

JULIUS-MAXIMILIANS UNIVERSITÄT
WÜRZBURG

DOCTORAL THESIS

**Quantitative genetics - from genome
assemblies to neural network aided
omics based prediction of
quantitative traits**

Author:

Jan Alexander
FREUDENTHAL

Supervisor:

Prof. Arthur KORTE

*A thesis submitted in fulfillment of the requirements
for the degree of Ph.D.*

in the

Research group for evolutionary genomics
GSLs

November 16, 2019

Declaration of Authorship

“Wit beyond measure is man’s greatest treasure”

Rowena Rawenclaw

JULIUS-MAXIMILIANS UNIVERSITÄT WÜRZBURG

Abstract

Faculty Name

GSLs

Ph.D.

**Quantitative genetics - from genome assemblies to neural network aided
omics based prediction of quantitative traits**

by Jan Alexander FREUDENTHAL

The Thesis Abstract is written here (and usually kept to just this page). The page is kept centered vertically so can expand into the blank space above the title too...

Acknowledgements

The acknowledgments and the people to thank go here, don't forget to include your project advisor...

Contents

Declaration of Authorship	iii
Abstract	vii
Acknowledgements	ix
1 Benchmarking of Chloroplast Genome Assembly tools	1
1.1 Introduction	1
1.1.1 Motivation	1
1.1.2 Extraction of chloroplast reads from whole genome data and general assembly workflow	4
Purpose and scope of benchmarking the landscape of chloro- plast assembly tools	6
1.2 Material and Methods	7
1.2.1 Methods	7
Data and code availability	7
Tools	7
Standardization and reproducibility	8
1.2.2 Data	9
Simulated	9
Real data set	10
Novel data sets	10
1.2.3 Evaluation	11
Quantitative	11

	Consistency	11
1.3	Results	12
1.3.1	Quantitative	12
	Simulated data	12
	Real data sets	14
	Consistency	16
	Novel	17
1.4	Discussion	19
1.5	Conclusion & outlook	22
2	Understanding the haplotype structure of Arabidopsis thaliana	25
2.1	Introduction	25
2.2	Haplotyping of A. thaliana	25
2.3	Results	25
2.4	Disucssion	25
3	GWAS-Flow a gpu-accelerated software for large-scale genome-wide as-	
	sociation studies	33
3.1	Introduction	33
3.2	Methods	35
	GWAS Model	35
	The GWAS-Flow Software	35
	Calculation of permutation-based thresholds for GWAS	36
	Benchmarking	37
3.3	Results	38
3.4	Discussion	40
4	Genomic prediction of phenotypic values of quantitative traits using	
	artificial neural networks	43
4.1	Introduction to machine learning	43

4.1.1	A brief history of machine learning	43
	The basic perceptron model	43
	Activation functions	46
	Gradient descent algorithm	49
	Optimizers	52
	Regularization parameters and overfitting	54
4.2	Introduction to genomic selection	56
4.2.1	On the nature of quantitative traits	56
4.2.2	Artificial selection in plant and animal breeding in the ge- nomics era	60
	Introduction to genomic selection	60
	Genomic prediction in recurrent selection and the breeders equation	62
	Genomic BLUP and Bayesian methods	66
4.2.3	Genomic selection using artificial neural networks	73
4.3	Proof of concept for ANN-based genomic selection	76
4.4	Material	78
4.4.1	DH populations derived from maize landraces	78
	Genomic maize data	79
	Phenotypic maize data	80
	Single environment prediction	80
4.4.2	A. thaliana	81
	Genomic data	81
	Phenotypic data	82
4.5	Methods	82
4.5.1	Validation scheme	82
4.5.2	ANN	82
4.5.3	GBLUP	84
4.6	Results	84

Results of <i>A. thaliana</i> prediction	84
4.6.1 Results of maize prediction	89
Across environments	89
Single environments	91
4.7 Discussion	93
5 GWAS	95
5.1 Introduction	95
5.2 Reevaluation of 46? phenotypes from the AraPheno database . . .	96
5.3 GWAS in DH landrace populations of maize across and within envi- ronments	96
5.3.1 Introduction	96
5.3.2 Material and Methods	96
5.3.3 Results	96
5.3.4 Results	96
5.3.5 Discussion	96
6 General Discussion	97
A Source code	99
A.1 GBLUP example	99
A.2 gwas.py	99
A.3 main.py	103
A.4 herit.py	107
B <i>A. thaliana</i> phenotypic data	109
C Genomic prediction	117
C.1 GP ANN	117
C.2 GBLUP script	122
C.3 Results of GP	127

List of Figures

1.1	Structure of a chloroplast genome	3
1.2	Chloroplast genome assembly workflow	6
1.3	Score of assemblies of simulated data sets	13
1.4	Scores of assemblies from real data sets	16
1.5	Comparison between two runs with the same assembler for consistency testing	17
1.6	Upset plot comparing the success rates for novel data sets	18
1.7	Upset plot comparing the success rates of of all assemblers	20
1.8	AliTV plot of alignments of assemblies of <i>Oryza brachyantha</i> of all assemblers	22
2.1	Haplotype strutcure of chromosome 1 of <i>A. thaliana</i>	26
2.2	Haplotype strutcure of chromosome 2 of <i>A. thaliana</i>	27
2.3	Haplotype strutcure of chromosome 3 of <i>A. thaliana</i>	28
2.4	Haplotype strutcure of chromosome 4 of <i>A. thaliana</i>	29
2.5	Haplotype strutcure of chromosome 5 of <i>A. thaliana</i>	30
2.6	blabl	31
3.1	Computations time vs accessions	39
3.2	Computation time vs number of markers	40
3.3	Computational time of GWA Analyses on real <i>A. thaliana</i> data sets	42
4.1	Basic perceptron model	44
4.2	Schematic layout of a simple multi-layer perceptron	45

4.3	Popular activation functions for neural networks	47
4.4	Training vs. validation loss over time	55
4.5	Truncation selection of a normal distributed phenotype	63
4.6	Scatterplot comparing prediction accuracies of ANN and GBLUP in <i>A. thaliana</i>	88
4.7	Violinplot comparing the results for GP in the DH population Ke- mater for ANN and GBLUP	89
4.8	Violinplot comparing the results for GP in the DH population Petkuser for ANN and GBLUP	90
4.9	Results of genomic prediction across single environments for Ke- mater and Petkuser DH populations	92

List of Tables

1.1	Data selection criteria for real data sets from SRA	10
1.2	Scores of assemblies of simulated data	14
1.3	Mean scores of chloroplast genome assemblers	15
4.1	Overview of properties of a variety of commonly applied Bayesian methods for genomic prediction. Table altered after KÄRKKÄINEN and SILLANPÄÄ, 2012	73
4.2	Simple simulated phenotypes and genotypes for genomic prediction with genotypes $G_1 \dots G_4$, Markers M_1 and M_2 and phenotypes based on additive effects or <i>and</i> , <i>or</i> , <i>xor</i> logic gates.	76
4.3	Results of genomic prediction from phenotypes and genotypes in table 4.2	77
4.4	Schematic representation of the enhanced genotype matrix for across environment prediction of maize phenotypes with DHs 1-2 with markers M 1-2 in environments E1-2	81
4.5	Prediction accuracies of <i>A. thaliana</i> phenotypes for GBLUP and ANN	84
4.6	Comparison of prediction results of ANN within locations and across locations for Kemater and Petkuser	93
4.7	ANN architectures of ANN resulting in highest prediction accuracies	93

List of Abbreviations

Adadelata	Adaptive delta
Adagrad	Adaptive Gradient Algorithm
Adam	Adaptive Moment estimation
ANN	Artificial Neural Network
API	Application Programming Interface
AUC	Area Under the Curve
BLUE	Best Linear Unbiased Estimator
BLUP	Best Linear Unbiased Predictor
BP	Base Pair
CPU	Core Processing Unit
DH	Doubled Haploid
DNA	DeoxyriboNucleic Acid
RNA	RiboNucleic Acid
EMMA	Efficient Mixed Model Associations
FCL	Fully Connected Layer
GBLUP	Genomic Best Linear Unbiased Predictor
GD	Gradient Descent
GEBC	Genomic Estimated Breeding Values
GPL	General Public License
GP	Genomic Prediction
GPU	Graphical Processing Unit
GRM	Genomic Relationship Matrix
GS	Genomic Selection

GUI	Graphical User Interface
GWAIS	Genome Wide Interaction Association Studies
GWAS	Genome Wide Association Studies
HL	Hidden Layer
HDF	Hierarchical Data Format
HPC	High Performance Computing
IR	Inverted Repeat
LCL	Locally Connected Layer
LD	Linkage Disequilibrium
LMM	Linear Mixed Model
LSC	Large Single Copy
MAF	Minor Allele Frequency
MBP	Mega Base Pair
MCMC	Markov Chain Monte Carlo
MLP	Multi Layer Perceptron
ML	Machine Learning
MSE	Mean Square Error
Nadam	Nesterov-accelerated Adaptive Moment Estimation
NAG	Nesterov Accelerated Momentum
NCBI	National Center for Biotechnological Information
QTL	Quantitative Trait Locus
ReLU	Rectified Linear Units
RKHS	Reproducing Kernel Hilbert Spaces
RMSE	Root Mean Square Error
RMSProp	Root Mean Square Propagation
ROC	Receiver Operating Characteristics
RSS	Residual Sum of Squares
SGD	Stochastic Gradient Descent

SNP	S ingle N ucleotide P olymorphism
SRA	S equence R ead A rchive
SSC	S mall S ingle C opy
TRN	T Rai N ing subset
TST	T e S Ting subset
WGS	W hole G enome S equencing
XOR	e X clusive O R

For/Dedicated to/To my...

1 Benchmarking of Chloroplast Genome Assembly tools

This chapter is oriented on FREUDENTHAL et al., 2019b. Only the chapters from the publication, which the author majorly contributed to, are included. If not cited otherwise the plots, even though they were published along the aforementioned paper, were designed and generated by the author of this thesis.

1.1 Introduction

1.1.1 Motivation

Some organelles like mitochondria and chloroplasts contain their own genetic information from which they are able to synthesize certain proteins independent of the core genome. Evolutionary this developed during endosymbiosis, a process which underlying theory seeks to explain how eukaryotic cells formed from prokaryotes MERESCHKOWSKY, 1905; KUTSCHERA and NIKLAS, 2005. This widely acknowledged hypothesis explains how in the early evolution of eukaryotes, other cells were incorporated in those cells from which today's known organelles descent. In the case of chloroplasts those were most likely photosynthetic bacteria or similar organisms ARCHIBALD, 2015. This process left its traces in the structure of chloroplast genomes until today, which resemble more that of a prokaryotic genome than that of its eukaryotic host cells. A typical chloroplast genome consists of circular DNA with a size between 120 kbp to 160 kbp PALMER, 1985, while

plant core genomes are linear, organized on chromosomes and larger by multiples of hundreds to tens of thousands.

The first chloroplasts have been sequenced as early as 1986 and were isolated from *Marchantia polymorpha* and *Nicotiana tabacum* OHYAMA et al., 1986; SHINOZAKI et al., 1986. Complete reviews on the structure of chloroplast genomes were authored by GREEN, 2011 and WICKE et al., 2011. Chloroplast genomics is widely applied in evolutionary studies aiding to elucidate the processes involved in endosymbiosis and the development of photosynthetic plants MARTIN et al., 2002; XIAO-MING et al., 2017. Over the course of natural adaptation the genome has been reduced in size through endosymbiotic gene transfer, a form of horizontal gene transfer, where fractions of plastid genomes are incorporated in the core DNA MARTIN et al., 2002; DEINER et al., 2017. This mechanism of evolution is still ongoing and can be observed *in vitro* and was proven experimentally BOCK, 2017; FUENTES et al., 2014; STEGEMANN and BOCK, 2009.

In the case of *Arabidopsis thaliana* this resulted in 14 % of the core genome's genes previously being located on the chloroplast, while 100-120 genes remain on the chloroplast itself WICKE et al., 2011, which by far would not suffice to allow the chloroplast to function independently of the host cell. Organelle genomes being much smaller and highly conserved with a large gene content leads to polymorphisms being more likely to cause functional changes in physiological processes. Another difference between organelle and core genomes is that single chloroplasts contain up to hundreds of copies of its own genome KUMAR, OLDENBURG, and BENDICH, 2014; BENDICH, 1987 and photosynthetic active cells again contain multiple chloroplasts. Therefore the copy number of the chloroplast's genomes is considerably higher than the number of core genomes per cell which in most cases is one.

Structurally chloroplast genomes are made up of four distinct regions. Two inverted repeats (IR), IR_A and IR_B , ranging from 10 kbp to 76 kbp in size, that divide the circular genome into two areas. The large single copy (LSC) and the

small single copy (SSC) as shown in figure 1.1 PALMER, 1985.

Taking into account that the majority of assembly tools has been designed to assemble linear core genomes, the structure of chloroplast genomes is an obstacle for the assembly pipelines, functioning with modern short read technologies, to overcome. This especially regards solving and aligning the IRs WANG et al., 2018.

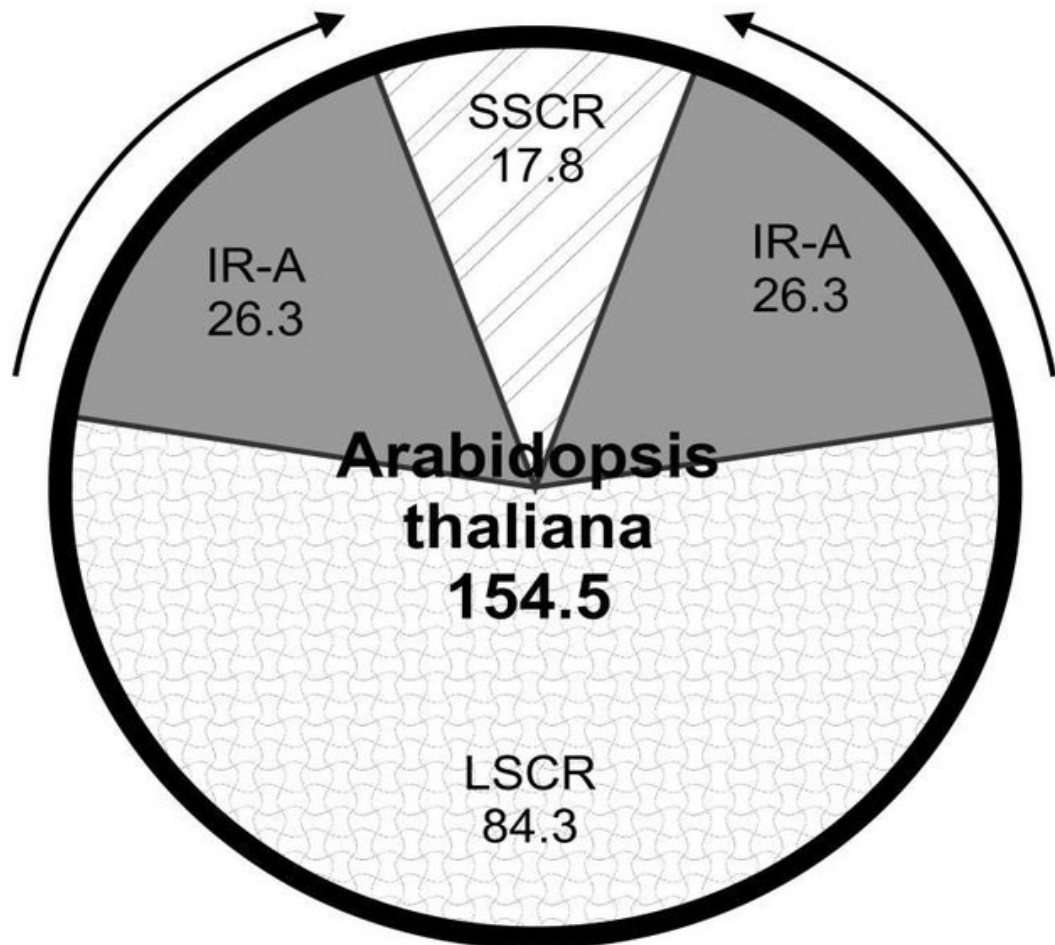


FIGURE 1.1: Structure of the chloroplast genome of *A. thaliana* with SSC-Region and LSC-Region. Length of the genome and its parts in kbp. Graphic from OLEJNICZAK et al., 2016

Another obstacle is heteroplasmy. It describes the phenomenon of co-existence of multiple versions of the chloroplast's genome in a single organism and even single cells of that respective organism, thus complicating genome assemblies and ongoing from there the downstream analyses CORRIVEAU and COLEMAN,

1988; CHAT et al., 2002. The underlying evolutionary mechanisms behind heteroplasmy are not fully elucidated and eventually existing fitness advantages fueling heteroplasmy cannot be explained satisfactory by standard evolutionary methods SCARCELLI et al., 2016.

Derived from a multitude of plant genome projects, there is a large variety of databases, containing short read data for species without assembled organelle genomes, available. E.g. NCBI's sequence read archive (SRA) LEINONEN et al., 2010. Because most plant DNA extraction protocols applied to procure raw input for sequencing use green leaf tissue as their basis, also contain a large amount of plastid DNA, providing a valuable basis for organelle genome assemblies pipelines. Which will be assessed in the course of this chapter.

Having larger numbers of assembled and annotated chloroplast genomes publicly available will be beneficial for evolutionary studies and are a useful addition to bar-coding and super-barcoding COISSAC et al., 2016, aside from other biotechnological applications DANIELL et al., 2016. To obtain those there is a variety of tools available. In the course of this chapter the availability, usability and overall performance of 7 of those assembly pipelines will be assessed. Ultimately, the newly gained insights will be utilized to attempt *de novo* to assemble more than 100 chloroplasts.

1.1.2 Extraction of chloroplast reads from whole genome data and general assembly workflow

There is large array of strategies to assemble chloroplast genomes from raw sequencing data TWYFORD and NESS, 2017. In general the process involves three steps: (i) extraction of plastid reads from the whole-genome sequencing (WGS) data, (ii) assembly of the plastid genome, (iii) solving the circular structure of the genome with the IRs. There are three approaches to address step (i). The first

one is to map all reads to a reference chloroplast VINGA et al., 2012, which works reasonably well if there is one available for the same or at least a closely related species. The second one is to make use of the much larger coverage of chloroplast DNA compared to core DNA, with a k-mer analysis CHAN and RAGAN, 2013, this is for example done by chloroExtractor ANKENBRAND et al., 2018. The third way to accomplish this is to combine both approaches as done by NOVOPlasty DIERCKXSENS, MARDULYN, and SMITS, 2017. Figure 1.2 shows the general workflow of chloroplast assembly tools with the bifurcation at step (ii).

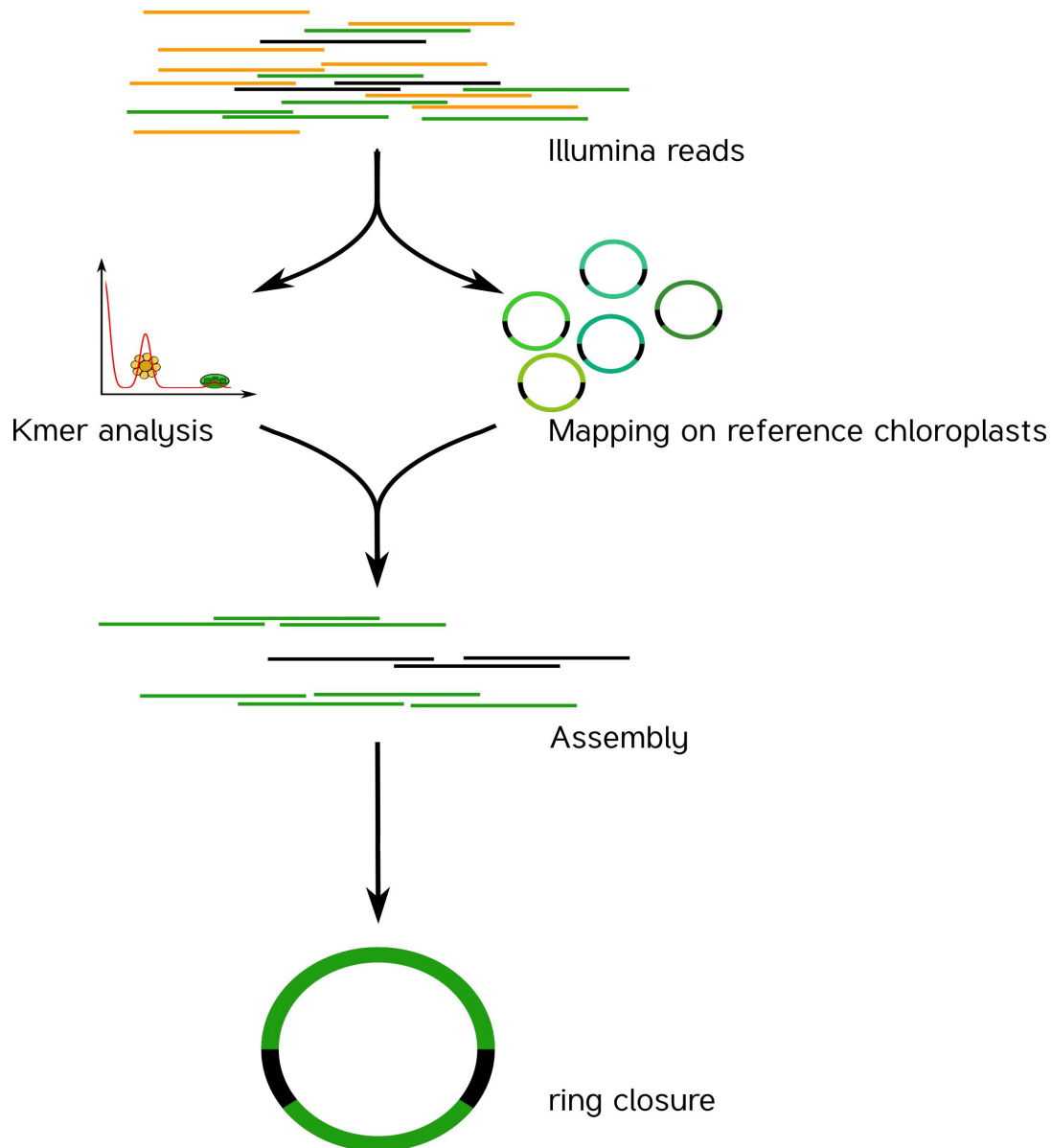


FIGURE 1.2: Standard workflow of chloroplast genome assembly.
Graphic from ANKENBRAND et al., 2018

Purpose and scope of benchmarking the landscape of chloroplast assembly tools

The purpose of this study is to provide insights into the landscape of chloroplast assembly tools, to recommend best practices for organelle genome assemblies and to contribute *de novo* assemblies for many species and families without a reference chloroplast available so far to the scientific community.

To be included into this study the software, including the source code, must be publicly available and published under the terms of a liberal, free open source software license e.g. GPL or MIT-license. The study was further restricted to paired-end Illumina data sets as their sole input source, because they were abundantly available for this benchmark. The seven tools that met the requirements and were therefore encompassed in this study were: chloroExtractor, ORG.Asm, Fast-Plast, IOGA, NOVOPlasty, GetOrganelle and Chloroplast assembly protocol. As later thoroughly described in section 1.3, there are huge differences between those tools and some will not be recommend to be used in scientific applications, while others outstand performance wise for most but not all cases.

1.2 Material and Methods

1.2.1 Methods

Data and code availability

All the source code and data used is publicly available under the terms of the MIT-License. The source code has been published on github [GitHub Repository for Benchmark Project](#) and archived on zenodo FÖRSTER and ANKENBRAND, 2019 . The docker images are available on dockerhub [Docker Hub Group for Benchmark Project](#).

Tools

As aforementioned there were certain requirements to be met to be included into the study. The only technical requirements was being able to assemble chloroplast genomes from paired-end Illumina reads. The other requirements were dictated by reproducibility. (i) The software must be open-source and available under the terms of a liberal software license. In the authors opinion obscuring the ability

to reproduce results behind paywalls cannot be considered good scientific practice. (ii) It has to be a command line tool since GUI-only tools are not suited for highly repetitive, automated analyses. In total there were 7 tools that met those conditions:

- (i) chloroExtractor ANKENBRAND et al., 2018
- (ii) Chloroplast assembly protocol SANCHO et al., 2018
- (iii) GetOrganelle JIN et al., 2018
- (iv) ORG.Asm COISSAC et al., 2016
- (v) IOGA BAKKER et al., 2016
- (vi) Fast-Plast MCKAIN and AFINIT, 2017
- (vii) NOVOPlasty DIERCKXSENS, MARDULYN, and SMITS, 2017

There are other tools available capable of assembling circular genomes that did not meet those requirements.

Standardization and reproducibility

The goal of this study was to provide deep insights into the landscape of chloroplast assembly tools. To accomplish that we tried to use the highest standards in bioinformatics in terms of standardization and reproducibility. Along with the study easy and ready-to-use versions of all the involved programs, working with standardized input, were published. For this purpose docker containers MERKEL, 2014 were implemented. To work with the containers in a closed HPC environment they were transformed into related singularity containers KURTZER, SOCHAT, and BAUER, 2017. To use the programs, novel users simply need to provide two files one for the forward reads (forward.fq) and one for the reverse reads (reverse.fq) and run the containers without any need for further configuration or installation besides docker or singularity itself. Both files are required to

be in FASTQ format. Besides the individual output files, recording the process of the respective program, all programs write the assembly products into files called `output.fa` in FASTA format. For the quantitative and consistency measurements the singularity containers were run on the Julia HPC-cluster of the University of Würzburg using the SLURM workload manager JETTE, YOO, and GRONDONA, 2002. All runs for all assemblies were set with a time limit of 48 hours. This was necessary because some assemblers e.g. I0GA, if not finishing after at least 12 hours, showed the tendency not to finish, even after weeks of running.

1.2.2 Data

Three different data sets were used:

- (i) simulated data from *A. thaliana* chloroplasts
- (ii) real data with known reference chloroplast to rate the success of the assemblies
- (iii) novel data sets from NCBI's SRA without a know reference chloroplast to apply the gained knowledge for the *de novo* assembly of more than 100 chloroplasts.

Simulated

As a first steps in any benchmarking process it is always useful to start with simulated data, allowing investigators to have full control over all the parameters involved. In the present case the data's input parameters, thought to be influential on the outcome, were: The read length, the ratio between chloroplast and core genome reads as well as the total size of the data set. The data simulations were based on real data from the TAIR10 genome of *A. thaliana* BERARDINI et al., 2015 and spawned using `seqkit` SHEN et al., 2016. Core to chloroplast ratios simulated were: 0:1, 1:10, 1:1000 and 1:1000, with read length of 150 and 250 bp. The

artificial data consisted either of 2 million read pairs or the full data available. The simulation process was documented and the code and the data is available on github and zenodo ANKENBRAND and FÖRSTER, 2019.

Real data set

Real data was selected from the SRA database. Table 1.1 lists the search terms that had to be met for a plant to be included in the study from SRA.

TABLE 1.1: Data selection criteria for real data sets from SRA

Choice	Option	Explanation
Organism	green plants	include only photosynthetic plants e.g. no algae
Strategy	wgs	only data from wgs projects included
Platform	Illumina	include only paired-end Illumina reads
Properties	biomol DNA	include only biomol. DNA samples (e.g. no RNA)
Layout	paired	exclude single-end reads
Selection	random	
Access	public	Only publicly available data included

In total this resulted in 369 data sets representing a broad variety of the plant kingdom with many different families and genera included.

Novel data sets

To assess the performance of assemblies without a published chloroplast on CpBase *CpBase* 105 data sets were selected from SRA. It was emphasized that the chosen read libraries were as distant as possible related to the next relatives with a reference chloroplast, related as possible in taxonomic terms according to NCBI *NCBI Taxonomy*. This was achieved by a phylogenetic analysis of the accessible data sets on SRA by Frank Förster described in FREUDENTHAL et al., 2019b.

1.2.3 Evaluation

Quantitative

Each assembly from each assembler was compared to their respective reference genome by alignment using minimap2 LI, 2018. Based on those alignments scores were calculated following equation 1.1 from 0 to 100, with 100 being a perfect score. Four different metrics contributed equally to the final score:

- (i) the coverage of the assembled genome compared to the reference genome cov_{ref} as an estimate for the completeness
- (ii) the vice versa case cov_{qry} as a measure for the correctness of the assembly
- (iii) the success of resolving the IR correct, estimated from the size difference from the reference and the newly assembled genome $\min \left\{ \frac{cov_{qry}}{cov_{ref}}, \frac{cov_{ref}}{cov_{qry}} \right\}$
- (iv) the number of total contigs were weighted as $\frac{1}{n_{contigs}}$ giving a chloroplast with one contig the optimal score.

$$score = \frac{1}{4} \cdot \left(cov_{ref} + cov_{qry} + \min \left\{ \frac{cov_{qry}}{cov_{ref}}, \frac{cov_{ref}}{cov_{qry}} \right\} + \frac{1}{n_{contigs}} \right) \cdot 100 \quad (1.1)$$

While it is difficult to evaluate the success or failure of assemblies on a continuous scale, equation 1.1 allows for objective and unbiased measurements. SNPs or other small variants do not influence the outcome of the score, because they are more likely due to in-species variation between plastid genomes and not caused by the assembly itself. Even if the latter is true it would be difficult to determine.

Consistency

For any given bioinformatical application consistency is a desired trait. Software ideally should repeatedly yield the same output when provided with the same

output and assembly tools are exception. To evaluate the reproducibility of the 7 tools, for all the 369 real data sets described in section 1.2.2, they were assembled and scored twice with each assembler. The correlations between the first and the second run's scores were used as the measure for the robustness of a program.

1.3 Results

1.3.1 Quantitative

Simulated data

The simulated data sets were assembled and scored with all the tools as described above. Figure 1.3 shows a tile plot with the results displaying a color scale from orange over light green to dark green representing the scores from 0 to 100. Blank spaces indicate the failure to produce any output in the given time frame of 48 hours.

While at first sight there is no clear correlation between the input data sets and the score, it is clearly visible that there are grave differences between the assemblers. Two programs, namely Chloroplast assembly protocol and IOGA, failed to correctly assemble a single chloroplast's genome. IOGA even fails to provide an output at all for the majority of the data sets. While those two stand out as negative examples, Fast-Plast and GetOrganelle stand out as positive examples, perfectly or nearly perfectly assembling all the data sets, with GetOrganelle surpassing the performance of Fast-Plast. In the middle of the field are chloroExtractor, ORG.Asm and NOVOPlasty performing reasonably well, but sometimes lacking to solve the IRs and the circular structure.

1.3. Results

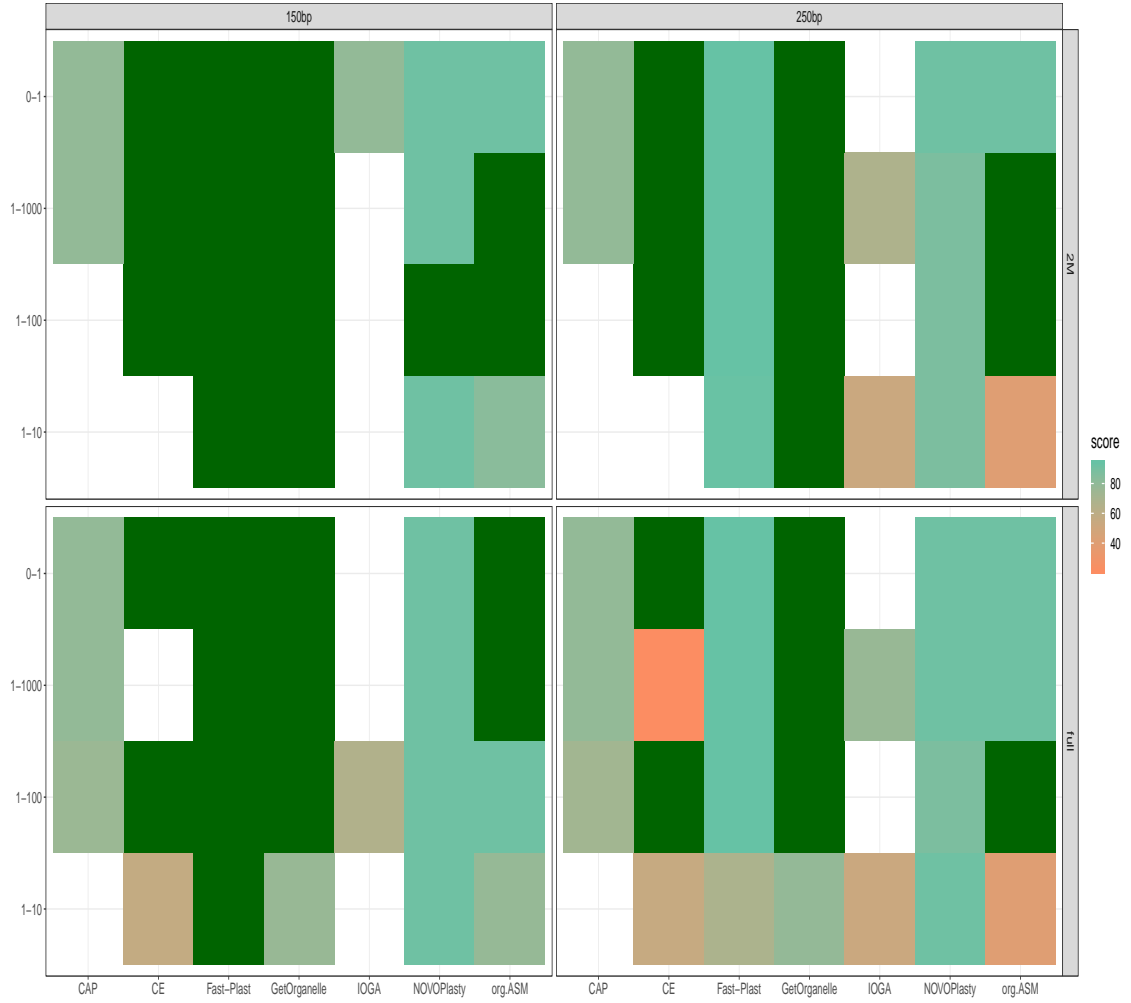


FIGURE 1.3: Results of assemblies executed with simulated data sets.

There is a significant difference between the performance of the assemblers, but generally the other varying input parameters, do not have as grave an influence as the choice of assembler. While Fast-Plast deals with the shorter reads of 150 bp much better than with the longer reads of 250 bp, the scores of the other assemblers do not seem to be influenced by the read length. There is no difference between the full and the subsampled data sets. And while all assemblers appear to be more challenged by low chloroplast to core genome ratios of 1:10, beyond a ratio of 1:10 it does not affect the quality of the assemblies. Table 1.2 shows all the individual results for all data sets and assemblers. For the fields with no entry

the respective assembler failed to provide an output.

TABLE 1.2: Scores of assemblies of simulated data

Set	Length	Ratio	CAP	CE	FP	GO	IOGA	NP	oA
full	150	0-1	79.10	100.00	99.48	100.00		91.52	100.00
2M	150	0-1	79.10	100.00	99.72	100.00	79.10	91.52	91.50
full	150	1-10		56.44	100.00	76.98		91.52	78.00
2M	150	1-10			99.97	100.00		91.52	82.72
full	150	1-100	75.72	100.00	99.48	100.00	66.09	91.52	91.50
2M	150	1-100		100.00	99.47	100.00		100.00	100.00
full	150	1-1000	79.10		99.72	100.00		91.52	100.00
2M	150	1-1000	79.10	100.00	99.72	100.00		91.52	100.00
full	250	0-1	79.10	100.00	93.82	100.00		91.52	91.50
2M	250	0-1	79.10	100.00	93.83	100.00		91.52	91.50
full	250	1-10		54.98	68.45	78.89	52.71	91.52	40.20
2M	250	1-10			93.00	100.00	52.67	87.40	40.20
full	250	1-100	72.81	100.00	93.82	100.00		87.40	100.00
2M	250	1-100		100.00	93.83	100.00		87.40	100.00
full	250	1-1000	79.10	21.30	93.83	100.00	76.96	91.52	91.50
2M	250	1-1000	79.10	100.00	93.83	100.00	67.55	87.40	100.00

CAP = Chloroplast assembly protocol; CE = chloroExtractor; FP = Fast-Plast; GO = GetOrganelle; NP = NOVOPlasty; oA = ORG. Asm; length in bp

Real data sets

Table 1.3 summarizes the results from the assemblies of 369 data sets with 7 the assemblers. Similar to the scores of the previous section there is a significant difference between the tools. Likewise GetOrganelle is the most successful assembler by a large margin with 210 of 369 chloroplast genomes perfectly assembled. It completely fails to provide output for only 9 data sets, resulting in a median score >99. Contrary Chloroplast assembly protocol and IOGA both failed to completely assemble a single genome. The performance of Fast-Plast is reasonably well in comparison, completing approximately half as many genomes as GetOrganelle and being the only other tool whose average score surpasses 90. Similar to the trials with the simulated data in chapter 1.3.1 chloroExtractor, NOVOPlasty and ORG. Asm are in the middle of the field.

1.3. Results

TABLE 1.3: Mean scores of chloroplast genome assemblers

Assembler	Median	IQR	n_perfect	n_tot
Chloroplast assembly protocol	45.25	50.19	0	369
chloroExtractor	56.55	71.50	14	369
Fast-Plast	92.80	23.59	113	369
GetOrganelle	99.83	20.94	210	360
IOGA	71.10	11.21	0	338
NOVOPlasty	75.95	48.69	58	369
ORG . Asm	67.35	91.69	46	348

Figure 1.4 emphasizes the large differences between the assemblers shown in table 1.3. The swarm plots show distinct bands for some assemblers e.g. NOVOPlasty and ORG . Asm, suggesting that multiple assemblies fail to be solved into a single contig genome at a certain point. As thoroughly discussed in section 1.4, solely from the swarm plot, it is debatable if all the tools should be recommended to be used for the purpose they were designed for.

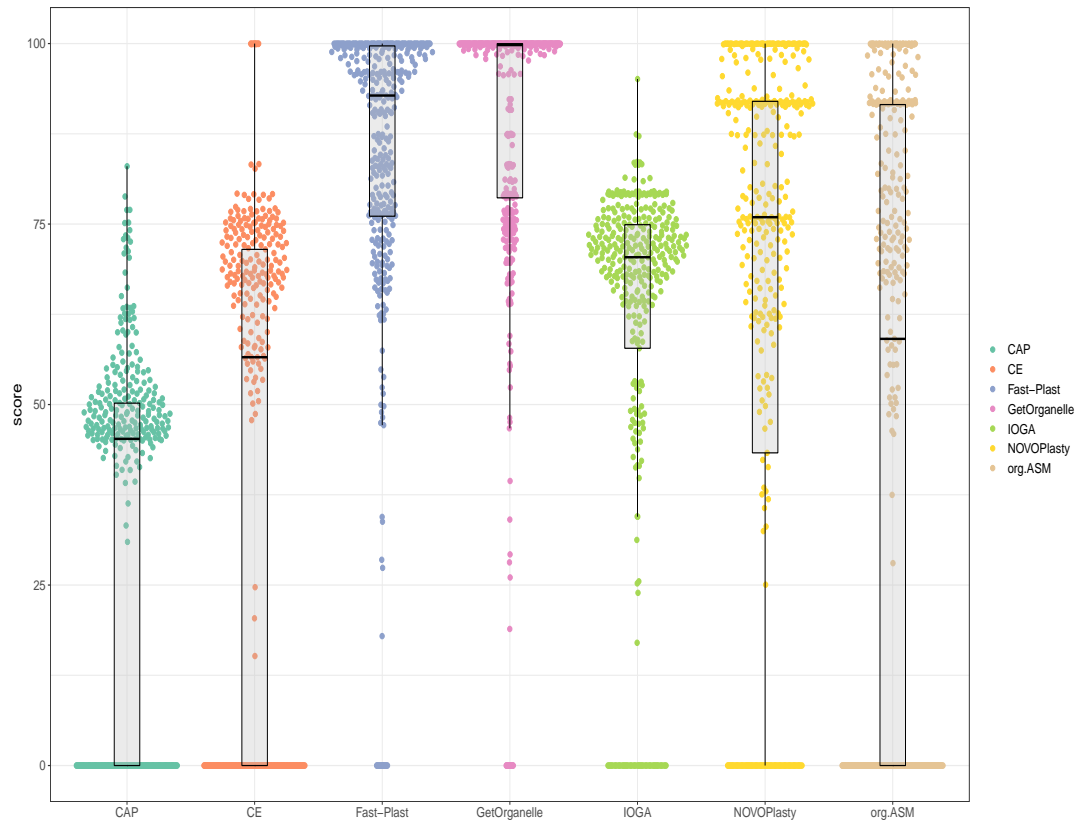


FIGURE 1.4: Box and swarm plots depicting the results from scoring shown calculated by 1.1

Consistency

Consistency testing was done by re-running every assembly for the real data sets and comparison of the two scores. `chloroExtractor` was the only tool that was 100 % consistent over both runs. Followed by `Fast-Plast` and `NOVOPlasty`. The consistency plot (figure 1.5) for both of them results in arrowhead shaped plots. With differences between the first and second run appearing in assemblies with the best scores. All other assemblers appear to produce the same output in the two runs, except if either run failed to complete the assembly at all. This is less pronounced for `Chloroplast assembly protocol` and `GetOrganelle` and is a grave issue for `ORG.Asm` and `IOGA`.

1.3. Results

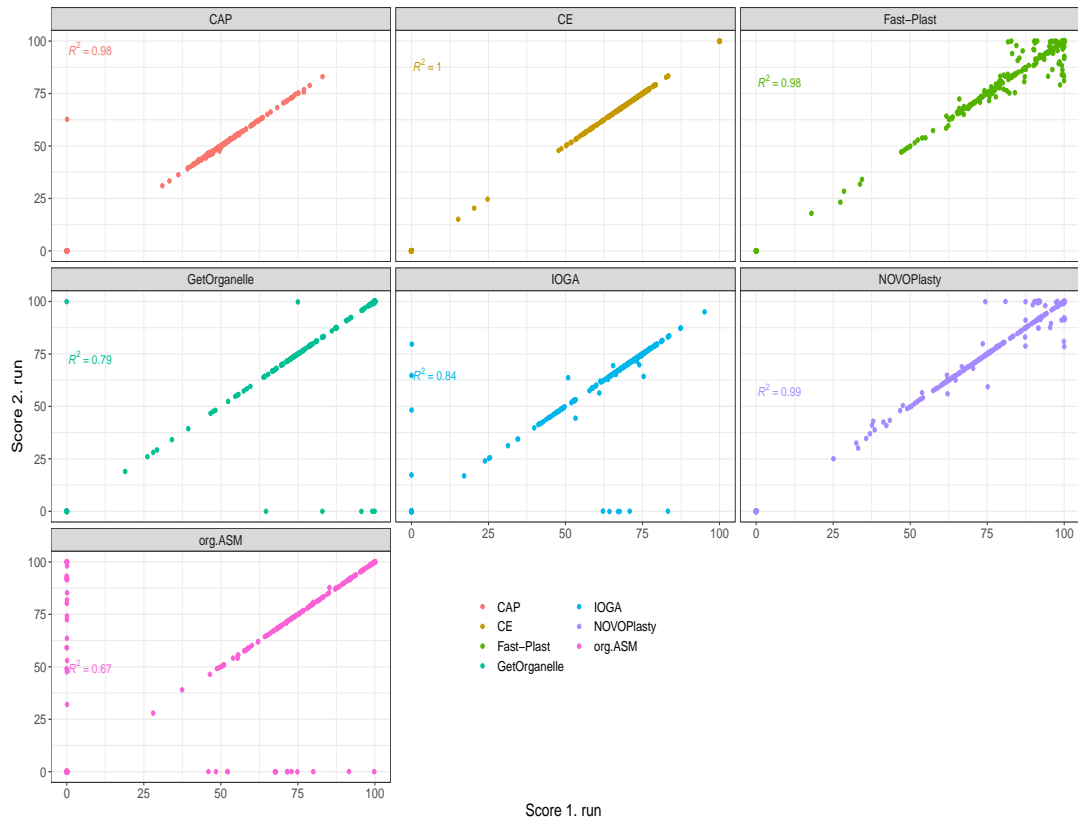


FIGURE 1.5: Swarm plots depict the results from the scoring shown in 1.1 for two independent runs for each assembler on each of the data sets

Novel

The final assessment in the evaluation of the assemblers was to test them on novel data sets without a published chloroplast. This step is important for two reasons.

(i) It is possible that certain tools perform well on known chloroplasts because they have knowledge of their structure, which would lead to a lack of generalization on unknown genomes. (ii) To apply and test the gained insights with the goal of providing the scientific community with a larger variety of published chloroplast genomes.

As in previous evaluations the most successful assembler was GetOrganelle, with 49 out of 105 novel data sets completely assembled.

Lacking a reference genome for alignment, the success had to be defined differently and equation 1.1 was not suitable to evaluate the novel assemblies. Metrics influencing the score of the novel assemblies were the number of contigs, solving the IRs and the size of the SSC and LSC. This, known to the author, might be biased and not true for all chloroplasts and assumes that all chloroplast genomes evolved according to the general structure described in chapter 1.1. Figure 1.6 compares the results of the assemblies with at least one successful assembly.

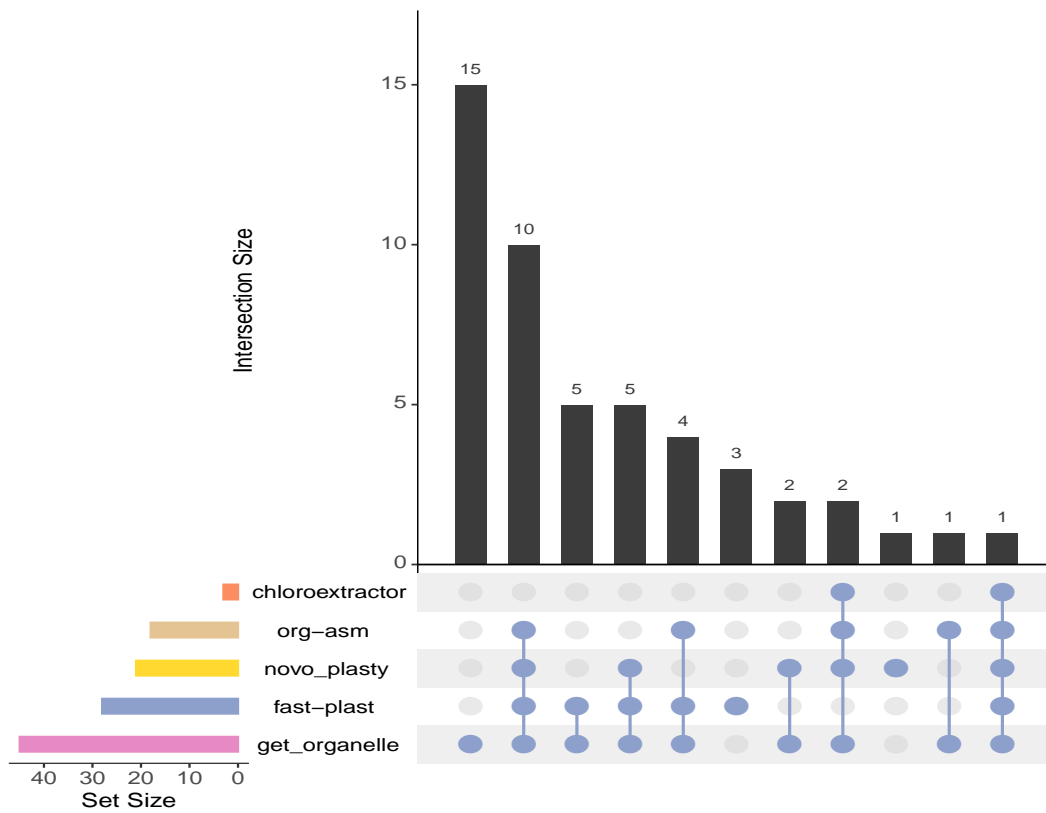


FIGURE 1.6: Upset plot comparing the success rates of the different assemblers. The colored, horizontal bar plot show the total amount of successful assemblies for each assemblers. The black, vertical barplot the size of the intersection indicated by the dots in the middle

1.4 Discussion

Recapitulating the study presented in this chapter so far consists of two goals. (i) To assess the overall performance of a variety of tools designed specifically for the assembly of circular chloroplast genomes from paired-end Illumina reads and (ii) to *de novo* assemble a variety of yet unpublished chloroplast genomes from existing data. To accomplish the first goal 16 simulated and 369 real data sets were used adding up to a total of 5166 assemblies for the real data sets and 112 for the simulated data, along 735 assemblies for the novel data sets, thus underlying the statistical powers of this benchmarking study. The most successful tools were GetOrganelle and Fast-Plast, which are recommended to be used complementary because, as shown in figure 1.7, they succeed for most data sets compared to other assemblers and accomplish to satisfactory assemble chloroplast genomes where the other fails. If both of them fail it might be worthwhile to repeat the runs because other results could be expected as shown in the scatter plots of figure 1.5, especially Fast-Plast might be able to improve the previously reached score. Only if both of them fail it might, even though improbable, that NOVOPlast might lead to a successful assembly. The other assemblers should be used with caution. While chloroExtractor might be good for a quick overview due to its relatively low demand in computational time FREUDENTHAL et al., 2019b; Chloroplast assembly protocol, ORG.Asm and IOGA are not recommended to be used as the primary tools in organelle genome assembly projects.

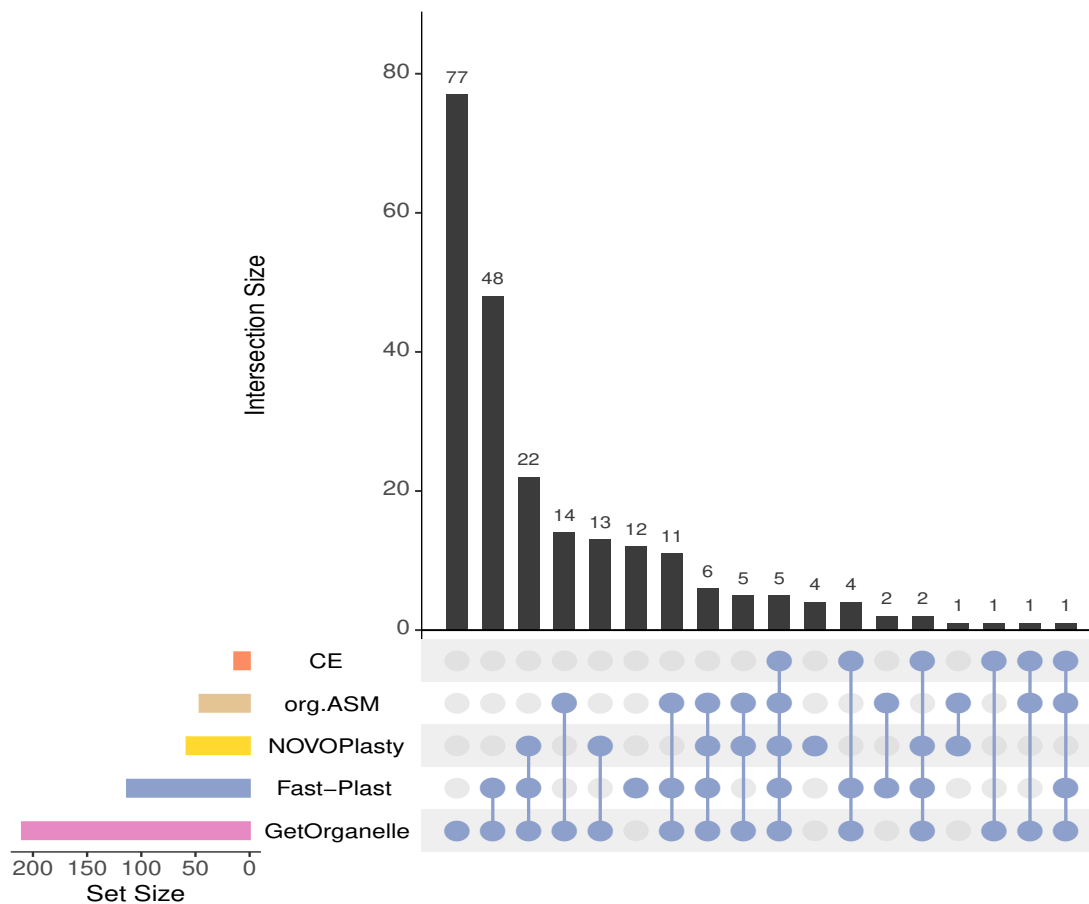


FIGURE 1.7: Upset plot showing the intersections of success rates between assemblers. A successful assembly was defined by a score >99 according to equation 1.1. The colored, horizontal barplot indicate the total number of successful assemblies for an individual tool. The black, vertical barplot gives the magnitude of the intersection between the assemblers indicated by the dots in the middle. Therefore the first and second vertical bars are to be interpreted as follows: 77 data sets were only successfully assembled by chloroExtractor, likewise 48 genomes were assembled completely by GetOrganelle and Fast-Plast and so on.

It might be possible that overall performance of a specific tool might change significantly by fine tuning the input parameters of the tool, which was purposely

not done in the scope of the present study because this study was designed to mimic the behavior of end-users and not developers of such tools. It is assumed that users with little experience in bioinformatics are inclined to use the basic configurations of such a tool.

While there are huge differences between all assemblers, they are presented with the same challenges and the bottlenecks are similar for all of them. However, the success rate of passing those differs. Figure 1.8 shows the alignment of the genomes, assembled with the 7 tools, of *Oryza brachyantha*, a grass distantly related to cultivated rice *Oryza sativa*, and the respective reference genome. For the need of a linear representation of the circular genome the convention is to present chloroplast genomes in the order LSC - IRa - SSC -IRb. *O. brachyantha* was chosen because multiple tools successfully or at least almost assembled the full genome. Chloroplast assembly protocol is singled out, which only managed to assemble a few fragments on the SCC and the IRs on many contigs. A common mistake is to return 3 contigs as IOGA did. They represent the LSC the SSC and one IR but failed to resolve those regions into a one circular contig. GetOrganelle and Fast-Plast were able to reproduce the structure of the reference, while chloroExtractor flipped the LSC and NOVOPlasty and ORG.Asm were not able to construct the single contig into the conventional structure. All of these are common mistakes appearing more or less rare in all the assemblers. This could be a good starting point for the developers to further improve their tools. In this example all but Chloroplast assembly protocol were able to construct all the parts of the chloroplast's genome, and the main mistake was to resolve the structure of the genome into a circular, one contig version.

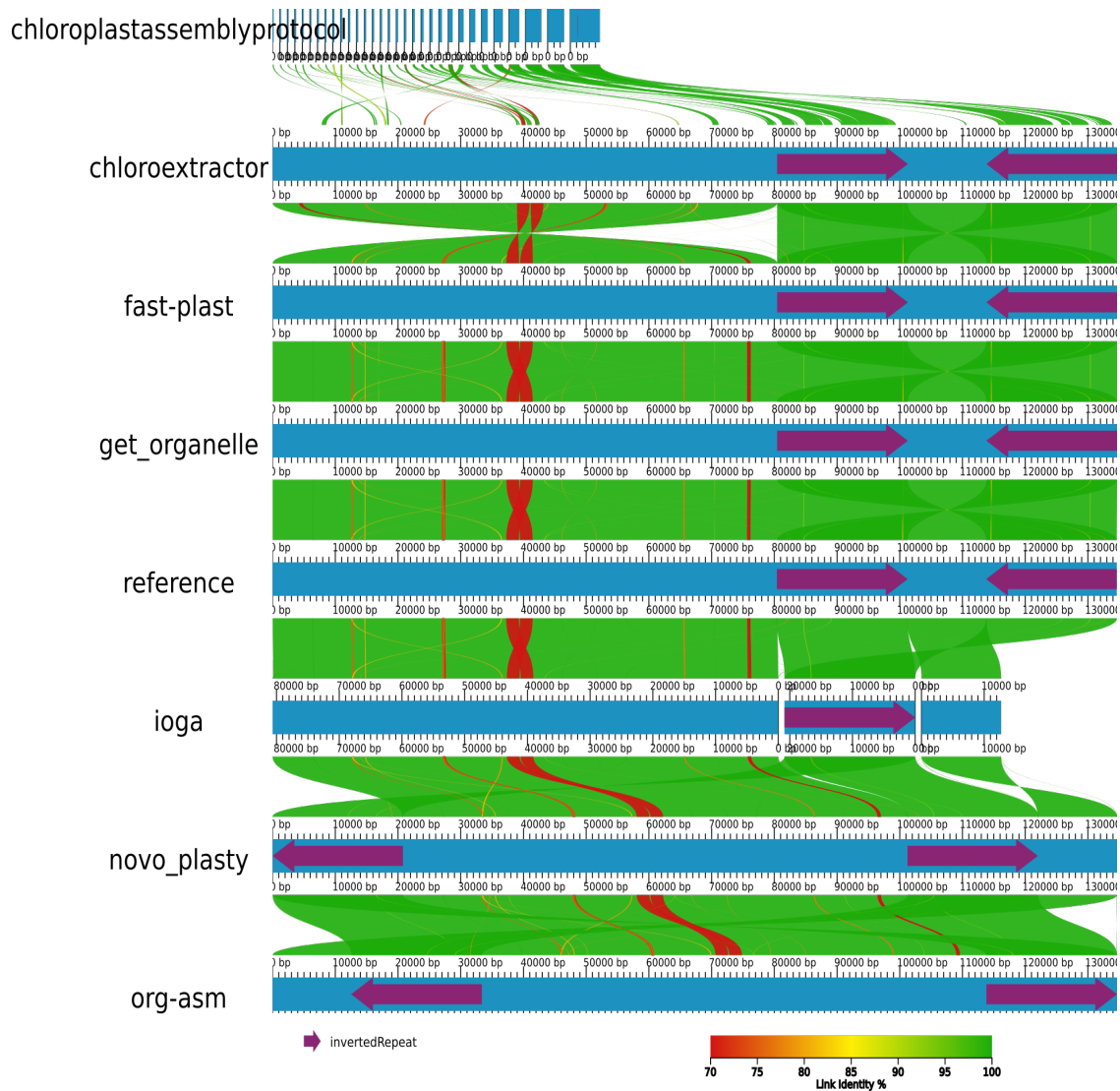


FIGURE 1.8: AliTV plot ANKENBRAND et al., 2017 from FREUDENTHAL et al., 2019b showing the alignments of *Oryza brachyantha* chloroplast genomes for all 7 assemblers. Regions in adjacent assemblies are connected with colored ribbons. The color codes of for the similarity between regions. The purple arrows indicate the IR regions

1.5 Conclusion & outlook

Organelle genomics is a promising field in plant genetics. As described in section 1.1 chloroplast genomes are well-suited for applications in evolutionary sciences, taxonomy and barcoding applications. Alike for its mother branch genomics,

for comparative chloroplast genomics it is just as crucial to obtain high quality genomes. The quality is mainly influenced by two factors: the quality of the genome sequencing protocol and the quality of the assembly. As shown the latter varies massively between tools and not all tools are recommend equally from the conclusions drawn from the experiments described above. All tools have room for improvement. This is not meant to criticize the respectable work of the developers, but to encourage them to further develop tools and publish them under terms of liberal software licenses for the greater benefit of the entire scientific community.

2 Understanding the haplotype structure of *Arabidopsis thaliana*

2.1 Introduction

Recombination and LD in *A. thaliana* KIM et al., 2007 LD in *A. thaliana* NORDBORG et al., 2002 Evolution of selfing TANG et al., 2007 Evolution and genetic differentiation among relatives of *Arabidopsis thaliana* KOCH and MATSCHINGER, 2007 FLC haplotypes LI et al., 2014

2.2 Haplotyping of *A. thaliana*

2.3 Results

2.4 Disucssion

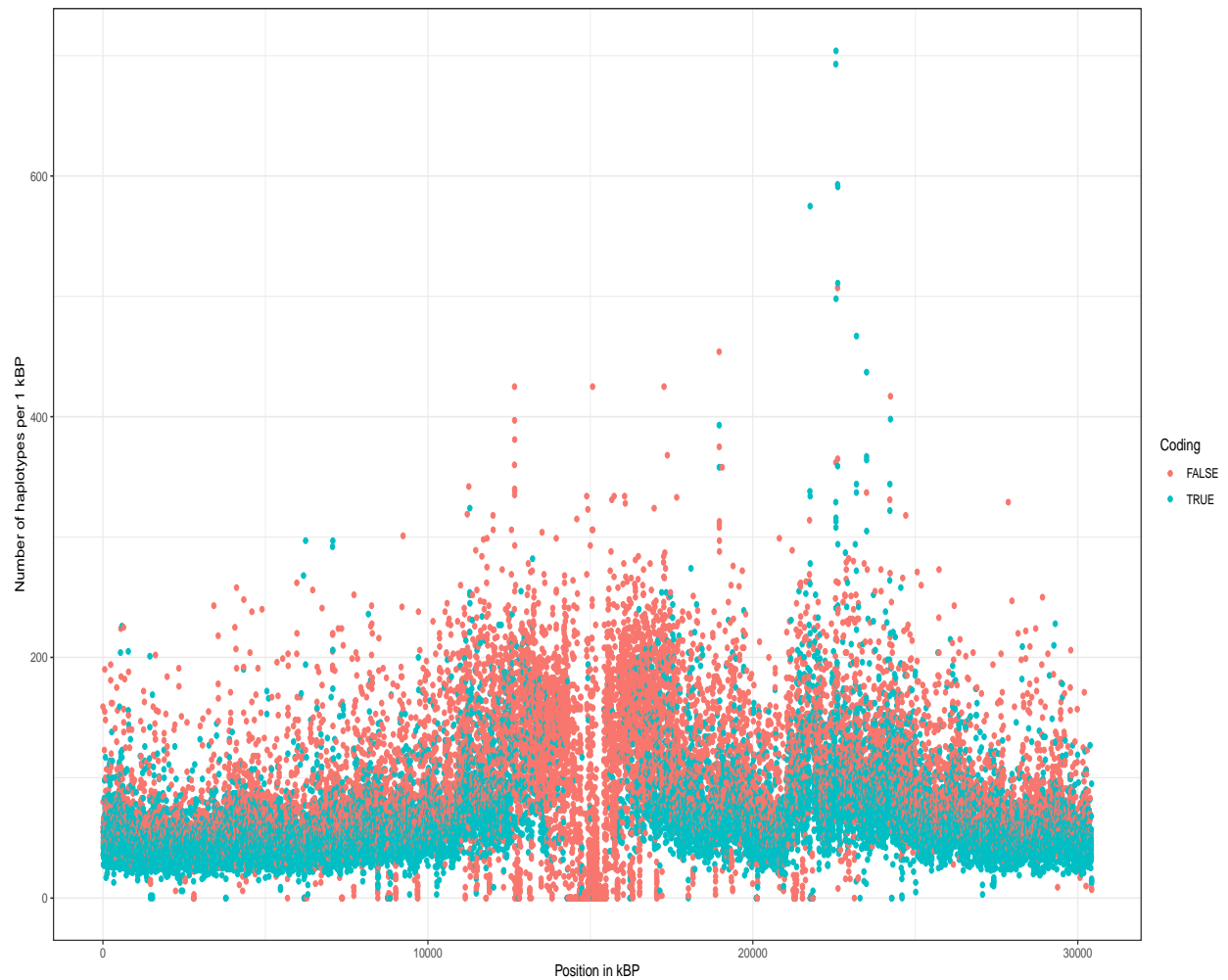


FIGURE 2.1: The number of segregating haplotypes with a polymorphism in at least one position over a stretch of 1 kBP.

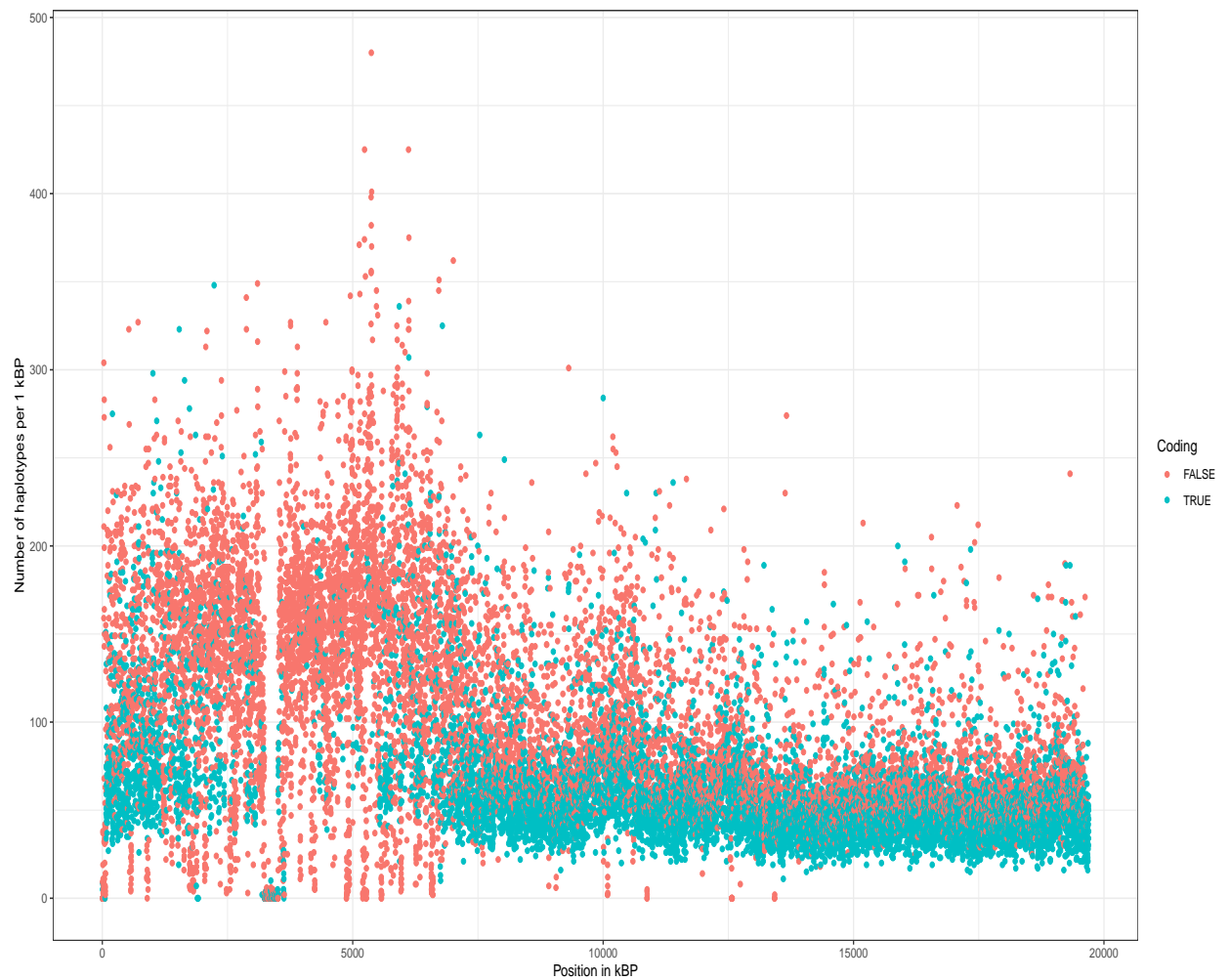


FIGURE 2.2: Number of segregating haplotypes with a polymorphism in at least one position over a stretch of 1 kBP.

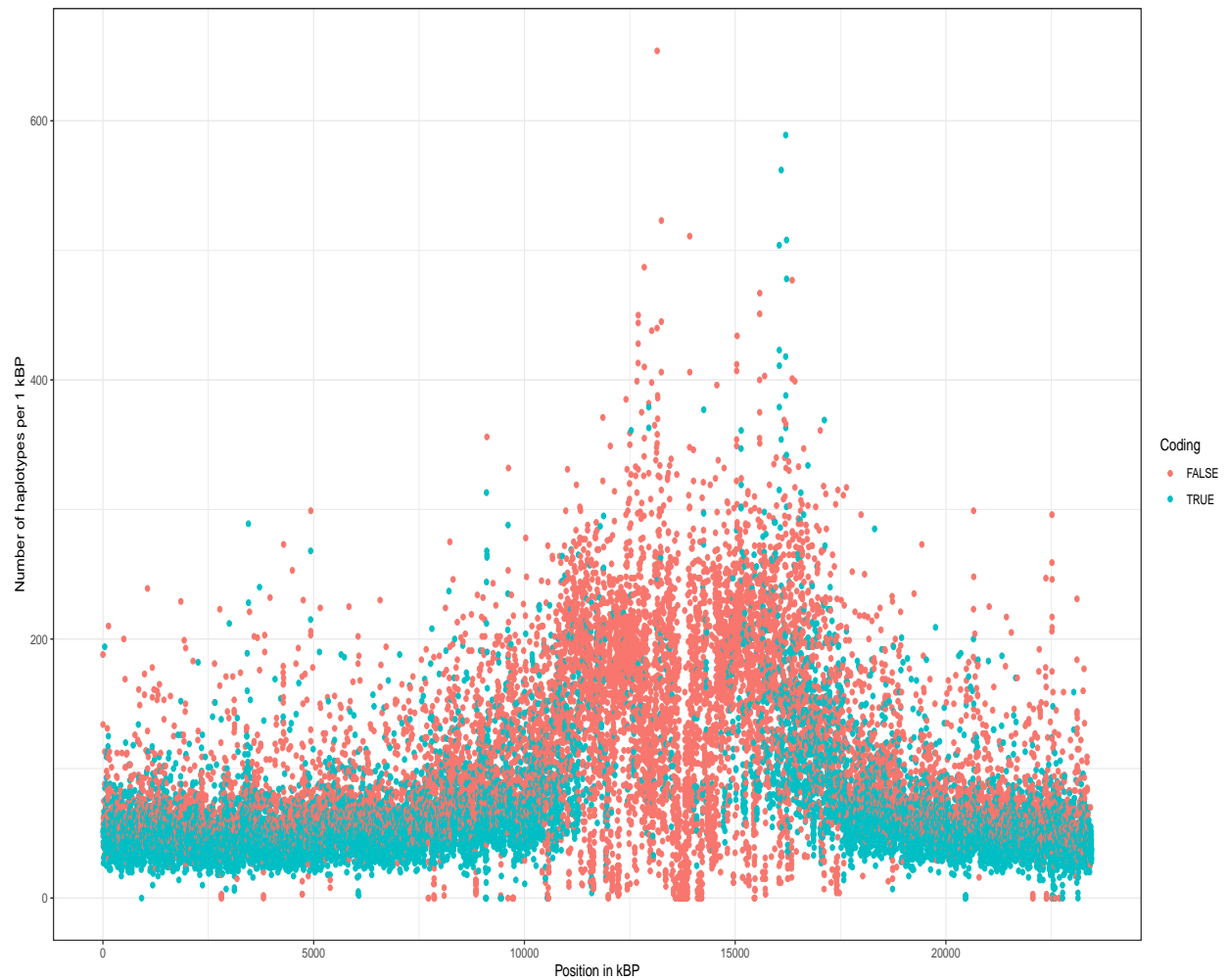


FIGURE 2.3: Number of segregating haplotypes with a polymorphism in at least one position over a stretch of 1 kBP.

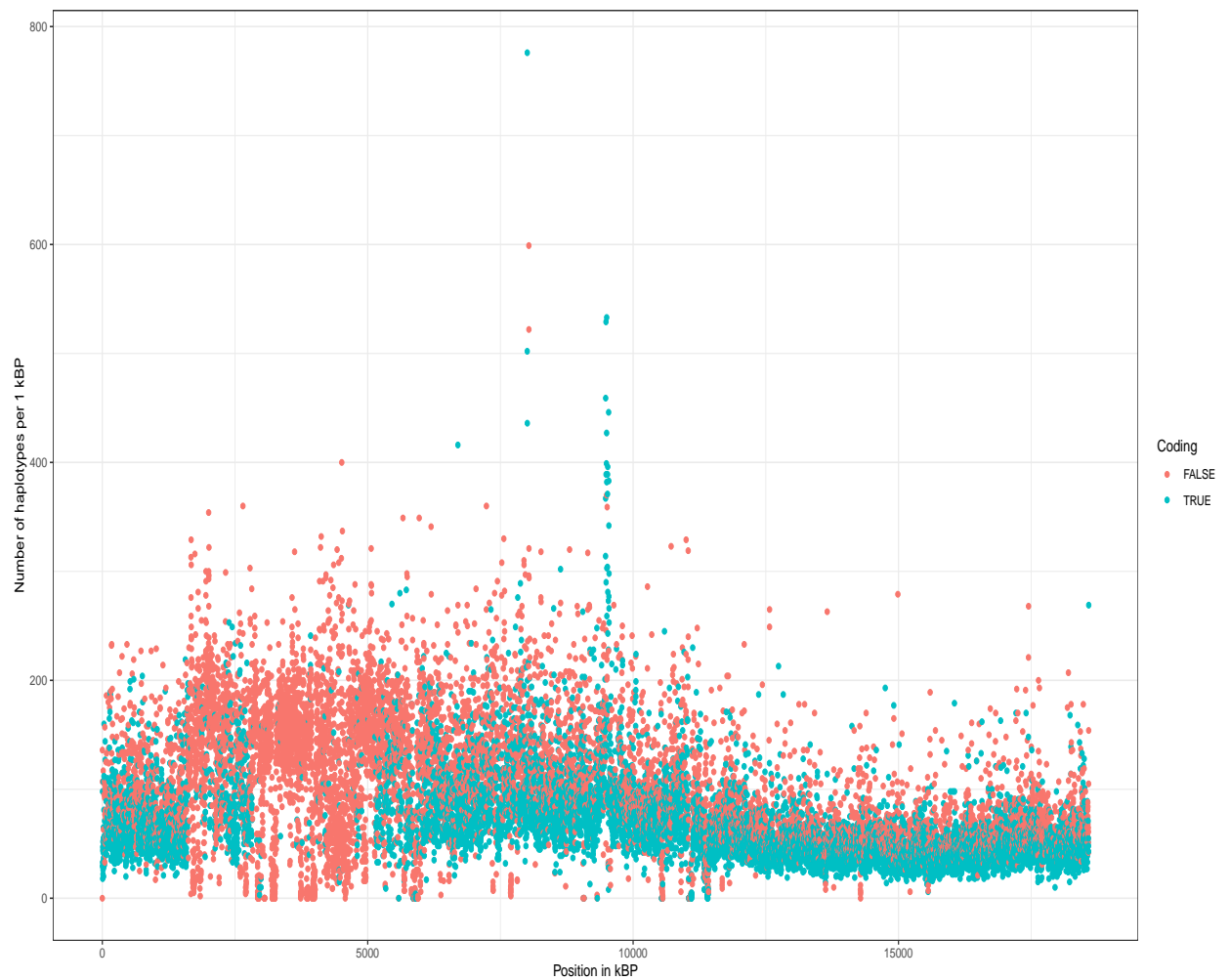


FIGURE 2.4: Number of segregating haplotypes with a polymorphism in at least one position over a stretch of 1 kBP.

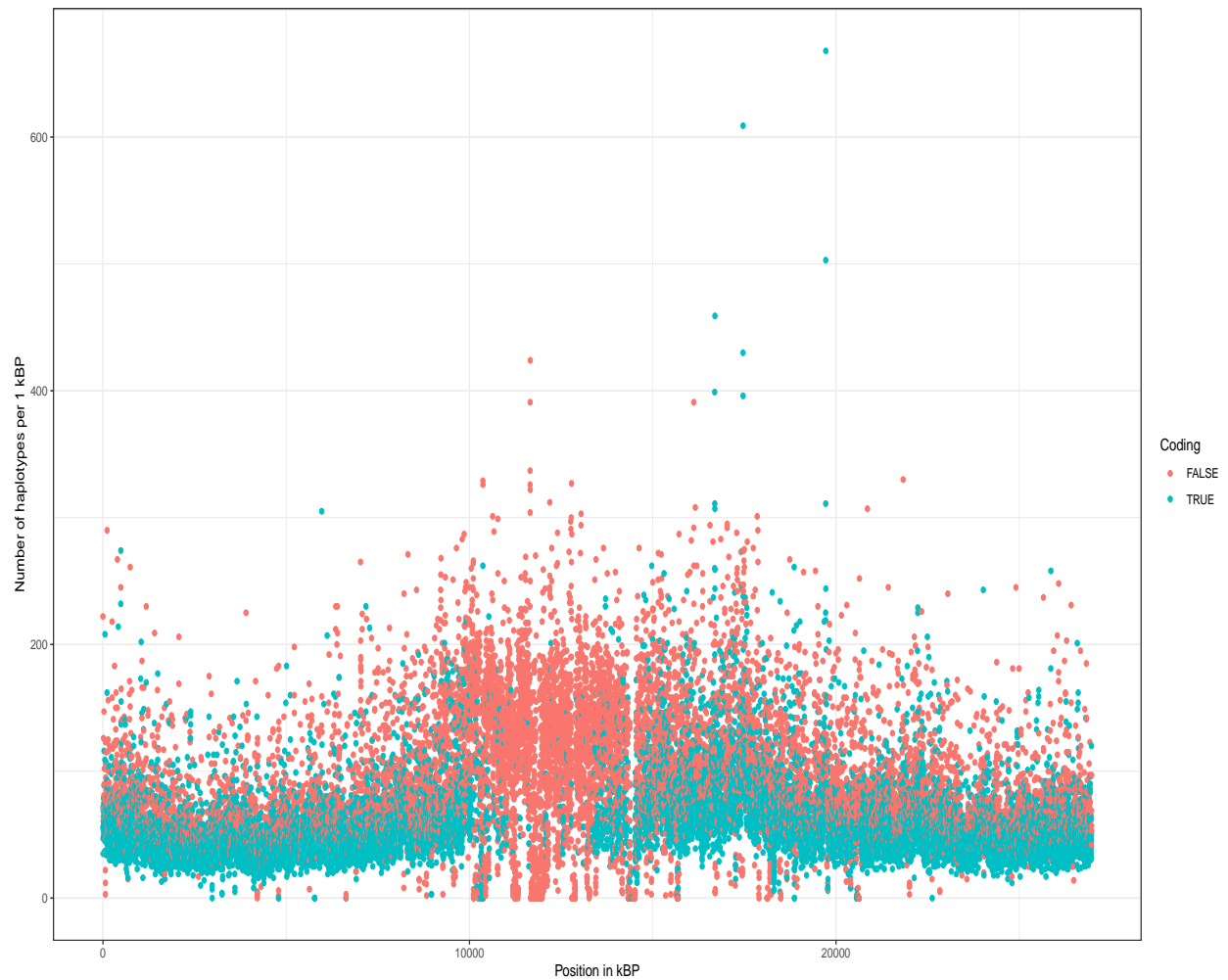


FIGURE 2.5: Number of segregating haplotypes with a polymorphism in at least one position over a stretch of 1 kBP.

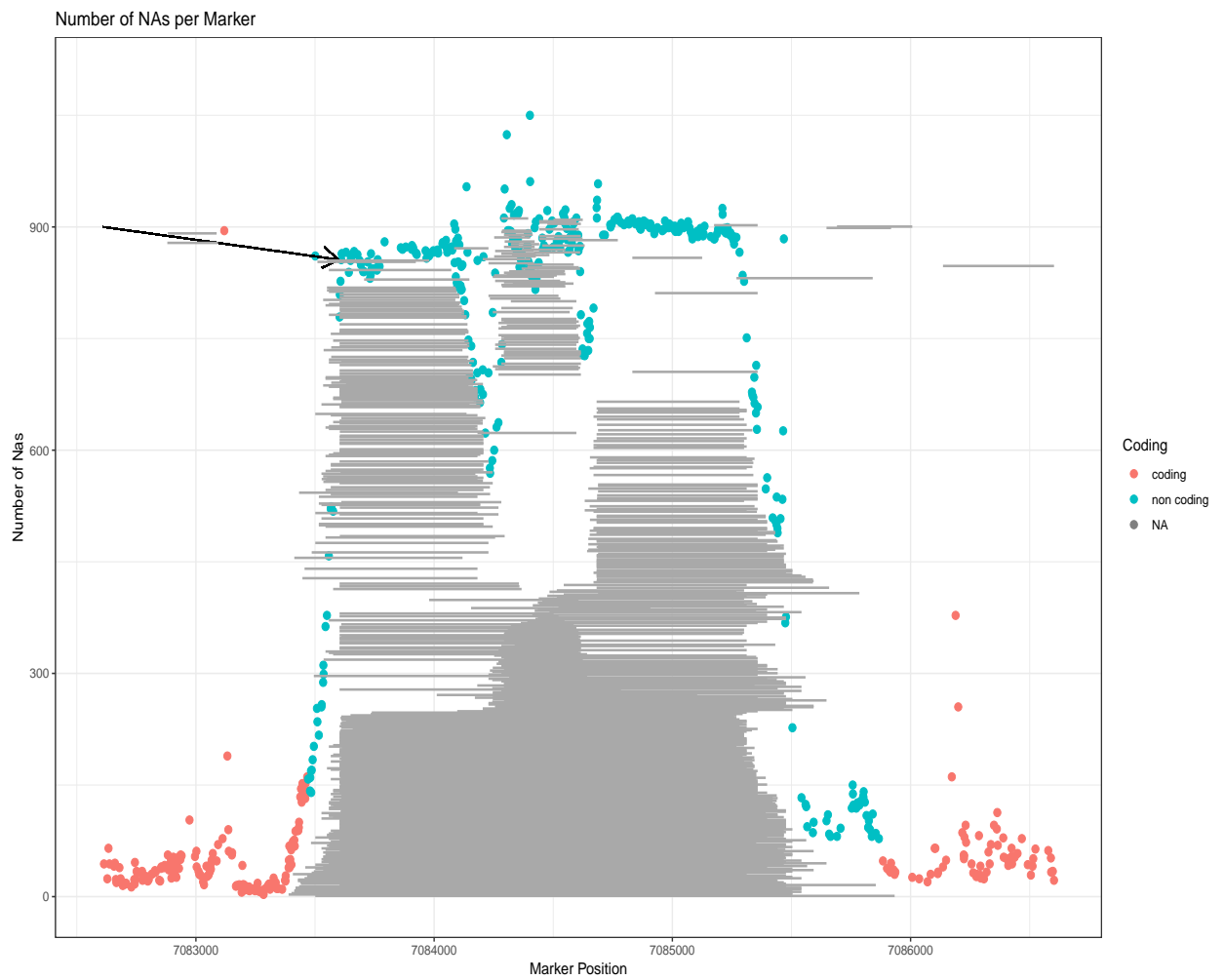


FIGURE 2.6: Number of segregating haplotypes with a polymorphism in at least one position over a stretch of 1 kBP.

3 GWAS-Flow a gpu-accelerated software for large-scale genome-wide association studies

The following chapter has been published in a similar version on the bioRxiv preprint server FREUDENTHAL et al., 2019a and has been submitted for publication to Oxford Bioinformatics. The experiments and the software were designed and conducted by the author. The manuscript has been prepared by the author, with minor corrections from Prof. Arthur Korte & Prof. Dominik Grimm. All authors approved of the final manuscript.

3.1 Introduction

Genome-wide association studies, pioneered in human genetics HIRSCHHORN and DALY, 2005 in the last decade, have become the predominant method to detect associations between phenotypes and the genetic variations present in a population. Understanding the genetic architecture of traits and mapping the underlying genomic polymorphisms is of paramount importance for successful breeding both in plants and animals, as well as for studying the genetic risk factors of diseases. Over the last decades, the cost for genotyping have been reduced dramatically. Early GWAS consisted of a few hundred individuals which have

been phenotyped and genotyped on a couple of hundreds to thousands of genomic markers. Nowadays, marker density for many species easily exceed millions of genomic polymorphisms. Albeit commonly SNPs are used for association studies, standard GWAS models are flexible to handle different genomic features as input. The *Arabidopsis* 1001 genomes project features for example 1135 sequenced *Arabidopsis thaliana* accessions with over 10 million genomic markers that segregate in the population ALONSO-BLANCO et al., 2016. Other genome projects also yielded large amounts of genomic data for a substantial amount of individuals, as exemplified in the 1000 genomes project for humans SIVA, 2008, the 2000 yeast genomes project or the 3000 rice genomes project LI, WANG, and ZEIGLER, 2014. Thus, there is an increasing demand for GWAS models that can analyze these data in a reasonable time frame. One critical step of GWAS is to determine the threshold at which an association is termed significant. Classically the conservative Bonferroni threshold is used, which accounts for the number of statistical tests that are performed, while many recent studies try to significance thresholds that are based on the false-discovery rate (FDR) STOREY and TIBSHIRANI, 2003. An alternative approach are permutation-based thresholds CHE et al., 2014. Permutation-based thresholds estimate the significance by shuffling phenotypes and genotypes before each GWAS run, thus any signal left in the data should not have a genetic cause, but might represent model mis-specifications or uneven phenotypic distributions. Typically this process is repeated hundreds to thousands of times and will lead to a distinct threshold for each phenotype analyzed TOGNINALLI et al., 2017. The computational demand of permutation-based thresholds is immense, as per analysis not one, but at least hundreds of GWAS need to be performed. Here the main limitation is the pure computational demand. Thus, faster GWAS models could easily make the estimation of permutation-based thresholds the default choice.

3.2 Methods

GWAS Model

The GWAS model used for GWAS-Flow is based on a fast approximation of the linear-mixed-model described in KANG et al., 2010; ZHANG et al., 2010, which estimates the variance components σ_g and σ_e only once in a null model that includes the genetic relationship matrix, but no distinct genetic markers. These components are thereafter used for the tests of each specific marker. Here, the underlying assumption is, that the ratio of these components stays constant, even if distinct genetic markers are included into the GWAS model. This holds true for nearly all markers and only markers which possess a big effect will alter this ratio slightly, where now σ_g would become smaller compared to the null model. Thus, the p-values calculated by the approximation might be a little higher (less significant) for strongly associated markers.

The GWAS-Flow Software

The GWAS-Flow software was designed to provide a fast and robust GWAS implementation that can easily handle large data and allows to perform permutations in a reasonable time frame. Traditional GWAS implementations that are implemented using Python VAN ROSSUM and DRAKE JR, 1995 or R R CORE TEAM, 2019 cannot always meet these demands. We tried to overcome those limitations by using TensorFlow ABADI et al., 2015, a multi-language machine learning framework published and developed by Google. GWAS calculations are composed of a series of matrix computations that can be highly parallelized, and easily integrated into the architecture provided by TensorFlow. Our implementation allows both, the classical parallelization of code on multiple processors (CPUs) and the use of graphical processing units (GPUs). GWAS-Flow is written using the Python TensorFlow API. Data import is done with *pandas* MCKINNEY, 2010 and/or *HDF5* for Python COLLETTE, 2013. Preprocessing of the data (e.g filtering by minor Allele

count (MAC)) is performed with *numpy* OLIPHANT, 2006. Variance components for residual and genomic effects are estimated with a slightly altered function based on the Python package *limix* LIPPERT et al., 2014. The GWAS model is based on the following linear mixed model that takes into account the effect of every marker with respect to the kinship:

$$Y = \beta_0 + X_i\beta_i + u + \epsilon, u \sim N(0, \sigma_g K), \epsilon \sim N(0, \sigma_e I) \quad (3.1)$$

From this LMM the residual sum of squares for marker i are calculated as described in 3.2

$$RSS_i = \sum Y - (X_i\beta_0 + I_i\beta_1) \quad (3.2)$$

The residuals are used to calculate a p-value for each marker according to an overall F-test that compares the model including a distinct genetic effect to a model without this genetic effect:

$$F = \frac{RSS_{env} - R1_{full}}{\frac{R1_{full}}{n-3}} \quad (3.3)$$

Apart from the p-values that derive from the F-distribution, GWAS-Flow also report summary statistics, such as the estimated effect size (β_i) and its standard error for each marker.

Calculation of permutation-based thresholds for GWAS

To calculate a permutation-based threshold, we essentially perform n repetitions ($n > 100$) of the GWAS on the same data with the sole difference that before each GWAS we randomize the phenotypic values. Thus any correlation between the phenotype and the genotype will be broken and indeed for over 90% of these analyses the estimated pseudo-heritability is close to zero. On the other hand, the phenotypic distribution will stay unaltered by this randomization. Hence,

any remaining signal in the GWAS has to be of a non-genetic origin and could be caused by e.g. model mis-specifications. Now we take the lowest p-value (after filtering for the desired minor allele count) for each permutation and take the 5% lowest value as the permutation-based threshold for the GWAS.

Benchmarking

For benchmarking of GWAS-Flow we used data from the *Arabidopsis* 1001 Genomes Project ALONSO-BLANCO et al., 2016. The genomic data we used were subsets between 10,000 and 100,000 markers. We chose not to include subsets that exceed 100,000 markers, because there is a linear relationship between the number of markers and the computational time demanded, as all markers are tested independently. We used phenotypic data for flowering time at ten degrees (FT10) for *A. thaliana*, published and downloaded from the AraPheno database SEREN et al., 2016. We down- and up-sampled sets to generate phenotypes for sets between 100 and 5000 accessions. For each set of phenotypes and markers we ran 10 permutations to assess the computational time needed. All analyses have been performed with a custom R script that has been used previously TOGNINALLI et al., 2017, GWAS-Flow using either a CPU or a GPU architecture and GEMMA ZHOU and STEPHENS, 2012. GEMMA is a fast and efficient implementation of the mixed model that is broadly used to perform GWAS. All calculations were run on the same machine using 16 i9 virtual CPUs. The GPU version ran on an NVIDIA Tesla P100 graphic card. Additionally to the analyses of the simulated data, we compared the times required by GEMMA and both GWAS-Flow implementations for > 200 different real datasets from *A. thaliana* that have been downloaded from the AraPheno SEREN et al., 2016 database and have been analyzed with the available fully imputed genomic dataset of ca. 10 million markers, filtered for a minor allele count greater five.

3.3 Results

The two main factors influencing the computational time for GWAS are the number of markers incorporated in such an analysis and the number of different accessions, while the latter has an approximate quadratic effect in classical GWAS implementations ZHOU and STEPHENS, 2012. Figure 3.1 shows the time demand as a function of the number of accessions used in the analysis with 10,000 markers. The quadratic increase in time demand is clearly visible for the custom R implementation, as well as for the CPU-based GWAS-Flow implementation and GEMMA. The GWAS-Flow implementation and GEMMA clearly outperforms the R implementation in general, while for a small number of accessions GWAS-Flow is slightly faster than GEMMA. For the GPU-based implementation the increase in run-time with larger sample sizes is much less pronounced. While for small ($< 1,000$ individuals) data, there is no benefit compared to running GWAS-Flow on CPUs or running GEMMA, the GPU-version clearly outperforms the other implementations if the number of accessions increases.

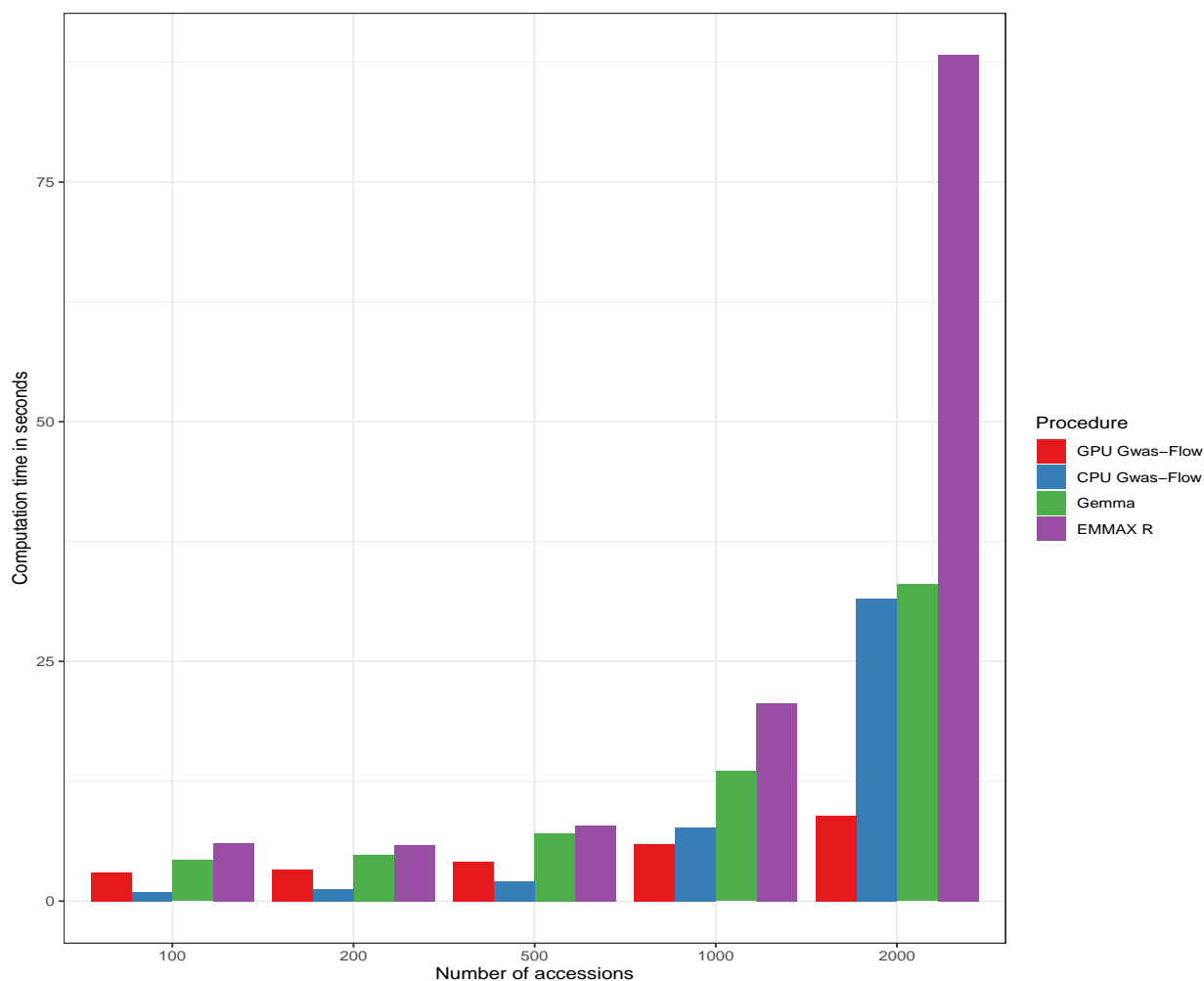


FIGURE 3.1: Computational time as a function of the number of accessions with 10000 markers each.

Figure 3.2 shows the computational time in relation to the number of markers and a fixed amount of 2000 accessions for the two different GWAS-Flow implementations. Here, a linear relationship is visible in both cases. To show the performance of GWAS-Flow not only for simulated data, we also run both implementations on more than 200 different real datasets downloaded from the AraPheno database. Figure 1C shows the computational time demands for all analyses comparing both GWAS-Flow implementation to GEMMA. Here, the CPU-based GWAS-Flow performs comparable to GEMMA, while the GPU-based implementation outperforms both, if the number of accessions is above 500. Importantly all

obtained GWAS results (p-values, beta estimates and standard errors of the beta estimates) are nearly (apart from some mathematical inaccuracies) identical between the three different implementations.

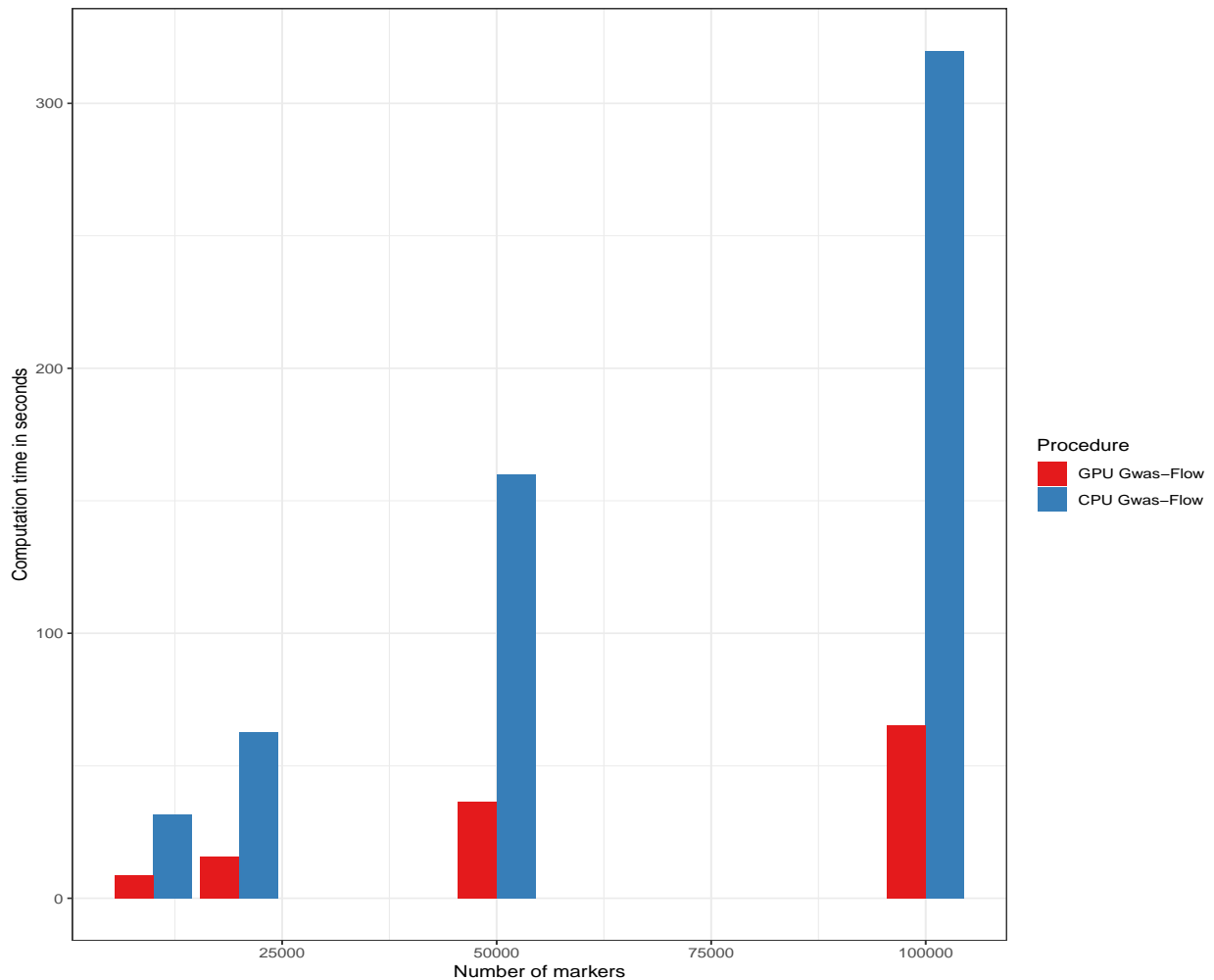


FIGURE 3.2: Computational time as a function of the number of genetic markers with constantly 2000 accessions for both GWAS-Flow versions

3.4 Discussion

We made use of recent developments of computational architecture and software to cope with the increasing computational demand in analyzing large GWAS

datasets. With GWAS-Flow we implemented both, a CPU- and a GPU-based version of the classical linear mixed model commonly used for GWAS. Both implementations outperform custom R scripts on simulated and real data. While the CPU-based version performs nearly identical compared to *GEMMA*, a commonly used GWAS implementation, the GPU-based implementation outperforms both, if the number of individuals, which have been phenotyped, increases. For analyzing big data, here the main limitation would be the RAM of the GPU, but as the individual test for each marker are independent, this can be easily overcome programmatically. The presented GWAS-Flow implementations are markedly faster compared to custom GWAS scripts and even outperform efficient fast implementations like *GEMMA* in terms of speed. This readily enables the use of permutation-based thresholds, as with GWAS-Flow hundred permutations can be performed in a reasonable time even for big data. Thus, it is possible for each analyzed phenotype to create a specific, permutation-based threshold that might present a more realistic scenario. Importantly the permutation-based threshold can be easily adjusted to different minor allele counts, generating different significance thresholds depending on the allele count. This could help to distinguish false and true associations even for rare alleles. GWAS-Flow is a versatile and fast software package. Currently GWAS-Flow is and will remain under active development to make the software more versatile. This will e.g. include the compatibility with TensorFlow v2.0.0 and enable data input formats, such as PLINK PURCELL et al., 2007. The whole framework is flexible, so it is easy to include predefined co-factors e.g. to enable multi-locus models SEGURA et al., 2012 or account for multi-variate models like the multi-trait mixed model KORTE et al., 2012. Standard GWAS are good in detecting additive effects with comparably large effect sizes, but lack the ability to detect epistatic interactions and their influence on complex traits MCKINNEY and PAJEWSKI, 2012; KORTE and FARLOW, 2013. To catch the effects of these gene-by-gene or SNP-by-SNP interactions, a variety of genome-wide association interaction studies (GWAIS) have been developed, thoroughly reviewed

in RITCHIE and VAN STEEN, 2018. Here, GWAS-Flow might provide a tool that enables to test the full pairwise interaction matrix of all SNPs. Although this might be a statistic nightmare, it now would be computationally feasible.

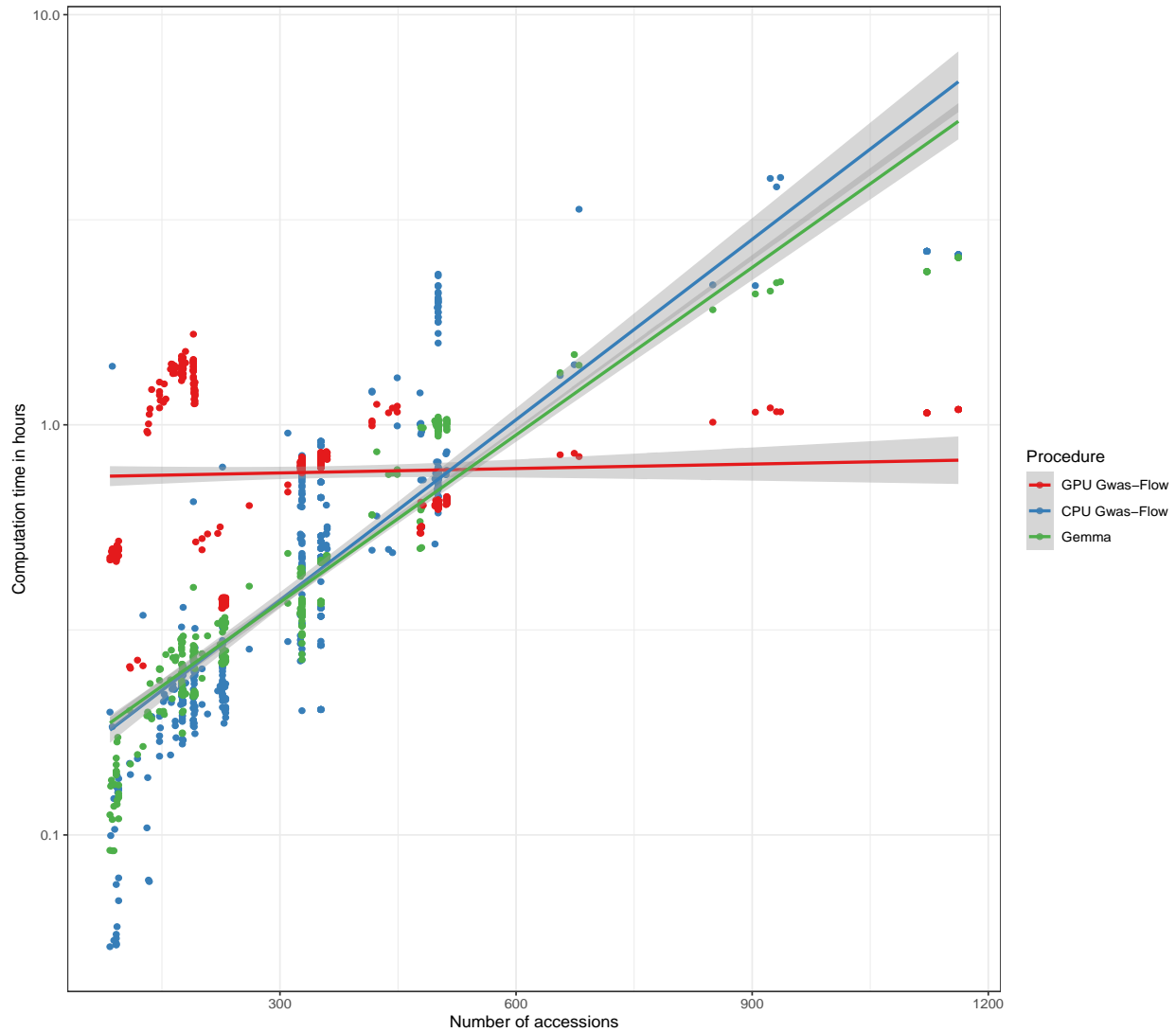


FIGURE 3.3: Comparison of the computational time for the analyses of > 200 phenotypes from *Arabidopsis thaliana* as a function of the number of accessions for GEMMA and the CPU- and GPU-based version of GWAS-Flow. GWAS was performed with a fully imputed genotype matrix containing 10.7 M markers and a minor allele filter of $MAC > 5$

4 Genomic prediction of phenotypic values of quantitative traits using artificial neural networks

4.1 Introduction to machine learning

4.1.1 A brief history of machine learning

The basic perceptron model

While machine learning, neural networks and deep learning became essential tools for many applications in more recent years, their mathematical principals date back to the early 1950s and 1960s. Figure 4.1 schematically shows the basic perceptron model as proposed by Rosenblatt, one of the founders of machine learning, as the set of related statistical algorithms would be defined today. Rosenblatt designed his perceptron to mimic the information flow in biological nervous systems ROSENBLATT, 1961.

This basic perceptron, which contrary to perceptrons used nowadays, does not have an embedded activation function, takes n binary inputs x_1, x_2, \dots, x_n and produces a single, likewise binary, output y after being processed. To achieve this Rosenblatt introduced the concept of weights, which determine a certain input's relative importance to the outcome of the output w_1, w_2, \dots, w_n . The output y is determined by the weighted sum of the weights $\sum_i w_i x_i$. If a certain threshold

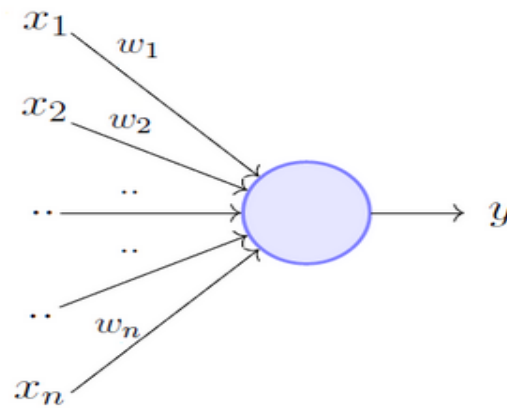


FIGURE 4.1: Basic perceptron model as proposed by Rosenblatt
ROSENBLATT, 1961

value is met the neuron is either activated and outputs 1 or not activated resulting in and output of 0. This is algebraically represented in equation 4.1:

$$0 = \text{if } \sum_i^n w_i x_i - \theta \leq 0 \quad (4.1a)$$

$$1 = \text{if } \sum_i^n w_i x_i - \theta > 0 \quad (4.1b)$$

Next to the weights w_n and the inputs x_n , a third term θ is introduced in equation 4.1, which represents the activation threshold and per definition is a negative value. A single perceptron is a linear classifier and can only be trained on linearly separable functions and can applied, as shown by ROSENBLATT, 1961, to solve simple logical operations as AND, OR and NOT. The basic perceptron fails, however, due to non-linearity to perform XOR operations, which was proven by MARVIN and SEYMOUR, 1969. This discovery led to a near stillstance in the research of artificial neural networks in the 1970s. That time period is now often referred to as the first AI-winter. Another reason that massively hindered the applications and research of machine learning during that span was the, compared to modern

times, incredibly small amount of computational power available NGUYEN and WIDROW, 1990.

More complex decision making, like solving XOR problems, requires more complex structures than a single perceptron can provide. Continuing the trend of mimicking human neural networks, multiple artificial neurons were stacked into layers and these layers were connected to each other allowing communication between the many perceptrons in such a network. Figure 4.2 schematically shows the basic structure of an artificial neural network, now harboring three types of layers.

- (i) the input layer
- (ii) one or more hidden layers
- (iii) the output layer, which in this case only consists of one only neuron

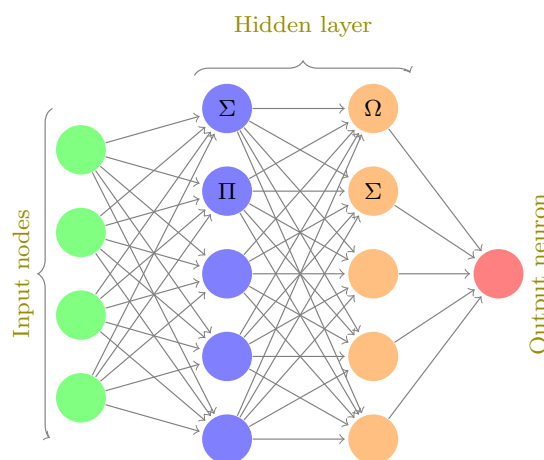


FIGURE 4.2: Schematic layout of a simple multi-layer perceptron

In the sample layout of figure 4.2 the neurons in the first column weigh the inputs and pass the gathered information to the neurons into the second layer. In the case above neurons in the first layer are connected to all neurons on the second layer. Such layers are referred to as fully-connected layers (FLC) and their resulting networks are often called multi-layer perceptrons (MLP) or fully-connected

networks. This architecture enables the network to perform more complex calculations resulting in more abstract decision making than single neurons or single layer architectures.

There are other architectures, where neurons in the previous layer are only connected with neighboring neurons in the succeeding layers. Those are known as locally-connected layers (LCL). Related to them are convolutional layers which share weights between selected neurons, building convolutional neural networks (CNN) LECUN et al., 1999.

Activation functions

The neurons discussed so far are only capable of outputting binary results, depending on whether threshold values are being reached or not. For more complex estimations it is desirable that small changes in the input also result in small changes of the output. This requirement cannot be easily met with binary outputs. Activation functions for a given node provide more sophisticated rules for the output in accordance to their inputs ŽILINSKAS, 2006.

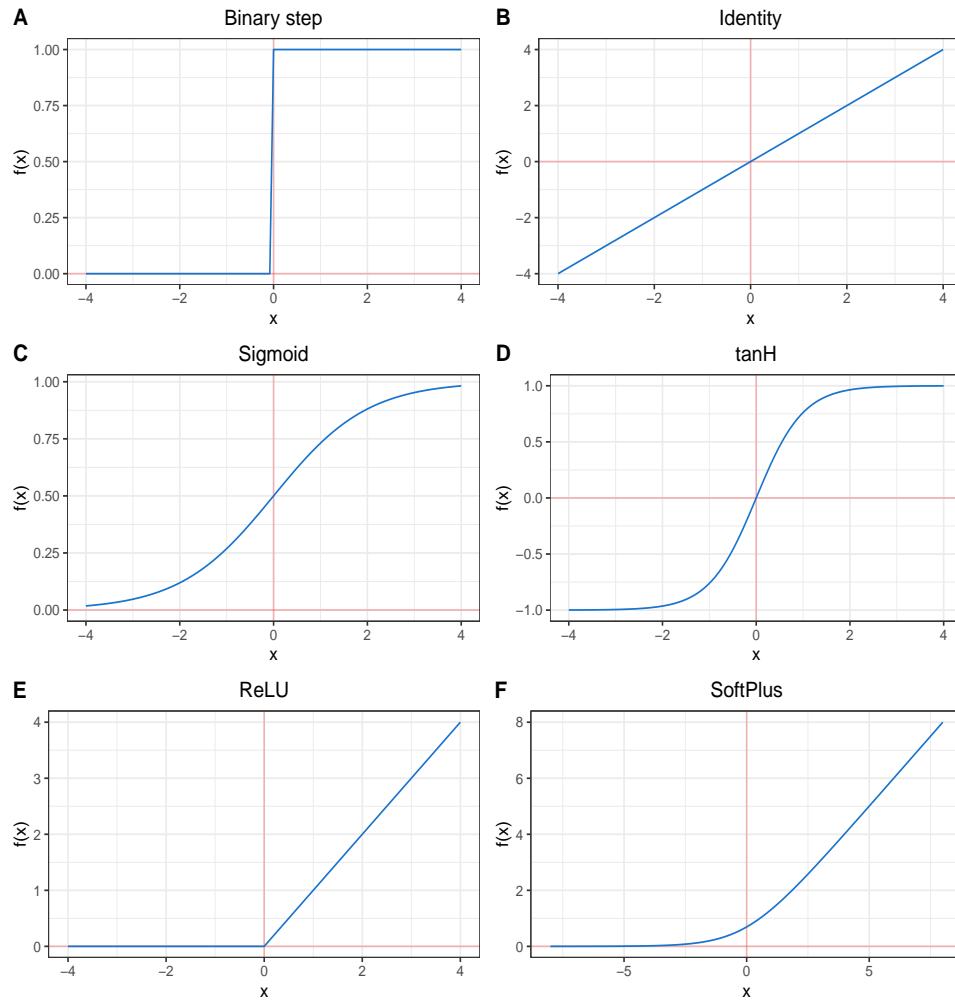


FIGURE 4.3: Popular activation functions used in neural networks.

- A** Binary step activation function
- B** Identity activation function
- C** Sigmoid or logistic activation function
- D** tangens hyperbolicus activation function
- E** rectified linear units activation function
- F** SoftPlus activation function

Figure 4.3 shows six of the most commonly used activation functions WARNER and MISRA, 1996. The simplest one, the binary step activation was already introduced (function **A** in equation 4.2), which properties have been discussed along the perceptron model. All other activation produce continuous outputs from given inputs.

Any mathematical function can serve as an activation function in neural nets, starting with a simple identity function (equation 4.3, figure 4.3 **B**). The sigmoid

function (figure 4.3 C, equation 4.4) and tanh (figure 4.3 D, equation 4.5), when $x \rightarrow \infty$ or $x \rightarrow -\infty$ have similar properties as the binary function, but produce continuous output around threshold values of 0.

$$f(x) = \sigma(x) = \begin{cases} 0 & \text{for } x < 0 \\ 1 & \text{for } x \geq 0 \end{cases} \quad (4.2)$$

$$f(x) = \sigma(x) = x \quad (4.3)$$

$$f(x) = \sigma(x) = \frac{1}{1 + e^{-x}} \quad (4.4)$$

$$f(x) = \sigma(x) = \frac{e^x - e^{-x}}{e^x + e^{-x}} \quad (4.5)$$

$$f(x) = \sigma(x) = \begin{cases} 0 & \text{for } x < 0 \\ x & \text{for } x \geq 0 \end{cases} \quad (4.6)$$

$$f(x) = \ln(1 + e^x) \quad (4.7)$$

ReLU (equation 4.6) and the softplus (equation 4.7) share similar properties as well, the latter one being a smoothed version of ReLU. Rectifiers as activation functions have been introduced in the 2000s HAHNLOSER et al., 2000 and have since then overtaken all others as the most popular activations functions in neural networks and deep learning LECUN, BENGIO, and HINTON, 2015. They have proven to be superior in many deep-learning applications over sigmoid or logistic functions. One of the advantages leading to the superiority of ReLUs is that with randomly initialized weights only half of the ReLU neurons are activated at start compared to tanh and sigmoid activation GLOT, BORDS, and BENGIO, 2011. All activation functions shown in figure 4.3, but the binary step function, share one common property: a small change of the input weight will result in

small changes of the output, while a small change of the input for the binary step function leads to either no or a complete change of the output, except for ReLU when $x < 0$. This property is, as described below, is an important prerequisite for networks being able to learn.

Gradient descent algorithm

Let a network alike the one shown in figure 4.2 be designed for the classification of an arbitrary phenotype like blue petals with $x_1 \dots x_4$ on the input layers being genetic markers as features. The output layer displays value from 0 to 1 giving the probability of the petals being blue or not. To quantify how well the network performs on predicting the color of the petals a loss function is applied SCHMID-HUBER, 2015.

There is a large variety of different loss functions available for neural networks like mean squared error (MSE), root mean squared error (RMSE) and cross-entropy among others. In generally MSE and RMSE are used for regression problems, with the latter being less popular, and cross-entropy also called log-loss is used for binary or multi-class classification settings JANOWSKI and CZARNECKI, 2017. Since all problems presented in due course are regression problems that use MSE as their loss function this will be the only loss function further elaborated upon in. MSE or the quadratic loss function can be written as:

$$MSE = \frac{1}{n} \sum_{i=1}^n (y_i - \hat{y})^2 \quad (4.8)$$

Equation 4.8 shows the MSE function which is the sum of the squares of the differences of all the predicted \hat{y} and the real values y_i . The same function can be rewritten with the previously used terminology of weights and biases in equation 4.8 with $L(w, b)$ as the loss.

$$L(w, b) = \frac{1}{2n} \sum_x \|y(x) - \hat{y}\|^2. \quad (4.9)$$

With w and b as the collection of all the weights and the biases in the network used to optimize the function $y(x)$. Giving the quadratic nature of the function $L(w, b)$ will always be positive. If $L(w, b) \rightarrow 0$ the loss is minimal, meaning that the real and predicted values are close together and the network found weights and biases that explain the output well.

A widely used function to find the optimum for such a loss function by finding its minimum is gradient descent (GD) BOTTOU, 1991. The idea behind GD or other optimizing algorithms is to start with randomly initialized weights and biases and repeatedly move them in direction Δw and Δb . This results in a change of the loss function which can be represented using partial derivatives as shown in equation 4.10.

$$\Delta L = \frac{\partial L}{\partial w} \Delta w + \frac{\partial L}{\partial b} \Delta b \quad (4.10)$$

Ideally ΔL is negative and the optimization algorithm found Δw and Δb that lead to a reduction of the loss. To simplify this problem let Δd be the vector of changes: $\Delta d = (\Delta w, \Delta b)^T$ and ∇L the vector of the partial derivatives as in equation 4.11.

$$\nabla L = \left(\frac{\partial L}{\partial w}, \frac{\partial L}{\partial b} \right)^T \quad (4.11)$$

Having defined ∇L and Δd the term 4.10 can be simplified to:

$$\Delta C = \nabla L * \Delta d \quad (4.12)$$

Now the task of gradient descent is to find Δd that results in ΔC being negative as shown in equation 4.13

$$\Delta d = -\eta \nabla L \quad (4.13)$$

Here η is a small positive decimal number, commonly referred to as the learning rate, which usually, but not exclusively, ranges from 0.1 to 0.001. Having found a way to ensure that ΔL always decreases according to equation 4.13 it can be utilized to repeatedly update the gradient ∇L over time steps T . To make the gradient descent algorithm efficient the learning rate η has to be chosen correctly. If η is too large the gradient ΔL possibly ends up being larger than zero leading to an increase of the loss. If the step size is too small convergence will either take too long or not take place at all BERGSTRÄ et al., 2011. In practical machine learning approaches different learning rates are tested. There are also algorithmic approaches available. Equation 4.10 only accounts for two inputs features but it can be generalized to compute n inputs as shown in equation 4.14.

$$\nabla L = \left(\frac{\partial L}{\partial w_1}, \dots, \frac{\partial L}{\partial w_n} \right)^T \quad (4.14)$$

Equation 4.15 shows the gradient descent how it is used to repetitively update the weights and biases to optimize the loss function $L(c, w)$ with w and b as the weight and bias matrices and the learning rate η . In machine learning each iterational update of the network is often called epoch or training epoch.

$$w = w_i - \eta \frac{\partial}{\partial w} L(w) \quad (4.15a)$$

$$b = b_i - \eta \frac{\partial}{\partial b} L(b) \quad (4.15b)$$

$$(4.15c)$$

Substituting the partial differentials with ∇L equation 4.15 simplifies to:

$$w = w_i - \eta \nabla L \quad (4.16)$$

Optimizers

The previous section introduced the concept of gradient descent, an algorithm to minimize the loss function of the weights and biases of a neural network. All other optimizers introduced in the following chapter are either variations or extensions of the basic gradient descent algorithm shown in equation 4.15.

One disadvantage of gradient descent is that if the data set grows larger the demand in memory for computation increases exponentially. Taking into consideration that machine learning is a popular method in big data applications this is a serious drawback.

Methods to solve that issue are stochastic gradient descent and mini batch gradient descent. The idea behind the latter is to randomly divide the entity of the training data into subsamples called mini batches BOTTOU and BOUSQUET, 2008. The network is then trained iteratively with all mini batches. The batch size has a significant influence on the accuracy and the training speed of the network and is a hyperparameter, which has to be tuned by iteratively testing different settings. If the batch size is one mini batch GD is also referred to as stochastic gradient descent (SGD).

During the optimization process optimizers can descent into local minima of the cost function without being able to overcome them enabling to reach the global minimum. An algorithm extending GD to accelerate the search of the global minimum is momentum, which allows the GD to speed up when the loss is decreasing and to slow down when going in the wrong direction, hence the loss function $L(w, b)$ is increasing. This is achieved by accounting for the gradient of the previous step in the calculation of the current step. This concept was introduced by POLYAK, 1964 and re-popularized alongside the introduction of backpropagation

learning by RUMELHART, HINTON, and WILLIAMS, 1988 an algorithm to efficiently update the weights and biases.

$$w = w_i - \eta \nabla L + \alpha \Delta w \quad (4.17)$$

Equation 4.17 shows how the momentum is mathematically represented in GD to update the weights w or likewise the biases. The delta of the weights multiplied by an coefficient α is the momentum. α is usually ranges from 0.1 to 0.9 and is another parameter to be tuned for successful training. If the momentum is too small the GD will not be able to overcome local minima and if α is too large the loss functions tends to oscillate without ever finding an optimum LE-CUN, BENGIO, and HINTON, 2015.

For both the momentum and the learning rate it is impractical to maintain the same level during all training epochs. After each epoch the loss function is either closer or further away from its global minima and depending on the distance to that minimum it is desirable to have larger or smaller learning rates and momenta. This can be achieved with naive approaches, for example using a step function to gradually decrease those values after each iteration, or to utilize algorithmic approaches MICHIE, SPIEGELHALTER, and TAYLOR, 1994. There is a large variety of optimizers trying to find optimal values for α and η and till today this field is under active research GOODFELLOW, BENGIO, and COURVILLE, 2016. Popular among those are: RMSprop HINTON, SRIVASTAVA, and SWERSKY, 2012; Nesterov momentum DOZAT, 2016; Adadelta ZEILER, 2012; Adagrad RUDER, 2016 and Adam KINGMA and BA, 2014. With Adam being the most popular optimizer today.

Nesterov momentum is slight change to the normal momentum algorithm, capable of having huge impacts in practical applications, because it helps avoiding oscillations around the minimum by using intermediate information to adapt the momentum.

RMSProp - root mean square propagation - is a method aiming to adapt the learning rate algorithmically, by choosing η for each iteration. Lastly the wide-spread Adam optimizer combines both of the features of momentum and RMSProp and adapts the learning rate as well as the momentum iteratively KINGMA and BA, 2014.

Regularization parameters and overfitting

A common problem in machine learning is over parameterize the model on the training data and losing the ability to generalize on validation data. This issue occurs because neural networks have hundreds of thousand of free parameters to be trained. Deeper neural networks even have billions or trillions of parameters. If training of the neural net continues for enough epochs eventually the loss function will approach a minimum. As $L(w, b) \rightarrow 0$ the initially drawn conclusion could mislead to assuming that training was successful. However, when trying to apply the trained network on the training data set (TRN) to a testing data set (TST) the loss and accuracy of the prediction of TST are very large or accordingly small. This phenomenon is known as overfitting and a lot of fine tuning of hyperparameters is devoted to minimizing this effect TETKO, LIVINGSTONE, and LUIK, 1995. Figure 4.4 visualizes this effects of during training GOODFELLOW, BENGIO, and COURVILLE, 2016 of a neural networks.

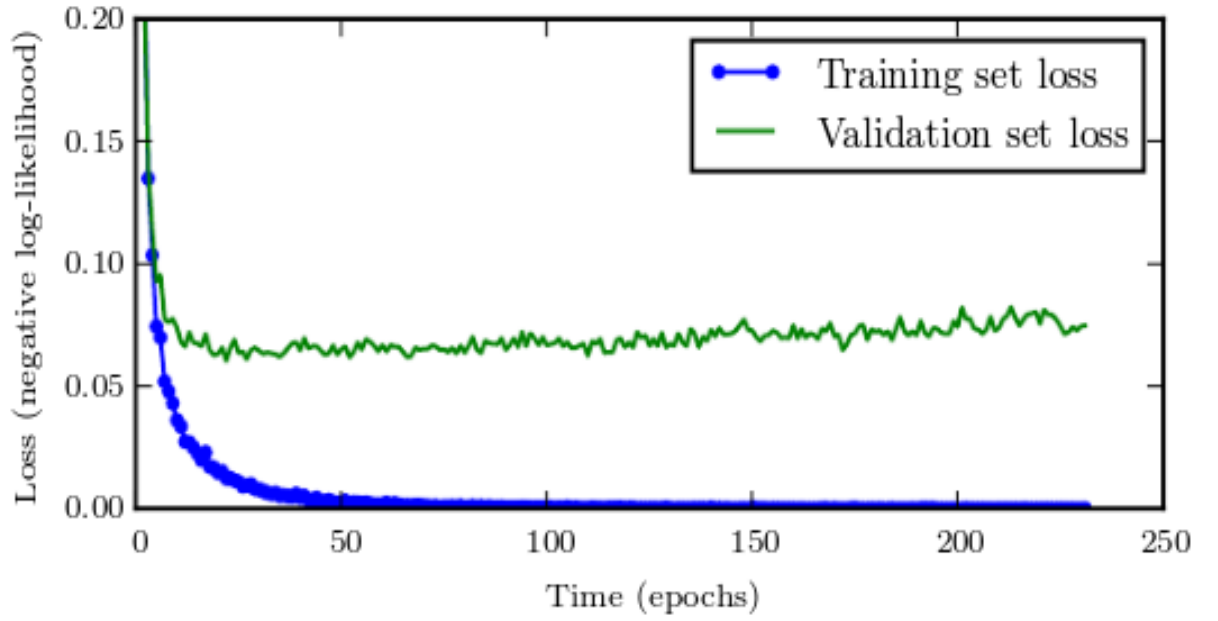


FIGURE 4.4: Learning curves showing how a loss function changes during training in the training and validation data set. While the training loss approaches 0 the validation loss starts increasing after hitting a minimum. This effect is due to overfitting on the training data set. Figure from GOODFELLOW, BENGIO, and COURVILLE, 2016.

Cross-validation

A method that is used in basically every training of neural networks is splitting up the data in multiple subsets. More specifically in a training set (TRN) and a testing set (TST). The training set is used to minimize the loss functions and its success is evaluated on the TRN set by comparison of the predicted values \hat{y} and the real values in TST y . For all neural nets in this study person's correlation coefficients were chosen as performance metric, calculated according to equation 4.18 SOPER et al., 1917.

$$\rho(y, \hat{y}) = \frac{\text{cov}(y, \hat{y})}{\sigma_y \sigma_{\hat{y}}} \quad (4.18)$$

There are other popular performance metrics, especially for classification problems, like AUC (area under the curve) and ROC (receiver operating characteristics), which evaluate the success of learning by weighing sensitivity and specificity.

In cross-validation compared to single validation the initial data set is split into TRN and TST multiple times, e.g. if the ratio is 80:20 five times, and each TRN-TST pair is evaluated individually. Sometimes it is necessary to use a third subset - the validation data set. Because hyperparameter tuning is performed with the TRN and TST sets, a third portion of the data is needed to assess whether the neural network is able to generalize on global data or not.

L1 and L2 loss

L1 and L2

Dropout

4.2 Introduction to genomic selection

4.2.1 On the nature of quantitative traits

According to the omnigenic model, which is an extension of the polygenic model, proposed by BOYLE, LI, and PRITCHARD, 2017 and thoroughly reviewed in TIMPSON et al., 2018, all traits or phenotypic values are influenced by a great number or even all genes in the genome. This therefore results in traits following gradual statistical distributions instead of being binned in classes or binary.

Intuitively this might be contradicting to the theoretical foundation of modern genetics - Mendel's three laws. They were derived from observations, which were mainly influenced by one locus. Using one of Mendel's phenotypes as an example - the round or wrinkled surfaces of peas (*Pisum sativum*)- an assessment of a couple of thousands peas would inevitably lead to the conclusion that from the

“roundest” to the “wrinkliest” pea any gradual step between those two classes is possible and observable.

Mendel’s third law of independent segregation also only holds true under certain assumptions. The most simplest one being that the traits under investigation have to be located on different linkage groups. Otherwise the seven traits used in Mendel’s initial studies would not have segregated independently. The odds of seven randomly selected traits being on seven different linkage groups are rather small, especially taking into account that the genome of the *P. sativum* consists of only 7 chromosomes itself KALO et al., 2004. Mendel most likely new about traits not following its own laws, as well as being aware of the quantitative nature of traits such as the constitution of pea’s surface or the color of its petals. However, being the pioneer of a then rather unexplored field of science, some of which big questions we fail to satisfactory answer today, he did not have the resources or the knowledge to explain traits that were not “mendeling”.

Initially thought to be contradicting to Mendel’s ideas, Darwin proposed the concept of evolution due to natural selection, which introduced the idea of traits following a gradual distributions DARWIN, 1859. This contrast led to a long lasting debate in the scientific community in the early 1900s between the Mendelians and the biometricians, who believed in the quantitative nature of continuous traits. This conflict has eventually been solved by Fisher’s fundamental work published in 1919 FISHER, 1919. His theories combined the then in all fields of science popular research on statistical distributions and genomics. He mathematically proved that traits influenced by many genes, with randomly-sampled alleles follow a continuous normal distribution in a population.

While this combined the ideas of Mendel and of the biometricians it opened an other long debated question of effect sizes and the overall genetic architecture of complex traits. While in the theory of monogenic traits the effect size of the single gene on the trait is 100 %, with an increasing number of genes influencing a complex trait the *per se* contribution of single gene has to decrease with an increasing

number of loci determining the value a given trait. Until the 1990s it has been believed that complex traits are predominantly controlled by few genes with a large to medium effect size, while others supposedly have a minimal influences ZHANG et al., 2018.

With the upcoming popularity of GWAS as the favored method to decipher genetic architectures of traits, having pioneered in human genetics, it became clear that the majority of effect sizes are tiny $< 1\%$, while there are very few loci which have a moderate effect on the phenotypic variance of a population with around 10% or less KORTE and FARLOW, 2013; STRINGER et al., 2011. This nature of quantitative traits presents great challenges to animal GODDARD and HAYES, 2009 and plant breeding WÜRSCHUM, 2012 in further improving crop or livestock performances, as well as complicating the decomposition of genomic causes for diseases like schizophrenia or autism in human medicine DE RUBEIS et al., 2014; PURCELL et al., 2014.

While the complex nature of the architecture of quantitative traits provides enough challenges as is, all traits are also influenced by the environment surrounding the individual.

Therefore the distribution of trait values in a given population can be expressed as the addition of the variances of its genetic and the environmental effects 4.19.

$$\sigma_P = \sigma_G + \sigma_E \quad (4.19)$$

The genomic and the environmental effects do not only influence the phenotypic variance directly, but the environment also has an influence on gene expression, methylation of DNA bases etc. and therefore the equation 4.19 extends by the variance of the gene-environment interactions $\sigma_{G \times E}$ to equation 4.20 LYNCH and WALSH, 1998; WALSH and LYNCH, 2018b.

$$\sigma_P = \sigma_G + \sigma_E + \sigma_{G \times E} \quad (4.20)$$

Equation 4.20 shows the decomposition of the phenotypic variance. To thoroughly understand the complex genetic architectures of traits the genetic variance needs to be decomposed further in its additive, dominance and epistatic components as in equation 4.21.

$$\sigma_G = \sigma_A + \sigma_D + \sigma_I \quad (4.21)$$

The additive effects are caused by single, for this model mostly homozygous, loci while the variance caused by dominance effects is caused by heterozygous loci with their resulting interactions being full-, over-, co- or underdominant. Lastly, the interaction effects are a result of two or more genes only having an impact if they co-occur in a certain state. The resulting variance is commonly known as the gene-gene interaction or epistasis FALCONER and MACKAY, 1996. Since possible interactions in a genome can appear between additive or dominant or a combination of those loci, the variance due to interaction effects σ_I can be further dissembled into the variances resulting from additive-additive σ_{AA} dominant-dominant σ_{DD} and additive-dominant σ_{AD} interactions as shown in equation 4.22.

$$\sigma_I = \sigma_{AxA} + \sigma_{DxD} + \sigma_{AxD} \quad (4.22)$$

Knowledge of the variance components involved in the expression of a trait in a given population leads up to the estimation of the total influence of all genetic variances and the environmental variance on the phenotypic distribution. This concept is called heritability.

The heritability of a trait H^2 accounts for the proportion of the phenotypic variance controlled by the total genetic variance as shown in equation 4.23. This is also referred to as broad sense heritability, because all genetic effects, including additive, dominance and epistatic effects, are included BROOKER, 1999.

$$H^2 = \frac{\sigma_A + \sigma_D + \sigma_I}{\sigma_P} \quad (4.23)$$

The concept of narrow-sense heritability 4.24 is similar to the broad-sense heritability, but only the additive genetic effects are included in the equation. This differentiation is important for natural and artificial selection and thus is commonly used in evolutionary genomics and breeding. Because in diploid species each parent only passes down on a single allele of a given locus, dominance effects or interaction effects are not commonly inherited from one parent. Therefore mainly the additive genetic effects of a parent influence its offspring. While the dominance and epistatic variances are controlled by the combination of the parents FALCONER and MACKAY, 1996, WALSH and LYNCH, 2018b.

$$h^2 = \frac{\sigma_A}{\sigma_P} \quad (4.24)$$

4.2.2 Artificial selection in plant and animal breeding in the genomics era

Introduction to genomic selection

Genomic prediction has been applied to almost all relevant crop and model species. This includes: *A.thaliana*; SHEN et al., 2013; HU et al., 2015. Alfalfa (*Medicago sativa*) LI and BRUMMER, 2012; ANNICCHIARICO et al., 2015; LI et al., 2015; BIAZZI et al., 2017; HAWKINS and YU, 2018.

Barley (*Hordeum vulgare*) ZHONG et al., 2009; OAKEY et al., 2016; NEYHART, LORENZ, and SMITH, 2019.

Cassava (*Manihot esculenta*) ELIAS et al., 2018a; ELIAS et al., 2018b. Cauliflower (*Brassica olearacea spp*) THORWARTH, YOUSEF, and SCHMID, 2018.

Cotton (*Gossypium spp.*) GAPARE et al., 2018.

Maize (*Zea mays*) RINCENT et al., 2012; WINDHAUSEN et al., 2012; TECHNOW, BÜRGER,

and MELCHINGER, 2013; RIEDELSHEIMER et al., 2013; GUO et al., 2013; PEIFFER et al., 2014; TECHNOW et al., 2014; LEHERMEIER et al., 2014; OWENS et al., 2014; MONTESINOS-LÓPEZ et al., 2015; BUSTOS-KORTS et al., 2016a; KADAM et al., 2016; SCHOPP et al., 2017a; SCHOPP et al., 2017b; SOUSA et al., 2017; BRAUNER et al., 2018; SCHRAG et al., 2018; MOEINIZADE et al., 2019; ALLIER et al., 2019.

Potato (*Solanum tuberosum*) ENCISO-RODRIGUEZ et al., 2018; ENDELMAN et al., 2018.

Rape seed (*Brassica naps*) SNOWDON and INIGUEZ LUY, 2012; WÜRSCHUM, ABEL, and ZHAO, 2014; QIAN, QIAN, and SNOWDON, 2014; JAN et al., 2016; LUO et al., 2017; WERNER et al., 2018.

Rice (*Oryza sativa*) XU, 2013; GRENIER et al., 2015; HASSEN et al., 2018; MOMEN et al., 2019.

Rye (*Secale cereale*) BERNAL-VASQUEZ et al., 2014; WANG et al., 2014; AUINGER et al., 2016; MARULANDA et al., 2016; BERNAL-VASQUEZ et al., 2017. Sugar beet (*Beta vulgaris*), WÜRSCHUM et al., 2013; BISCARINI et al., 2014.

Sugar cane (*Saccharum officinarum*) GOUY et al., 2013.

Soybean (*Glycine max*) JARQUIN, SPECHT, and LORENZ, 2016; XAVIER, MUIR, and RAINEY, 2016; STEWART-BROWN et al., 2019. Switchgrass (*Panicum virgatum*) RAMSTEIN et al., 2016; POUDEL et al., 2019; RAMSTEIN and CASLER, 2019.

Wheat (*Triticum aestivum*) THAVAMANIKUMAR, DOLFERUS, and THUMMA, 2015; LOPEZ-CRUZ et al., 2015; SUKUMARAN et al., 2016; BUSTOS-KORTS et al., 2016b; GIANOLA et al., 2016; CROSSA et al., 2016; RINCENT et al., 2018; NORMAN et al., 2018; BELAMKAR et al., 2018; OVENDEN et al., 2018; CUEVAS et al., 2019a; HOWARD et al., 2019; KRAUSE et al., 2019.

As well as various tree species HOLLIDAY, WANG, and AITKEN, 2012; RESENDE et al., 2012; ZAPATA-VALENZUELA et al., 2013; JARAMILLO-CORREA et al., 2014; KUMAR et al., 2015; EL-DIEN et al., 2016; RINCENT et al., 2018; RATCLIFFE et al., 2017; KAINER et al., 2018; ALMEIDA FILHO et al., 2019.

Even though GS finds broad applications in plant breeding it has been originally developed for the use in animal breeding HAYES and GODDARD, 2010; GODDARD,

HAYES, and MEUWISSEN, 2011. The gold standard is a method known as genomic BLUP VANRADEN, 2008, which utilizes a relationship matrix based on the co-occurrence of genetic markers. This method is derived from the pre-genomic era in animal breeding, where the relationship matrix was constructed after pedigrees according to the best linear unbiased predictors based on the linear mixed model equations developed by HENDERSON, 1975.

GBLUP accounts only for additive-genetic effects VANRADEN, 2008. There are other methods that are able to account for more complex genomic effects that are non-additive. Popular among those are for example Reproducing Kernel Hilbert Spaces (RKHS) GIANOLA and KAAM, 2008. Alternatively to Henderson's linear mixed models a large variety of different Bayesian methods became popular HAYES and GODDARD, 2001; GIANOLA et al., 2009; HABIER et al., 2011; GIANOLA, 2013; CROSSA et al., 2017.

Genomic prediction in recurrent selection and the breeders equation

While the quantitative genetic methods breeders utilize are complex their goals can be defined in one sentence: To genetically improve plant germplasms for agriculture. The breeding process started at the same time as farming around 10,000 BC in the region between the Euphrat and Tigris rivers known as the fertile crescent KINGSBURY, 2009. This changed the phenotypic appearance of the early crops dramatically to the point where they share little external traits with their wild ancestors. Those changes have been deeply carved into the genomes, which underwent serious alterations, including hybridization, duplications etc. This lead to most crop plants not having any wild ancestors with whom they could naturally mate. For example wheat (*Triticum aestivum*), one of the three most important sources of food on a global scale, underwent multiple hybridization steps OZKAN, LEVY, and FELDMAN, 2001. Wheat is a hybrid from either the diploid emmer (*T. diccoides*) or durum wheat (*T. durum*) and *Aegilops tauschii*, while emmer and durum are hybrids derived from wild emmer, which is a hybrid of wild grass

of the genus of *Aegilops* and *T. urata* FRIEBE et al., 2000; FELDMAN and LEVY, 2012. While being ignorant of modern genetics early “plant breeders” must have had an intuitive, yet naive, understanding of the general concept of heritability in a way that they must have comprehended that offsprings share properties with their parents, which motivated them to regrow individuals with desired traits generations after generation. This induced many changes including that artificial selected plants are commonly largely inbred. That process could be considered an early form of recurrent truncation selection. Truncation selection on a normal distributed phenotype is shown in figure 4.5.

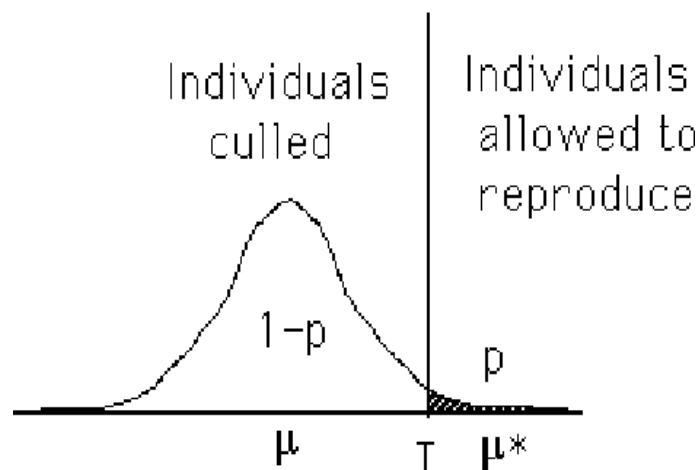


FIGURE 4.5: Truncation selection from a normal distributed phenotype with selection a threshold value of T , μ as the mean of the total population and μ^* as the mean of the selected phenotypes. Graphic from WALSH and LYNCH, 2018a

Like the early breeders modern breeders have to determine a selection threshold T to divide the total population with the mean μ into two groups: the individuals culled and the ones allowed to reproduce with the mean μ^* . The difference between those two is the selection differential S :

$$S = \mu^* - \mu \quad (4.25)$$

In the case of normal distributed data as depicted in figure 4.5 S can be expressed as:

$$S = \varphi\left(\frac{T - \mu}{\sigma}\right) \frac{\sigma}{p} \quad (4.26)$$

From which we can obtain the selection intensity i , which makes i solely a function of p .

$$i = \frac{S}{\sigma} = \frac{\varphi(z_{|1-p|})}{p} \quad (4.27)$$

With recurrent truncation selection over many generations the population mean of the trait μ will change (hopefully in the desired direction), if the heritability (in this case the narrow sense heritability) $h^2 > 0$. It is impossible to breed for traits that do not contain any genetic components in their architecture WALSH and LYNCH, 2018b.

Next to i the selection intensity and h^2 the accuracy of the selection process r_{uA} is important for the success of a breeding program. Those three terms can be applied to estimate the gain of selection R over one generation (equation 4.28). Due to its importance in the evaluation of breeding schemes it is known as the breeder's equation MOUSSEAU and ROFF, 1987; FALCONER and MACKAY, 1996; KINGSOLVER et al., 2001.

$$R = i r_{uA} \sigma_A \quad (4.28)$$

The accuracy r_{uA} of equation 4.28 in cases when only phenotypic selection is conducted is the narrow-sense heritability and in cases where the selection process is aided by genomic prediction it is the prediction accuracy. According to the breeder's equation there are three parameters, which can be influenced through genomic prediction.

- (i) The prediction accuracy, which is usually smaller than the heritability, varies for different prediction equations and an increase in the accuracy will lead to an proportional increase in R . For this reason since 2001, in quantitative genetics one very active field of research was and still is to find new, better algorithms for GS as presented in the next chapter (4.2.2. As later evaluated on more than 150 phenotypes in chapter 4.7 h^2 is always larger than r_{uA} . Which if it was the only variable factor in equation 4.28, would make genomic selection inferior to phenotypic selection, which from a certain point of view it is. Phenotypic trials are better approximations for phenotypic appearance as GEBVs. However, as the cost of genotyping has decreased dramatically in the last 20 years, phenotyping with field trials remains tedious, laborious and mostly vastly expensive. Taking into account that field trials have to be repeated in several years and locations to produce reliable accounts it becomes clear that genotyping 10th of thousands of accessions is much cheaper than conducting field trials with 1000 of them.
- (ii) The selection intensity can be much stricter if the total population that is selected from is larger. In genomic prediction settings they are, because breeders can select from two pools. First the pool of plants with known phenotypes and known genotype information and from those where just genomic data is available. When selecting from a pool of 1000 with $p = 0.05$ with the goal to keep 50 plants in the next breeding cycle, the same goal can be reached when genomically selecting from a pool of 10000 with an intensity of $p = 0.005$.
- (iii) The decrease in time per generation is probably the largest advantage of genomic selection, when applied to breeding. While in field trials it is only possible to have one generation per year, genomic selection does not require the plants to be grown in the field. For GS it is only necessary to grow the

plants large enough, that DNA can be extracted from the tissues and evaluated. After selection only the ones above the threshold are grown until they bear seeds (or other reproductive organs) and be used for the next selection cycle, allowing up to ten generations per year. This development has led to the rise to a new branch of breeding: speed breeding GHOSH et al., 2018; WATSON et al., 2018. In practical, company-level breeding, genomic prediction has largely contributed to an increase by a factor of 2 to the gain in selection in recent years (personal communication with breeding company employees).

The last term in equation 4.28, the additive genetic variance σ_A , is not directly, yet heavily influenced by the described breeding scheme. Artificial selection has similar effects on the genetic variance as bottlenecks do in natural selection have. It decreases, thus making it harder to increase R in later selection cycles WALSH and LYNCH, 2018b.

Genomic BLUP and Bayesian methods

All methods share a common statistical obstacle, which is commonly referred to as the $n \gg p$ problem, which arises because the number n of markers is usually significantly larger than the number of observations p . In practical applications it is not uncommon to have more than 100k markers while the number of phenotypes is no larger than 100. This does not allow to obtain genomic estimated breeding values (GEBV) by single marker regression as done by GWAS, which estimates highly inflated SNP-effects KORTE and FARLOW, 2013. One possibility is to include effect sizes as random effects and make prior assumptions about their distribution. The difference in prior distribution is the main distinction between the many methods of the Bayesian alphabet introduced in the following chapter GIANOLA, 2013.

Genomic BLUP

In the early years of research on genomic prediction algorithms were not solely benchmarked against each other, but had to compete with the previously popular pedigree methods. Quickly in the course of the first decade of this millennium the superiority of the genomic methods were elucidated in livestock and plant breeding HABIER, FERNANDO, and DEKKERS, 2007; VANRADEN, 2008; VANRADEN et al., 2008; HARRIS, JOHNSON, and SPELMAN, 2009. While the genomic methods are superior to non-genomic methods, there is no clear evidence that either of the genomic methods are superior to each other and there is lack of empirical evidence that the Bayesian methods generally outperform GBLUP MOSER et al., 2009 ; BERNARDO, 2010; AZODI et al., 2019.

Like pedigree BLUP for genomic BLUP the co-variance between related individuals is used for the predictions. In the latter case it is calculated from marker information.¹

The general genomic prediction model (equation 4.29) is derived from mixed models HENDERSON, 1975; VANRADEN, 2008 and implemented as:

$$Y = X\beta + Zu + \varepsilon \quad (4.29)$$

where Y is and $n \times 1$ vector of phenotypic observations, X the matrix of the fixed effects and β the vector of the fixed effects. Z is the incidence matrix for the combined marker effects and u is a $n \times 1$ vector of the additive genetic effect the vector of the residuals ε .

To construct a GBLUP model let's assume a matrix of size $(n \times m)$ with n individuals and m loci M containing marker information for three individuals on four loci, thus being of size 3×4 . The four markers of matrix 4.30 can take values of

¹In the GWAS terminology the relationship matrix is referred to as K for kinship, while in GS circumstances it is called GRM (genomic relationship matrix) or abbreviated as G . This study will remain consistent with the circumstantial literature and therefore purposely inconsistent within itself. In the chapter addressing GWAS it will be called K for kinship matrix and in the following chapter elucidating GBLUP it will be referred to as G .

−1, 0 and 1, translating into minor allele, heterozygous locus and major allele. ²

$$M = \begin{pmatrix} -1 & 0 & 1 & -1 \\ -1 & 0 & 0 & 0 \\ 0 & 1 & 1 & -1 \end{pmatrix} \quad (4.30)$$

The M matrix contains all the information that are necessary for the computation of the K matrix and other viable genetic parameters. The MM' matrix of size $n \times n$ (4.31) bears additional parameters.

$$MM' = \begin{pmatrix} 3 & 1 & 2 \\ -1 & 1 & 0 \\ 2 & 0 & 3 \end{pmatrix} \quad (4.31)$$

The diagonal shows the number of homozygous loci per individual, while the other elements of the matrix indicate the number of markers shared by related individuals. This is an indicator for the distance of the relationship between individuals, as defined by identity-by-descent VANRADEN, 2008; MISZTAL et al., 2013. While matrix 4.31 calculates the metrics per individual, the $M'M$ matrix (4.32) accounts for metrics per marker. Likewise the diagonal contains the number of homozygous individuals per marker.

$$M'M = \begin{pmatrix} 3 & -1 & 0 & 0 \\ -1 & 1 & 1 & 1 \\ 0 & 1 & 2 & 1 \\ 0 & 1 & 1 & 2 \end{pmatrix} \quad (4.32)$$

The next step is to obtain a matrix of the allele frequencies at each locus also of size $n \times m$ like matrix M . For the design of matrix P (4.33) let the minor allele frequencies $p_1 \dots p_4$ be $\{0.3, 0.2, 0.1, 0.15\}$. The allele frequency of the i^{th} column

²This example calculation has been adapted from ISIK, 2013.

of P is expressed according to the n^{th} marker of matrix M as $P_i = 2(p_i - 0.5)$ resulting in:

$$P = \begin{pmatrix} -0.4 & -0.6 & -0.8 & -0.7 \\ -0.4 & -0.6 & -0.8 & -0.7 \\ -0.4 & -0.6 & -0.8 & -0.7 \end{pmatrix} \quad (4.33)$$

The allele frequencies, as in this simulated example, should be drawn from the entire population and not only the subsample used for the calculation VANRADEN, 2008. The final step to obtain the Z matrix for the us in equation 4.29 is to subtract the P matrix from the M matrix $Z = M - P$ resulting in:

$$Z = \begin{pmatrix} 1.4 & 0.6 & 1.8 & -0.3 \\ -0.6 & 0.6 & 0.8 & 0.7 \\ 0.4 & 1.6 & 1.8 & -0.3 \end{pmatrix} \quad (4.34)$$

In Z the mean values of the allele effects are set to 0 and the subtraction of P emphasizes the effect of rare variants VANRADEN, 2008. There is a large variety of methods to generate the genomic relationship matrices and here lies the major difference between different genomic BLUP methods, but K is always of size $n \times n$.

- (i) The naive approach is to iterate over each individual and count the common markers with every other individual. This approach is suited for inbred or doubled-haploid populations, less so for outcrossed populations with high degrees of heterozygosity, because as in the sample implementation it does only account for homozygous loci. This method becomes computationally intense when the data sets grow larger as common today (personal observation).

- (ii) Probably the most popular method in GS is to obtain K as proposed by VAN-RADEN, 2008 designed after Wright's WRIGHT, 1922 equations for the covariance in structured populations, as described by equation 4.35 with Z as in 4.34.

$$G = \frac{ZZ'}{2\sum p_i(1 - p_i)} \quad (4.35)$$

- (iii) The unified additive relationship G_{UAR} according to YANG et al., 2010 and equation 4.36

$$G_{UAR} = A_{jk} = \frac{1}{N} \sum_i A_{ijk} = \begin{cases} \frac{1}{N} \sum_i \frac{(x_{ij} - 2p_i)(x_{ik} - 2p_i)}{2p_i(1 - p_i)}, j \neq k \\ 1 + \frac{1}{N} \sum_i \frac{x_{ij}^2(1 + 2p_i)x_{ij} + 2p_i^2}{2p_i(1 - p_i)}, j = k \end{cases} \quad (4.36)$$

where p_i is the allele frequency at locus i and x_{ij} the genotype for the j^{th} individual at the i^{th} locus. Another method also proposed by YANG et al., 2010 is to adjust G_{UAR} with β as in equation 4.37

$$G_{UARadj} = \begin{cases} \beta A_{jk}, j \neq k \\ 1 + \beta(A_{jk} - 1), j = k \end{cases} \quad (4.37)$$

- (iv) Another approach is to weigh marker by the reciprocals of their expected variance according to the model 4.38. This was originally designed to investigate population structures in human genomics LEUTENEGGER et al., 2003; AMIN, VAN DUIJN, and AULCHENKO, 2007.

$$G = ZDZ', \text{ with} \quad (4.38)$$

$$D_{ii} = \frac{1}{m|2p_i(1 - p_i)|}$$

- (v) Other methods like the gaussian kernel compute kinship between individuals by the euclidean distance between the respective genotypes MOROTA and GIANOLA, 2014.

$$\begin{aligned} K(x_i, x_j) &= \exp(-\theta d_{ij}^2) \\ &= \prod_{k=1}^m \exp(-\theta (x_{ik} - x_{jk})^2) \end{aligned} \quad (4.39)$$

with $d_{ij} = \sqrt{(x_{i1} - x_{j1})^2 + \dots + (x_{ik} - x_{jk})^2 + \dots + (x_{im} - x_{ja})^2}$ and x_{ik} ($i, j = 1, \dots, n, k = 1, \dots, m$) and x_{ik} as the i^{th} individual at SNP k .

The linear model of equation 4.29 $Y = X\beta + Zu + \varepsilon$, with β as the vector fixed effects and u as the vector of additive genetic effects, can be solved to obtain genomic estimated breeding values as:

$$\begin{pmatrix} X'X & X'Z & 0 \\ Z'X & Z'Z + G^{11} & G^{12} \\ 0 & G^{21} & G^{22} \end{pmatrix} \begin{pmatrix} \hat{b} \\ \hat{y}_1 \\ \hat{y}_2 \end{pmatrix} = \begin{pmatrix} X'y \\ Z'y \\ 0 \end{pmatrix} \quad (4.40)$$

with G^{12} as the part of G^{-1} containing individuals with phenotypic data and with G^{22} as the part of G^{-1} containing individuals without phenotypic data and just marker information available.

This can be algebraically solved to compute the GEBV of the unknown phenotypes \hat{y}_2 as:

$$\hat{y}_2 = - \left(G^{22} \right)^{-1} G^{21} \hat{y}_1 \quad (4.41)$$

GBLUP is fairly easy compared to more complex Bayesian methods and can be quickly implemented in any programming language capable of solving liner equations like R or Python R CORE TEAM, 2018; VAN ROSSUM and DRAKE JR, 1995. Computational as the number of phenotypes in the study increases in numbers

the timed demand grows exponentially, because the kinship matrix quadruples in size and it becomes more complicated to compute the inverse of G (personal observations).

Bayesian methods

Next to the universal GBLUP a set of related algorithms became popular for solving the mixed models involved in genomic selection, known as the Bayesian alphabet GIANOLA et al., 2009; GIANOLA, 2013. They are all based on Bayes' fundamental theorem (equation 4.42).

$$P(\theta|y) = \frac{P(\theta)P(y|\theta)}{P(y)} \quad (4.42)$$

with $P(\theta)$ as the prior distribution, $P(y|\theta)$ as the likelihood and $P(y)$ as the marginal density of y . The prior distribution in GS assume that y was drawn from a certain distribution. Infinitesimal models assume that the genetic effects follow a normal distribution LEGARRA, LOURENCO, and VITEZICA, 2018, while the Bayesian frameworks, however, will assume non-normal distributed marker effects. This can be explained by a two-step hierarchical distribution. Stage one assumes that every marker has *a priori* a different variance LEGARRA, LOURENCO, and VITEZICA, 2018.

$$p(a_i|\sigma_{ai}^2) = N(0, \sigma_{ai}^1) \quad (4.43)$$

The second stage assumes prior distributions for the variances.

$$p(a_i|variable) = P(\dots) \quad (4.44)$$

with *variable* standing for the large variety of prior distributions. In total there are more than >20 different Bayesian models known to the author. Their main

difference “simply” lies in the *a priori* assumptions of prior distributions. This change can make some methods mathematically much more complicated than others. As shown in later chapters none of the methods is completely superior over others in terms of prediction accuracy.

Approximation to the solution of the linear equations is usually performed by Gibb’s sampling using Markov Chain Monte Carlo (MCMC) simulations DE LOS CAMPOS et al., 2009; CAMPOS and RODRIGUEZ, 2016. Table 4.1 summarizes commonly applied Bayesian methods for genomic prediction indicating their key differences.

TABLE 4.1: Overview of properties of a variety of commonly applied Bayesian methods for genomic prediction. Table altered after KÄRKKÄINEN and SILLANPÄÄ, 2012

Name	Reference	Prior	Indicator	Hierarchy	Hyperprior	Estimation
BayesA	HAYES and GODDARD, 2001	Student	No	Yes	No	MCMC
BayesB	HAYES and GODDARD, 2001	Student	Yes	Yes	No	MCMC
BayesC	VERBYLA et al., 2009	Student	Yes	Yes	No	MCMC
BL	XU, 2010	Laplace	No	Yes	No	EM
BayesD π	HABIER et al., 2011	Student	Yes	Yes	Yes	MCMC

The name is given by the author. The prior column tells which shrinkage prior is used.

4.2.3 Genomic selection using artificial neural networks

As mentioned in 4.2.2 genomic selection (GS) has been successfully applied in animal HAYES and GODDARD, 2010; GIANOLA and ROSA, 2015 and plant breeding CROSSA et al., 2010; HEFFNER et al., 2010; DESTA and ORTIZ, 2014; CROSSA et al., 2017 as well as in medical applications since it was first reported HAYES and GODDARD, 2001. Since then the repertoire of methods for predicting phenotypic values has increased rapidly e.g. DE LOS CAMPOS et al., 2009; HABIER et al., 2011; GIANOLA, 2013; CROSSA et al., 2017. Genomic prediction has repeatedly been proven to outperform pedigree-based methods CROSSA et al., 2010; ALBRECHT et al., 2011 and

is nowadays used in many plant and animal breeding schemes. It has also been shown that using whole-genome information is superior to using only feature-selected markers with known QTLs for a given trait BERNARDO and YU, 2007; HEFFNER, JANNINK, and SORRELLS, 2011 in most cases. A more recent study AZODI et al., 2019 compared 11 different genomic prediction algorithms with a variety of data sets and found contradicting results, indicating that feature selection can be useful for some cases when whole genome regression is performed by neural nets.

While every new method is a valuable addition to the toolbox of genomic selection, some fundamental problems remain unsolved and are the same for every algorithm, of which the $n \gg p$ problematic stands out. Usually in genomic selection settings the size of the training population (TRN) with n phenotypes is substantially smaller than the number of markers p FAN, HAN, and LIU, 2014, making the number of trainable features immensely large. Furthermore every marker is treated as an independent observation neglecting collinearity and linkage disequilibrium (LD) between them. More difficulties arise through non-additive, epistatic and dominance marker effects. The main issue with epistasis in quantitative genetics is the almost infinite amount of different marker combinations, which cannot be represented within the size of TRN in the thousands. The same problems arise in GWA studies KORTE and FARLOW, 2013. With already large p the number of possible additive SNP-SNP interactions potentiates to $p^{(p-1)}$. Methods that attempt to overcome those issues are EG-BLUP, which uses an enhanced epistatic kinship matrix and reproducing kernel Hilbert space regression (RKHS) JIANG and REIF, 2015; MARTINI et al., 2017.

In the past 10 years, due to increasing availability of high performance computational hardware with decreasing costs and parallel development of free easy-to-use software, most prominent being googles library TensorFlow ABADI et al., 2016 and Keras CHOLLET, 2015, machine learning (ML) has experienced a renaissance. ML is a set of methods and algorithms used widely for regression and

classification problems. Popular among those are e.g. support vector machines, multi-layer perceptrons (MLP) and convolutional neural networks. ML has been widely applied in many biological fields MIN, LEE, and YOON, 2017; LAN et al., 2018; MAMOSHINA et al., 2016; ANGERMUELLER et al., 2016; WEBB, 2018; RAMPASEK and GOLDENBERG, 2016.

A variety of studies assessed the usability of ML in genomic prediction GONZÁLEZ-CAMACHO et al., 2018; GONZÁLEZ-CAMACHO et al., 2016; OGUTU, PIEPHO, and SCHULZ-STREECK, 2011; MONTESINOS-LÓPEZ et al., 2019a; GRINBERG, ORHOBOR, and KING, 2018; CUEVAS et al., 2019b; MONTESINOS-LÓPEZ et al., 2019b; MA et al., 2017; QIU et al., 2016; GONZÁLEZ-CAMACHO et al., 2012; LI et al., 2018. Through all those studies the common denominator is that there is no such thing as a gold standard for genomic prediction. No single algorithm was able to outperform all the others tested in a single of those studies, let alone in all. While the general aptitude of ML for genomic selection has been repeatedly proven, there is no evidence exists that neural networks can generally outperform mixed-model approaches as GBLUP HAYES and GODDARD, 2001.

In other fields like image classification neural networks have up to 100s of hidden layers HE et al., 2016. The commonly used fully-connected networks in genomic prediction tend to have one to three hidden layers. With one layer networks often being the most successful among those. Contradicting to the idea behind machine learning in genomic selection one hidden layer networks will be inapt to capture interactions between loci and thus only account for additive effects. As shown in AZODI et al., 2019 convolutional networks perform worse than fully-connected networks in genomic selection, which again is contradicting to other fields where convolutional layers are applied successfully, e.g natural language processing DOS SANTOS and GATTI, 2014 or medical image analysis LITJENS et al., 2017. Instead of using convolutional layers and fully-connected layers only, as shown in Pook et al 2019, we also propose to use locally-connected layer in combination with fully-connected layers. While CL and LCL are closely related they

have a significant difference. In CL weights are shared between neurons and in LCLs each neuron as its own weight. This leads to a reduced number of parameters to be trained in the following FCLs and should therefore theoretically lead to a decrease in overfitting. To evaluate the usefulness of machine learning in GS the data sets generated in the scope of the 1001 genome project of *A. thaliana* ALONSO-BLANCO et al., 2016 and the MAZE project were used.

4.3 Proof of concept for ANN-based genomic selection

Having established the quantitative architecture of traits in section 4.2.1 and the basics of machine learning and neural nets in section 4.1.1, that knowledge can be used to provide a proof of concept that neural networks are a candidate for GP. Table 4.2 provides all the possible genotypes $G_1 \dots G_4$ that can be derived by two bi-allelic markers M_1, M_2 on a fictional haploid organism. In this simulation the effect sizes for each marker β_1 and β_2 are constant with a value of 1.

TABLE 4.2: Simple simulated phenotypes and genotypes for genomic prediction with genotypes $G_1 \dots G_4$, Markers M_1 and M_2 and phenotypes based on additive effects or *and*, *or*, *xor* logic gates.

	M_1	M_2	Y_{ADD}	Y_{AND}	Y_{OR}	Y_{XOR}
G_1	0	0	0	0	0	0
G_2	0	1	1	0	1	1
G_3	1	0	1	0	1	1
G_4	1	1	2	1	1	0

The four phenotypes Y_{ADD} , Y_{AND} , Y_{OR} and Y_{XOR} , which were derived from their respective marker effects, were used for GP. Y_{ADD} is a phenotype with purely additive effects. So in the nomenclature introduced in chapter 4.2.1 $\sigma_A = \sigma_G$ and $\sigma_I = 0$. Since the hypothetical organism is haploid there are no dominance

effects to be accounted for $\sigma_D = 0$ and since all the genetic effects are caused by additive effects and there are also no environmental effects σ_E . The narrow sense heritability h^2 - equation 4.24 - and the broad sense heritability H^2 - equation 4.23 - are equally 1. The other three phenotypes are base on epistatic effects σ_I , generated by passing the markers M_1 and M_2 through their respective logic gates. This theoretically results in $h^2 = 0$ and $H^2 = 1$ because there should be no additive effects. For y_{AND} , however, $h \approx 0.5$ because there is a correlation between Y_{ADD} and Y_{AND} . In practical applications this allows methods like GBLUP, designed to account for additive genetic effects, to capture some of the epistatic effects of σ_I VIEIRA et al., 2017.

According to chapter 4.1.1 a single perceptron fails to solve *xor* gates. While a network with multiple nodes and layers should be able to overcome that deficit. A relatively simple neural network with two fully-connected hidden layers with 10 and 5 nodes was trained for the prediction of the phenotypes. To keep the simulation as simple possible, no regularization parameters like dropout etc. were included. The activation function was ReLU (4.6) with an Adam optimizer. The results of the prediction are shown in table 4.3.

TABLE 4.3: Results of genomic prediction from phenotypes and genotypes in table 4.2

	M_1	M_2	\hat{Y}_{ADD}	\hat{Y}_{AND}	\hat{Y}_{OR}	\hat{Y}_{XOR}
G_1	0	0	0.01	0.00	0.00	0.01
G_2	0	1	0.99	0.01	0.99	0.98
G_3	1	0	0.99	0.00	0.99	1.01
G_4	1	1	1.99	0.98	1.01	0.02

Not surprisingly, the simple network is able to solve all four problems and predict the phenotypes accurately. The task was rather easy because the training data set and the testing data set were the same, but it served the purpose of showing that neural networks are generally apt to solve different marker interactions.

In natura those interactions and the overall genetic architecture are much more complex, of course. Effect sizes are not constant and epistasis may be caused by interactions with more than just two markers. With an increasing number of markers n the number of possible two way interactions increases even more to $2^n - 1$. Smaller interaction effects could be obscured under larger additive effects. Gene-environment interactions might have a significant influence resulting in a model that does not converge.

4.4 Material

Two different data sets were used for the genomic prediction trials. A set of doubled-haploid (DH) populations derived from maize landraces and *A. thaliana* data sets with genomic data procured along the 1001 genomic project ALONSO-BLANCO et al., 2016 and various phenotypic trials SEREN et al., 2016.

4.4.1 DH populations derived from maize landraces

The DH populations were produced, propagated and phenotyped in the scope of the MAZE project phase I, funded by the Federal Ministry of Education and Research (BMBF) (Funding ID: 031B0195, project “MAZE”) as well as the KWS SAAT SE, by various project partners at the Technical University of Munich, University of Hohenheim and the KWS. A thorough description of the germplasm selection and phenotyping was recently published by HÖLKER et al., 2019.

Modern maize cultivars are almost exclusively high-performing hybrids from two inbreed lines originating from different heterotic pools. Commonly hybrids are derived from a cross of European Flint and American Dent maize SANTOS DIAS et al., 2004; BRAUNER et al., 2019. Before hybrid breeding became the predominant method in maize breeding in the 1960s, landraces were grown by farmers. Landraces are dynamic, open-pollinated, locally highly-adapted populations. They did not derive from modern breeding, but from locally confined

selection and adaption by farmers to often very specific needs ARTEAGA et al., 2016. The hybrids grown today are derived from just a few landraces as founder lines, while the majority of landraces has been nearly forgotten. This and high intensity selection over many generation has led to a loss of genetic diversity σ_G in modern maize cultivars.

The landrace germplasm present an important and essential stock of genetic variability for continuous success in maize breeding. The utilization of those germplasms would be impossible without the invaluable work of institutions like the IPK Gatersleben, whose goal as genebanks is to maintain and store genetic material for long time periods. From European three landraces representing large phenotypic and genetic heterogeneity were chosen to be assessed in the scope of the MAZE project:

- (i) Kemater Landmais Gelb (KE, Austria)
- (ii) Petkuser Ferdinand Rot (PE, Germany)
- (iii) Lalin (LL, Spain).

They represent 95% of the molecular variance in a set of 35 landraces analyzed in a preceding project by MAYER et al., 2017.

In total 1015 DH lines (516 KE, 432 PE, 67 LL) were produced with *in vivo* haploid induction with an inducer line as described in ROEBER, GORDILLO, and GEIGER, 2005.

Genomic maize data

The genomic maize data was provided by the TUM as described by HÖLKER et al., 2019.

Genotyping was performed with the 600k Affymetrix® Axiom® Maize array UNTERSEER et al., 2014. The markers were quality filtered and missing values were imputed individually for each landrace population using Beagle 5.0 BROWNING

and BROWNING, 2007; BROWNING, ZHOU, and BROWNING, 2018. After LD pruning and further quality control 29833 markers remained for 471 Kemater and 403 PE DHs. LL was excluded from further analyses due to insufficient amounts of genotypes.

Phenotypic maze data

The phenotype data was provided by the TUM as described by HÖLKER et al., 2019.

The traits were evaluated with lattice design in 6 different locations across Europe. Those traits were:

- (i) early Vigor (EV) at three different stages (V3, V4, V6)
- (ii) plant height (PH) at two developing stages (V4,V6)
- (iii) the final plant height (PH_final)
- (iv) male flowering time: days till tasseling (DtTAS)
- (v) female flowering time: days till silking (DtSILK))
- (vi) root lodging (RL)

To account for GxE best linear unbiased estimators were calculated according to Henderson's model HENDERSON, 1975 and used for further prediction. Once the BLUEs were calculated across all environments and once they were calculated for the DHs in the six environments individually.

Single environment prediction

Next to the across environment BLUEs used for prediction the single environment BLUEs were used for prediction to able to gain insights of the structure of $\sigma_{G \times E}$ of the maize traits. This resulted in 2246 genotype x environment combinations for Kemater and 1975 for Petkuser with at least one data point. This

number is lower than the maximum number of n DHs per populations times the 6 environments, because naturally not all genotypes yielded reliable data in the environments. Each DH \times environment was treated as an individual in for the across environment prediction. The marker matrix was enhanced with the environmental origin as cofactors as show in table 4.4 with one-hot encoded markers.

TABLE 4.4: Schematic representation of the enhanced genotype matrix for across environment prediction of maize phenotypes with DHs 1-2 with markers M 1-2 in environments E1-2

	M-1	M-2	E-1	E-2
DH1-E1	0	1	1	0
DH2-E1	1	0	1	0
DH1-E2	0	1	0	1
DH2-E2	1	0	0	1

4.4.2 A. thaliana

Genomic data

The genomic data was generated during the course of the 1001 genome project of *A. thaliana* ALONSO-BLANCO et al., 2016 producing completed sequenced and assembled genomes from 1035 genomes, along 600k marker data for 1307 accessions with a small overlap between those groups resulting in a total of 2029 genotyped accessions. With more than 10 mio. SNPs and Indels on the 5 chromosomes of e *A. thaliana*. Imputation of missing data and upsampling of the 600k subsets was performed with Beagle3 BROWNING and BROWNING, 2007. For every one of the 164 phenotypes used for prediction subsets were sampled, LD pruned and MAF filtered. LD pruning was executed with the R-package SNPRelate ZHENG, 2013 with a relatively strict LD threshold of 0.65 and $MAF > 10$. This resulted in data sets with approximately 150.000 markers for each phenotype.

Phenotypic data

A complete list of the phenotypes used can be found in Appendix B with the according study references. The phenotypic trials ranged from 100 to more than 1000 accessions per data set ATWELL et al., 2010; LI et al., 2010; STRAUCH et al., 2015; MEIJÓ et al., 2014.

4.5 Methods

The theoretical backgrounds of the methods used for genomic prediction were described in section 4.1.1 for the ANNs and section 4.2.2 for the Bayesian methods and GBLUP. The next sections are devoted to explaining who those methods were adapted and implemented for the prediction of maize and *Arabidopsis* traits.

4.5.1 Validation scheme

The validation approach in this study was a little different than common 5 fold cross validation. All predictions were run 50 times with different splits of TST and TRN. For the full data set randomly 20% were assigned to TST and 80% to TRN. This process was repeated 50 times, reducing the chance of biases due to any TST-TRN combination being randomly more predictable for one or the other method. The validation scheme was generated *a priori* and stored in cross-validation files to allow reusing the validation sets.

4.5.2 ANN

The scripts for ANN based GS were written in python using the lower level API TensorFlow ABADI et al., 2016 and the higher level API Keras CHOLLET, 2015. Both are very versatile, well-documented and are capable of performing a large variety of machine learning applications. For those reasons they are the most used ML libraries. Another advantage is that they work well on GPUs, which allows

ML algorithms to run a reasonable amount of time compared to CPU-based calculations. Prior to training the data was split into TRN and TST. The markers of TRN served as the input layer for the network while the phenotypes were trained upon in the output layer, which in the present cases consisted of only one node, because GS in the cases applied here is a regression problem. Preliminary trials showed Adam is the superior optimizer for GS and hence was the only one further used. Likewise relu was the activation of choice being superior to sigmoid or other non rectifiers. All the weights and the biases of the kernel were initialized with truncated normal distributed values. The loss function used was always MSE.

Having a few hyperparameters fixed, the other ones were optimized via grid search. For each TRN multiple networks were trained to fine tune the input parameters. Those were the number of layers, the nodes per layer, the magnitude of the dropout, the type of dropout used, whether the first layer was locally-connected for fully-connected and the duration of training via the training epochs. This amount to a total of a little shy of 260000 trained networks for the 146 *A. thaliana* data sets alone.

After another set preliminary runs LCL as the first layer seemed to result in higher accuracies then FLC as the first layer and where henceforth exclusively used and applied with a stride length of 7. The stride length determines how many node of the input layer, in this case markers, where combined in the first hidden layer. The type of drop out used (alpha dropout, Gaussian noise or normal dropout) did not show an effect therefore the normal dropout function was used. The network training was iterated over the different number epochs, architecture, drop out values the the cross validation cycles, thus explaining the tremendous amount of total networks trained. Epochs from 5 to 60 in steps 5 and several 1, 2 or 3 Layer architectures following the locally-connected layer.

4.5.3 GBLUP

The evaluation of the genomic BLUP was performed with the R-package BGLR CAMPOS and RODRIGUEZ, 2016. To allow pairwise comparison of the individual validation runs the same validation scheme as for the ANNs was used with the same TST and TRN sets.

4.6 Results

Results of *A. thaliana* prediction

Table 4.5 show the results for genomic prediction for 146 *A. thaliana* phenotypes with ANNs and GBLUP and the architecture, determined via grid search, yielding the highest prediction accuracies. Figure C.3 contains scatter plots for the comparison of accuracies for GBLUP and the respective ANNs for 50 validation sets for all phenotypes. In table 4.5 phenotypes were ANN outperformed the genomic BLUP are indicated in red. At first sight ANN can surpass with GBLUP for traits with high accuracies, compete at an intermediate level and fails to reach to level of GBLUP when overall accuracies are low.

TABLE 4.5: Prediction accuracies of *A. thaliana* phenotypes for GBLUP and ANN

Phenotype	GBLUP	ANN	Architecture	Epochs
FT16	0.8237	0.8215	100	10
2W	0.8156	0.8205	50, 30	35
FT10	0.8249	0.8191	48	50
LD	0.8128	0.8159	150	30
DTF sweden 2009 (1st experiment)	0.8063	0.8141	48	30
DTF sweden 2009 (2nd experiment)	0.8035	0.8091	50, 30	20
DTF sweden 2008 (2nd experiment)	0.7986	0.8057	150	25
4W	0.795	0.8052	50, 35, 15	30
FT22	0.8009	0.8043	150	15
DTF spain 2008 (2nd experiment)	0.7975	0.8032	150	40
LN16	0.7996	0.7999	50, 30	20
DTF spain 2009 (2nd experiment)	0.7917	0.7988	150	55
LDV	0.8158	0.7975	150	15
0W GH FT	0.7873	0.7942	50, 30	15

4.6. Results

DTFmainEffect2009	0.7794	0.7855	50, 35, 15	35
SD	0.7905	0.7848	48	30
DTFplantingSummer2008	0.75	0.7746	50, 30	20
FT GH	0.7693	0.7702	50, 30	15
DTFlocSweden2009	0.7595	0.7626	50, 30	60
DTFplantingSummer2009	0.7521	0.7584	50, 30	50
0W	0.7488	0.7473	48	40
DTF spain 2009 (1st experiment)	0.7691	0.7425	48	40
DTF sweden 2008 (1st experiment)	0.727	0.728	50, 30	20
DTFlocSweden2008	0.7161	0.7271	50, 30	55
Seed Dormancy	0.7014	0.7241	50, 30	35
DTFmainEffect2008	0.7102	0.7142	50, 30	20
8W	0.7259	0.7083	150	50
LN22	0.7004	0.7069	50, 30	20
Size sweden 2009 (1st experiment)	0.6905	0.6994	48	50
LN10	0.6934	0.698	50, 30	20
DTF spain 2008 (1st experiment)	0.6944	0.677	150	25
SDV	0.6775	0.6728	150	15
8W GH FT	0.7001	0.6546	48	40
0W GH LN	0.6568	0.654	50, 30	20
Storage 7 days	0.6496	0.65	50, 30	25
Storage 28 days	0.6627	0.6483	50, 30	55
8W GH LN	0.671	0.6434	48	70
Size sweden 2009 (2nd experiment)	0.6114	0.6268	48	50
SizeLocSweden2009	0.6144	0.619	150	35
FLC	0.6118	0.6161	50, 30	30
LFS GH	0.6178	0.6136	150	35
FT Field	0.7324	0.6112	150	60
LY	0.6072	0.6088	150	60
Storage 56 days	0.6085	0.5788	150	15
LES	0.56	0.5764	150	50
M216T665	0.5155	0.5674	50, 30	50
LC Duration GH	0.5799	0.5664	150	55
M172T666	0.5165	0.5487	150	60
Trichome avg JA	0.588	0.5343	150	55
Secondary Dormancy	0.5184	0.5264	150	30
SizeMainEffect2009	0.52	0.5171	48	50
DSDS50	0.4754	0.5006	50, 30	60
avrPphB	0.5054	0.4942	150	60
Hypocotyl length	0.4934	0.4807	150	50
Size spain 2009 (1st experiment)	0.5121	0.4751	150	50
Yield spain 2009 (1st experiment)	0.5205	0.4719	50, 30	50
Leaf serr 10	0.4636	0.4683	150	55
Size spain 2009 (2nd experiment)	0.471	0.4623	48	50
Trichome avg C	0.4617	0.4385	48	40
Germ in dark	0.4447	0.4382	150	15
YieldMainEffect2009	0.505	0.4345	150	30

FT Diameter Field	0.5004	0.4274	150	15
Bacterial titer	0.5406	0.417	150	55
FRI	0.4011	0.4119	48	30
Rosette Erect 22	0.3973	0.3934	48	30
Area sweden 2009 (1st experiment)	0.4203	0.3895	50, 35, 15	30
Width 10	0.3932	0.3784	50, 30	60
Silique 22	0.4339	0.377	50, 30	50
avrRpt2	0.3757	0.3737	50, 30	30
M130T666	0.4381	0.3733	150	60
SizePlantingSummer2009	0.3769	0.3615	150	5
Area sweden 2009 (2nd experiment)	0.359	0.3542	48	45
FW	0.3397	0.3522	50, 30	25
P31	0.3632	0.3419	50, 30	45
MT GH	0.4016	0.3397	150	50
avrB	0.3304	0.3384	50, 30	30
avrRpm1	0.361	0.3368	50, 30	20
Seed bank 133-91	0.3446	0.3334	150	5
Mg25	0.5321	0.3288	50, 30	60
Leaf roll 10	0.3558	0.3272	48	40
Yield spain 2009 (2nd experiment)	0.4184	0.3197	20, 10	40
Noco2	0.3051	0.3174	48	30
Emwa1	0.3226	0.3124	50, 30	30
FT Duration GH	0.2659	0.3123	48	5
Leaf serr 22	0.3021	0.3108	150	60
Anthocyanin 10	0.3198	0.3107	50, 35, 15	60
Cd114	0.3345	0.3069	50, 30	50
Leaf serr 16	0.2895	0.3011	48	40
Fe56	0.2802	0.3006	150	35
YieldLocSweden2009	0.3431	0.2993	150	60
Width 16	0.3463	0.2983	150	50
Co59	0.2738	0.2953	50, 35, 15	25
K39	0.3036	0.2952	50, 30	60
Leaf roll 16	0.3072	0.2886	150	15
DTFplantingLoc2008	0.2971	0.275	50, 30	5
SizePlantingSummerLocSweden2009	0.2803	0.2704	50, 30	60
Mn55	0.2775	0.2662	50, 30	20
Anthocyanin 22	0.2731	0.2635	150	15
As75	0.254	0.2619	50, 30	35
Na23	0.2564	0.2598	50, 30	15
Ni60	0.2894	0.2539	150	25
Mo98	0.2765	0.2537	50, 30	35
Chlorosis 22	0.2622	0.2453	50, 35, 15	10
Hiks1	0.2441	0.2452	20, 10	20
Zn66	0.2553	0.2444	150	35
B11	0.2891	0.2392	48	40
Germ 16	0.2987	0.2356	50, 30	41
At2	0.2147	0.216	150	15

4.6. Results

Emco5	0.166	0.2101	150, 30	20
Se82	0.2192	0.2075	150	25
Mature cell length	0.1987	0.2052	150	45
DW	0.2878	0.2048	50, 30	60
Yield sweden 2009 (1st experiment)	0.2274	0.2033	150	55
As2	0.1774	0.1962	150	15
Meristem zone length	0.1976	0.195	150	50
Germ 10	0.2073	0.1873	20, 10	40
Anthocyanin 16	0.2433	0.1867	20, 10	10
Width 22	0.2224	0.1856	50, 30	50
YieldPlantingSummerLocSweden2009	0.2146	0.18	150	55
DTFplantingSummerLocSweden2009	0.2032	0.1775	150	55
Bs	0.2161	0.1656	50, 30	60
Bs CFU2	0.1672	0.1584	50, 35, 15	15
Germ 22	0.1267	0.1533	50, 30	35
Leaf roll 22	0.1135	0.1511	48	45
RP GH	0.1755	0.1458	150	15
Cu65	0.1543	0.1315	150	5
Li7	0.1611	0.1297	150	60
As	0.1089	0.1227	100	20
At1	0.1473	0.1197	48	40
S34	0.1045	0.11	50, 30	60
YieldPlantingSummer2009	0.1265	0.0984	150	50
Silique 16	0.2366	0.0884	50, 30	60
Chlorosis 10	0.0243	0.088	50, 35, 15	55
Ca43	0.3333	0.0732	50, 35, 15	55
Seedling Growth	0.0813	0.0636	48	30
Vern Growth	-0.0096	0.0422	150	15
At2 CFU2	0.0694	0.0378	150	25
Yield sweden 2009 (2nd experiment)	0.0536	0.0355	150	25
As CFU2	0.0312	0.035	150	5
At1 CFU2	0.0818	0.0319	50, 30	50
Aphid number	-0.0246	0.029	50, 35, 15	10
After Vern Growth	-0.1433	0.0057	50, 35, 15	5
Chlorosis 16	-0.0313	-0.0121	150	5
As2 CFU2	0.0504	-0.0325	50, 30	60

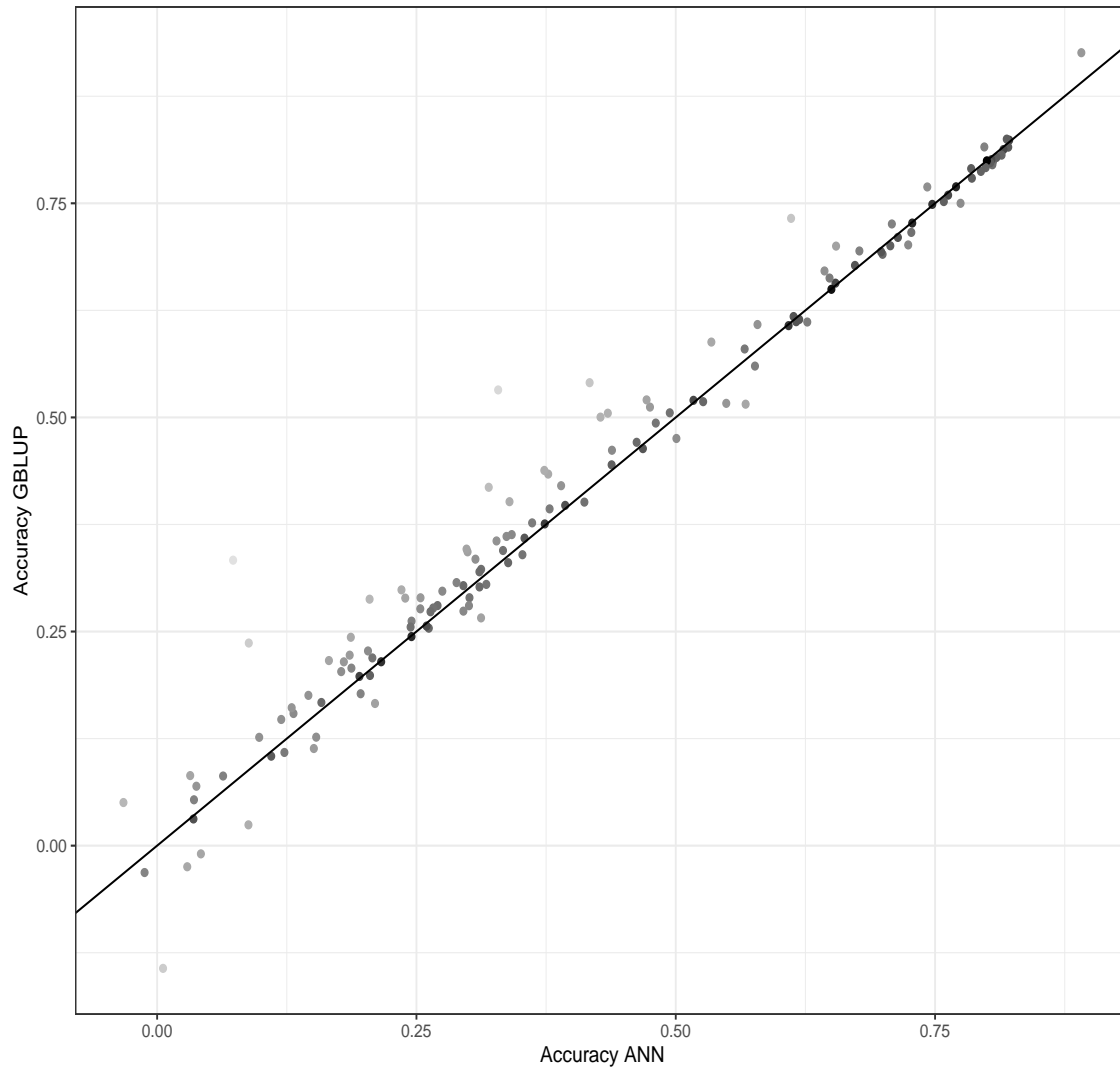


FIGURE 4.6: Scatterplot comparing prediction accuracies of ANN and GBLUP in *A. thaliana*. Greyscale indicates the magnitude of the difference between the methods

4.6.1 Results of maize prediction

Across environments

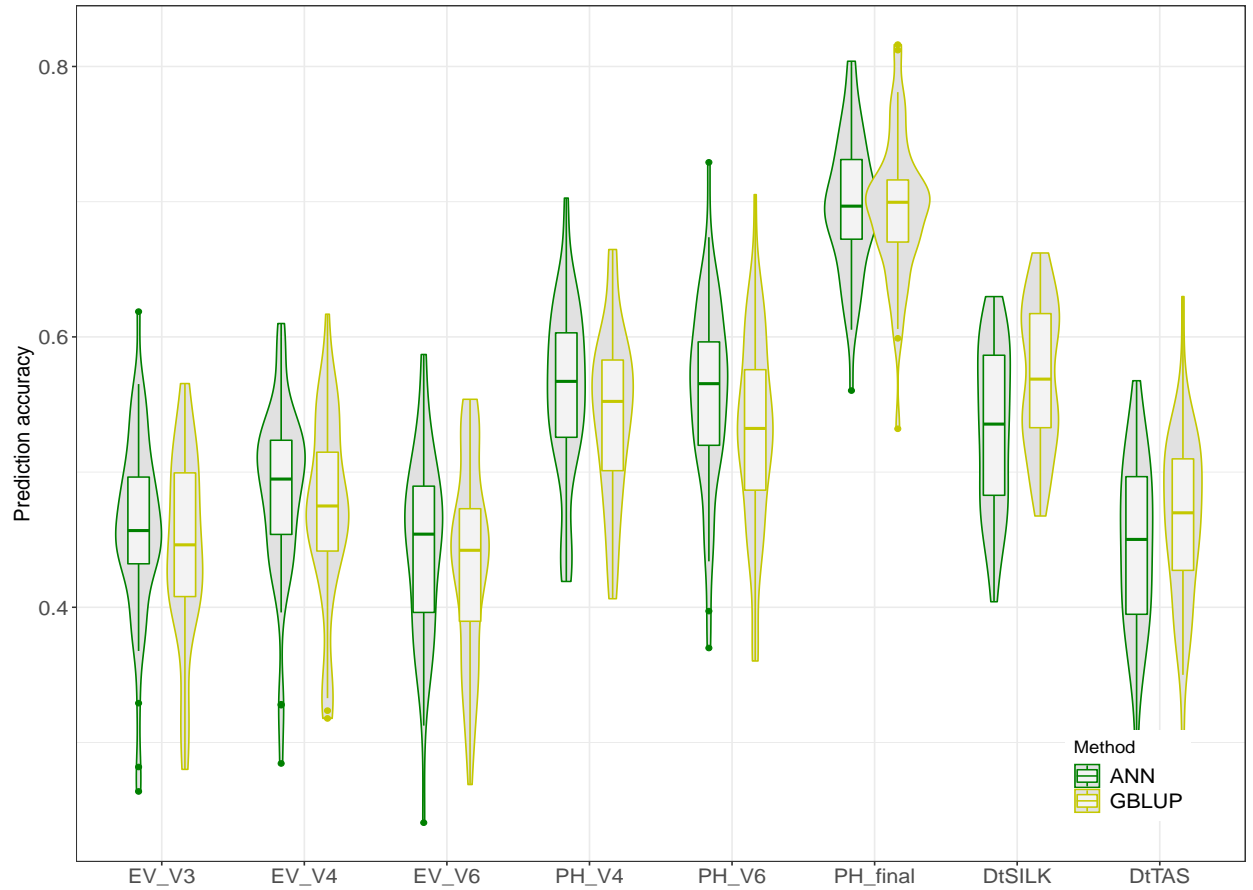


FIGURE 4.7: Violinplot comparing the results for GP in the DH population Kemater for ANN and GBLUP

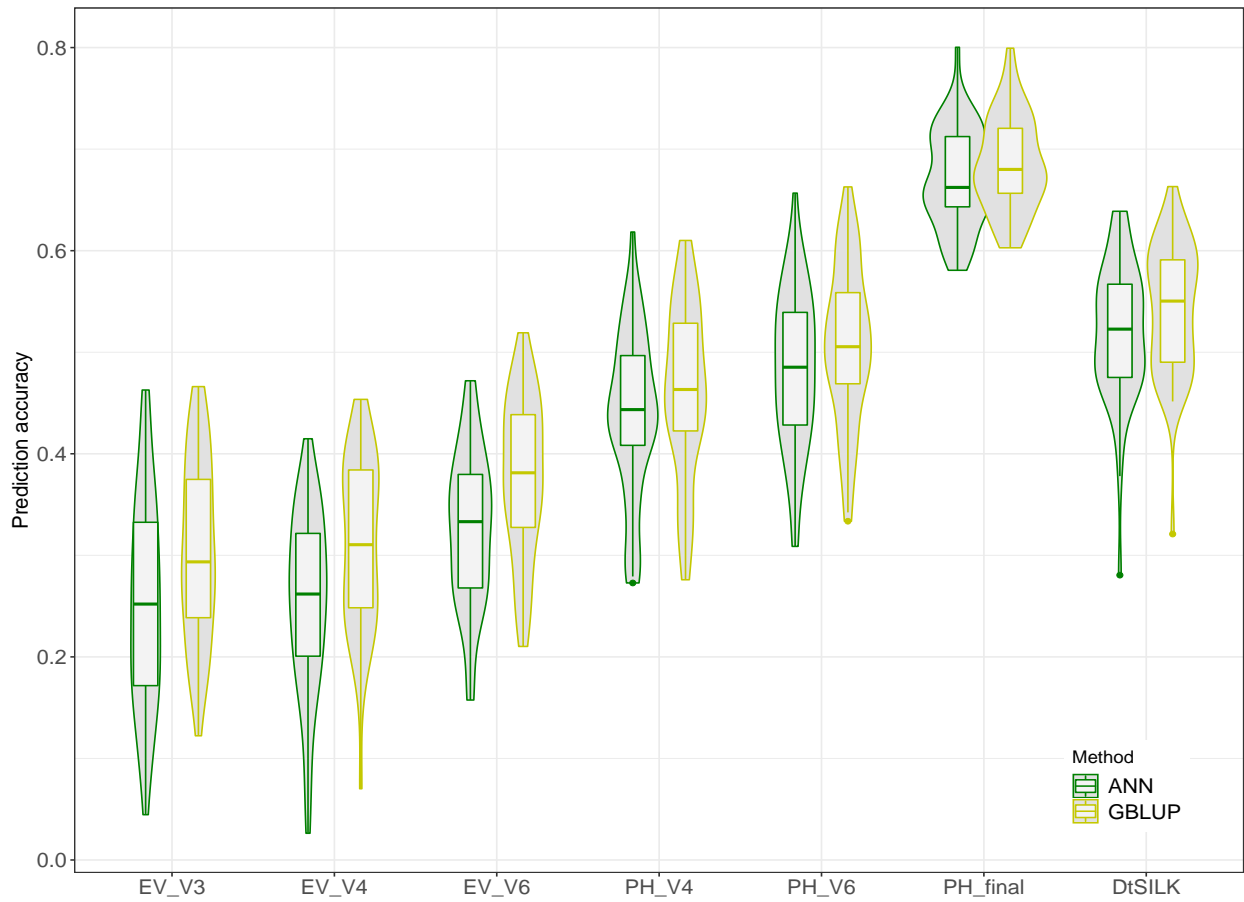


FIGURE 4.8: Violinplot comparing the results for GP in the DH population Petkuser for ANN and GBLUP

Phenotype	Kemater		Petkuser	
	GBLUP	ANN	GBLUP	ANN
EV_V3	0.44	0.46	0.31	0.25
EV_V4	0.47	0.49	0.31	0.25
EV_V6	0.43	0.44	0.38	0.33
DtTAS	0.47	0.44		
PH_V4_mean	0.54	0.56	0.46	0.44
PH_V6_mean	0.53	0.56	0.51	0.48
PH_final	0.69	0.70	0.68	0.67
DtSILK	0.57	0.53	0.54	0.52

Single environments

The prediction of the single environment BLUEs with the environmentally enhanced marker matrix yielded substantially higher prediction accuracies than the prediction with the across environment BLUEs (previous section)-

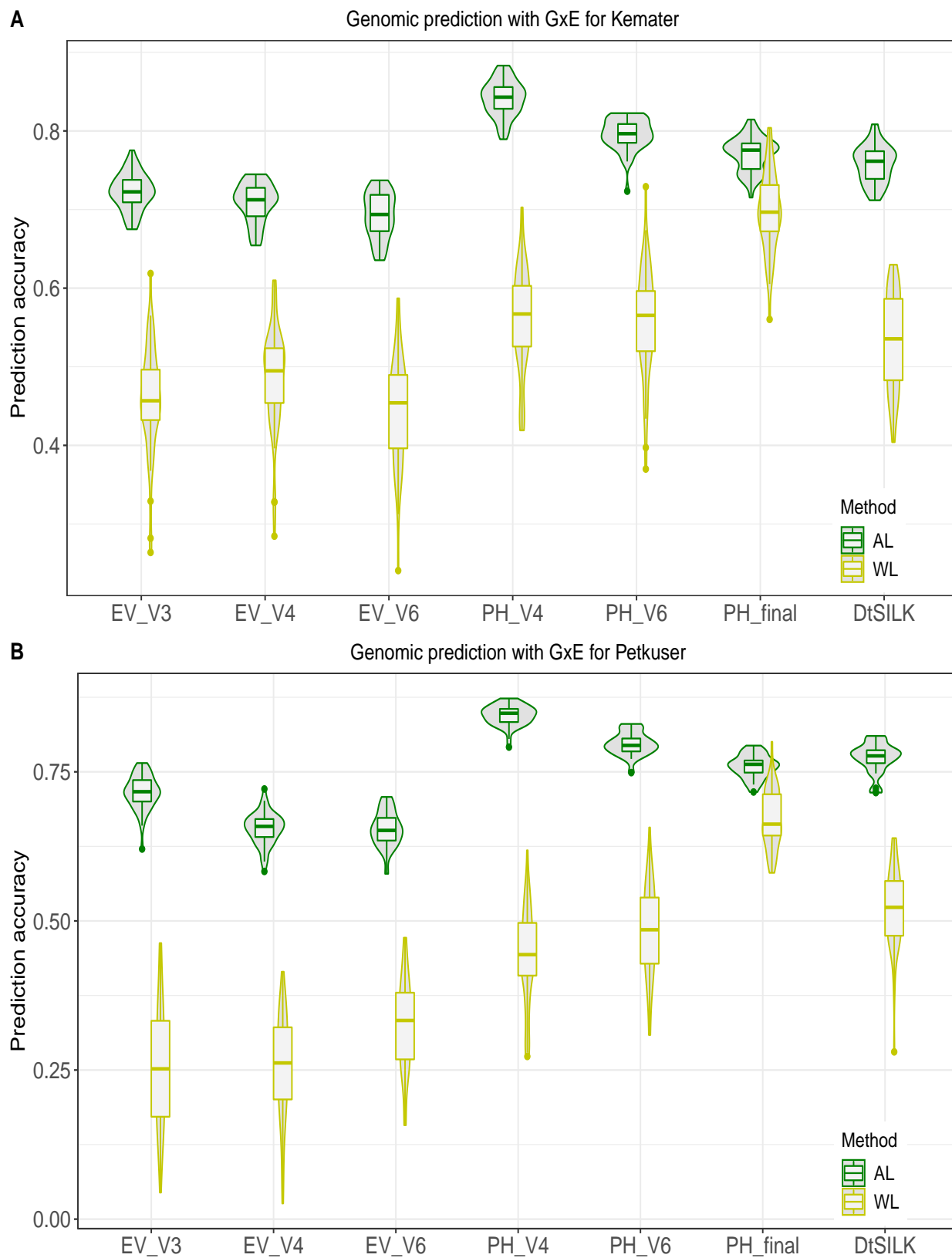


FIGURE 4.9: Results of genomic prediction across single environments for **A** Kemater and **B** Petkuser DH populations

TABLE 4.6: Comparison of prediction results of ANN within locations (WL) and across locations (AL) for Kemater and Petkuser

Phenotype	Kemater			Petkuser		
	AL	WL	Δ	AL	WL	Δ
EV_V3	0.73	0.46	0.27	0.72	0.25	0.47
EV_V4	0.72	0.49	0.23	0.66	0.25	0.40
EV_V6	0.70	0.44	0.26	0.65	0.33	0.33
PH_V4	0.84	0.56	0.28	0.84	0.44	0.41
PH_V6	0.80	0.56	0.25	0.80	0.48	0.31
PH_final	0.78	0.70	0.08	0.76	0.67	0.09
DtSILK	0.76	0.53	0.23	0.77	0.52	0.25

4.7 Discussion

TABLE 4.7: ANN architectures resulting in highest prediction accuracies, with number of hidden layer (HL) and the total count (n)

LCL	Architecture	HL	n
True	150	2	56
True	50, 30	3	47
True	48	2	23
True	50, 35, 15	4	11
True	20, 10	3	5
True	100	2	2
True	150, 30	3	

5 GWAS

5.1 Introduction

Chapter 2 or 3 introduced a new framework for high throughput GWAS. GWAS-Flow enables to execute GWAS analysis on GPU and thus gains an incredible performance advantage compared to other state of the art GWAS technologies. This enabled the research group of evolutionary genomics at the CCTB to evaluate 462 (oder so) data sets from Arapheno with the full 10 mio data set originally imputed with Beagle version 3. Those GWAS have been repeated 100 times with shuffled phenotypes to estimate permutation based thresholds. Additionally all phenotypes were re-evaluated with a recently generated data set which based the imputation on the more recent Beagle version 5, which supposingly is more accurate (Pook et al). In the scope of this chapter it will be assessed if this does influence the outcome of the GWAS. Furthermore was GWAS-Flow used to evaluate some of the common practices in GWAS, that a prior do not seam relevant to the author. Sometimes yet uncommon in the literature it is recommend to use transformations for the pheonotypic values prior to performing GWAS to account for non-normal distributed data, transformations or calculated with the log, square root or boxcox. Another common practice is to use principal components from PCA to account for population structure. This however should be covered sufficiently by the K matrix which is part of basically any mixed linear model based GWAS approach.

5.2 Reevaluation of 46? phenotypes from the Arapheno database

The Arapheno data base recently has been extended by several 100 new data sets. GWAS-Flow was applied to estimate the permutation based of those and the old data sets totaling in 461 phenotypes. In total approximately 50000 GWAS were run with a total of 10 million markers each. Additionally for each data sets three transformed phenotypes were tested and also re-evaluated with the Beagle 5.0 imputed genomic matrix.

5.3 GWAS in DH landrace populations of maize across and within environments

5.3.1 Introduction

5.3.2 Material and Methods

5.3.3 Results

5.3.4 Results

5.3.5 Discussion

6 General Discussion

Nothing here yet.

10000s of genome assemblies Almost 1 million neural nets trained and the same amount of GWAS run. Awesome stuff !

A Source code

A.1 GBLUP example

```
1 M <- matrix(c(1,-1,0,0,0,1,1,0,1,-1,0,-1),nrow=3)
2 MtM <- M %*% t(M)
3 MtM
4      [,1] [,2] [,3]
5 [1,]    3  -1    2
6 [2,]   -1    1    0
7 [3,]    2    0    3
8 tMM <- t(M) %*% t(M)
9 tMM
10     [,1] [,2] [,3] [,4]
11 [1,]    2    0    1  -1
12 [2,]    0    1    1  -1
13 [3,]    1    1    2  -2
14 [4,]   -1   -1   -2    2
15
16 P = matrix(rep(2*(mafs - 0.5),3),nrow=3,byrow=T)
17 P
18     [,1] [,2] [,3] [,4]
19 [1,] -0.4 -0.6 -0.8 -0.7
20 [2,] -0.4 -0.6 -0.8 -0.7
21 [3,] -0.4 -0.6 -0.8 -0.7
```

A.2 gwas.py

```
1 import os
2 import sys
3 import time
4 import numpy as np
```

```

5 import pandas as pd
6 import main
7 import h5py
8
9 # set defaults
10 mac_min = 1
11 batch_size = 500000
12 out_file = "results.csv"
13 m = 'phenotype_value'
14 perm = 1
15 mac_min= 6
16
17 X_file = 'gwas_sample_data/AT_geno.hdf5'
18 Y_file = 'gwas_sample_data/phenotype.csv'
19 K_file = 'gwas_sample_data/kinship_ibs_binary_mac5.h5py'
20
21
22
23 for i in range (1,len(sys.argv),2):
24     if sys.argv[i] == "-x" or sys.argv[i] == "--genotype":
25         X_file = sys.argv[i+1]
26     elif sys.argv[i] == "-y" or sys.argv[i] == "--phenotype":
27         Y_file = sys.argv[i+1]
28     elif sys.argv[i] == "-k" or sys.argv[i] == "--kinship":
29         K_file = sys.argv[i+1]
30     elif sys.argv[i] == "-m":
31         m = sys.argv[i+1]
32     elif sys.argv[i] == "-a" or sys.argv[i] == "--mac_min":
33         mac_min = int(sys.argv[i+1])
34     elif sys.argv[i] == "-bs" or sys.argv[i] == "--batch-size":
35         batch_size = int(sys.argv[i+1])
36     elif sys.argv[i] == "-p" or sys.argv[i] == "--perm":
37         perm = int(sys.argv[i+1])
38     elif sys.argv[i] == "-o" or sys.argv[i] == "--out":
39         out_file = sys.argv[i+1]
40     elif sys.argv[i] == "-h" or sys.argv[i] == "--help":
41         print("-x , --genotype :file containing marker information
in csv or hdf5 format of size")

```

```

42     print("-y , --phenotype: file container phenotype
information in csv format" )
43     print("-k , --kinship : file containing kinship matrix of
size k X k in csv or hdf5 format")
44     print("-m : name of columnn containing the phenotype :
default m = phenotype_value")
45     print("-a , --mac_min : integer specifying the minimum
minor allele count necessary for a marker to be included.
Default a = 1" )
46     print("-bs, --batch-size : integer specifying the number of
markers processed at once. Default -bs 500000" )
47     print("-p , --perm : single integer specifying the number
of permutations. Default 1 == no perm ")
48     print("-o , --out : name of output file. Default -o results
.csv ")
49     print("-h , --help : prints help and command line options")
50     quit()
51     else:
52         print('unknown option ' + str(sys.argv[i]))
53         quit()
54
55
56
57 print("parsed commandline args")
58
59 start = time.time()
60
61 X,K,Y_,markers = main.load_and_prepare_data(X_file,Y_file,K_file,m)
62
63
64 ## MAF filterin
65 markers_used , X , macs = main.mac_filter(mac_min,X,markers)
66
67 ## prepare
68 print("Begin performing GWAS on ", Y_file)
69
70 if perm == 1:
71     output = main.gwas(X,K,Y_,batch_size)

```

```

72     if( X_file.split(".")[ -1] == 'csv'):
73         chr_pos = np.array(list(map(lambda x : x.split("- "),
markers_used)))
74     else:
75         chr_reg = h5py.File(X_file, 'r')['positions'].attrs['
chr_regions']
76         mk_index= np.array(range(len(markers)),dtype=int)[macs >=
mac_min]
77         chr_pos = np.array([list(map(lambda x: sum(x > chr_reg
[: ,1]) + 1, mk_index)), markers_used]).T
78         my_time = np.repeat((time.time()-start),len(chr_pos))
79     pd.DataFrame({
80         'chr' : chr_pos[:,0] ,
81         'pos' : chr_pos[:,1] ,
82         'pval': output[:,0] ,
83         'mac' : np.array(macs[macs >= mac_min],dtype=np.int) ,
84         'eff_size': output[:,1] ,
85         'SE' : output[:,2]}).to_csv(out_file,index=False)
86 elif perm > 1:
87     min_pval = []
88     perm_seeds = []
89     my_time = []
90     for i in range(perm):
91         start_perm = time.time()
92         print("Running permutation ", i+1, " of ",perm)
93         my_seed = np.asscalar(np.random.randint(9999,size=1))
94         perm_seeds.append(my_seed)
95         np.random.seed(my_seed)
96         Y_perm = np.random.permutation(Y_)
97         output = main.gwas(X,K,Y_perm,batch_size)
98         min_pval.append(np.min(output[:,0]))
99         print("Elapsed time for permutatation",i+1 ," with p_min",
min_pval[i]," is",": ", round(time.time() - start_perm,2))
100         my_time.append(time.time()-start_perm)
101     pd.DataFrame({
102         'time': my_time ,
103         'seed': perm_seeds ,
104         'min_p': min_pval }).to_csv(out_file,index=False)

```


A.3. *main.py*

```
105
106 print("done")
107
108 end = time.time()
109 eltime = np.round(end - start,2)
110
111 if eltime <= 59:
112     print("Total time elapsed", eltime, "seconds")
113 elif eltime > 59 and eltime <= 3600:
114     print("Total time elapsed", np.round(eltime / 60,2) , "minutes
115 ")
116 elif eltime > 3600 :
117     print("Total time elapsed", np.round(eltime / 60 / 60,2), "
118 hours")
```

A.3 main.py

```
1 import pandas as pd
2 import numpy as np
3 from scipy.stats import f
4 import tensorflow as tf
5 import limix
6 import herit
7 import h5py
8 import limix
9 import multiprocessing as mlt
10
11 def load_and_prepare_data(X_file,Y_file,K_file,m):
12     type_K = K_file.split(".")[1]
13     type_X = X_file.split(".")[1]
14
15     ## load and preprocess genotype matrix
16     Y = pd.read_csv(Y_file,engine='python').sort_values(['
17 accession_id']).groupby('accession_id').mean()
18     Y = pd.DataFrame({'accession_id' : Y.index, 'phenotype_value'
19 : Y[m]})
```

```

18     if type_X == 'hdf5' or type_X == 'h5py' :
19         SNP = h5py.File(X_file, 'r')
20         markers = np.asarray(SNP['positions'])
21         acc_X = np.asarray(SNP['accessions'][:, :], dtype=np.int)
22     elif type_X == 'csv' :
23         X = pd.read_csv(X_file, index_col=0)
24         markers = X.columns.values
25         acc_X = X.index
26         X = np.asarray(X, dtype=np.float32)/2
27     else :
28         sys.exit("Only hdf5, h5py and csv files are supported")
29
30     if type_K == 'hdf5' or type_K == 'h5py':
31         k = h5py.File(K_file, 'r')
32         acc_K = np.asarray(k['accessions'][:, :], dtype=np.int)
33     elif type_K == 'csv':
34         k = pd.read_csv(K_file, index_col=0)
35         acc_K = k.index
36         k = np.array(k, dtype=np.float32)
37
38     acc_Y = np.asarray(Y[['accession_id']]).flatten()
39     acc_isec = [isec for isec in acc_X if isec in acc_Y]
40
41     idx_acc = list(map(lambda x: x in acc_isec, acc_X))
42     idy_acc = list(map(lambda x: x in acc_isec, acc_Y))
43     idk_acc = list(map(lambda x: x in acc_isec, acc_K))
44
45     Y_ = np.asarray(Y.drop('accession_id', 1), dtype=np.float32)[
46         idy_acc, :]
47
48     if type_X == 'hdf5' or type_X == 'h5py' :
49         X = np.asarray(SNP['snps'][0:(len(SNP['snps'])+1), :], dtype=
50             np.float32)[: , idx_acc].T
51         X = X[np.argsort(acc_X[idx_acc]), :]
52         k1 = np.asarray(k['kinship'][:, :])[idk_acc, :]
53         K = k1[:, idk_acc]
54         K = K[np.argsort(acc_X[idx_acc]), :]
55         K = K[:, np.argsort(acc_X[idx_acc])]

```

```
54     else:
55         X = X[idx_acc,:]
56         k1 = k[idk_acc,:]
57         K = k1[:,idk_acc]
58
59
60     print("data has been imported")
61     return X,K,Y_,markers
62
63
64 def mac_filter(mac_min, X, markers):
65     ac1 = np.sum(X,axis=0)
66     ac0 = X.shape[0] - ac1
67     macs = np.minimum(ac1,ac0)
68     markers_used = markers[macs >= mac_min]
69     X = X[:,macs >= mac_min]
70     return markers_used, X, macs
71
72 def gwas(X,K,Y,batch_size):
73     n_marker = X.shape[1]
74     n = len(Y)
75     ## REML
76     K_stand = (n-1)/np.sum((np.identity(n) - np.ones((n,n))/n) * K)
77     * K
78     vg, delta, ve = herit.estimate(Y,"normal",K_stand,verbose =
79     False)
80     print(" Pseudo-heritability is " , vg / (ve + vg + delta))
81     print(" Performing GWAS on ", n , " phenotypes and ", n_marker
82     ,"markers")
83     ## Transform kinship-matrix, phenotypes and estimate intercpt
84     Xo = np.ones(K.shape[0]).flatten()
85     M = np.transpose(np.linalg.inv(np.linalg.cholesky(vg * K_stand
86     + ve * np.identity(n))))).astype(np.float32)
87     Y_t = np.sum(np.multiply(np.transpose(M),Y),axis=1).astype(np.
88     float32)
89     int_t = np.sum(np.multiply(np.transpose(M),np.ones(n)),axis=1).
90     astype(np.float32)
91     ## EMMAX Scan
```

```

86     RSS_env = (np.linalg.lstsq(np.reshape(int_t,(n,-1)) , np.
reshape(Y_t,(n,-1)))[1]).astype(np.float32)
87     ## calculate betas and se of betas
88     def stderr(a,M,Y_t2d,int_t):
89         x = tf.stack((int_t,tf.squeeze(tf.matmul(M.T,tf.reshape(a
,(n,-1))))),axis=1)
90         coeff = tf.matmul(tf.matmul(tf.linalg.inv(tf.matmul(tf.
transpose(x),x)),tf.transpose(x)),Y_t2d)
91         SSE = tf.reduce_sum(tf.math.square(tf.math.subtract(Y_t,tf
.math.add(tf.math.multiply(x[:,1],coeff[0,0]),tf.math.multiply(x
[:,1],coeff[1,0])))))
92         SE = tf.math.sqrt(SSE/(471-(1+2)))
93         StdERR = tf.sqrt(tf.linalg.diag_part(tf.math.multiply(SE ,
tf.linalg.inv(tf.matmul(tf.transpose(x),x)))[1]
94         return tf.stack((coeff[1,0],StdERR))
95     ## calculate residual sum squares
96     def rss(a,M,y,int_t):
97         x_t = tf.reduce_sum(tf.math.multiply(M.T,a),axis=1)
98         lm_res = tf.linalg.lstsq(tf.transpose(tf.stack((int_t,x_t)
,axis=0)),Y_t2d)
99         lm_x = tf.concat((tf.squeeze(lm_res),x_t),axis=0)
100        return tf.reduce_sum(tf.math.square(tf.math.subtract(tf.
squeeze(Y_t2d),tf.math.add(tf.math.multiply(lm_x[1],lm_x[2:]),
tf.multiply(lm_x[0],int_t)))))
101    ## loop over the batches
102    for i in range(int(np.ceil(n_marker/batch_size))):
103        tf.reset_default_graph()
104        if n_marker < batch_size:
105            X_sub = X
106        else:
107            lower_limit = batch_size * i
108            upper_limit = batch_size * i + batch_size
109            if upper_limit <= n_marker :
110                X_sub = X[:,lower_limit:upper_limit]
111                print("Working on markers ", lower_limit , " to ",
upper_limit, " of ", n_marker )
112            else:
113                X_sub = X[:,lower_limit:]

```

```

114         print("Working on markers ", lower_limit , " to ",
n_marker, " of ", n_marker )
115         config = tf.ConfigProto()
116         n_cores = mlt.cpu_count()
117         config.intra_op_parallelism_threads = n_cores
118         config.inter_op_parallelism_threads = n_cores
119         sess = tf.Session(config=config)
120         Y_t2d = tf.cast(tf.reshape(Y_t,(n,-1)),dtype=tf.float32)
121         y_tensor = tf.convert_to_tensor(Y_t,dtype = tf.float32)
122         StdERR = tf.map_fn(lambda a : stderr(a,M,Y_t2d,int_t),
X_sub.T)
123         R1_full = tf.map_fn(lambda a: rss(a,M,Y_t2d,int_t), X_sub.T
)
124         F_1 = tf.divide(tf.subtract(RSS_env, R1_full),tf.divide(
R1_full,(n-3)))
125         if i == 0 :
126             output = sess.run(tf.concat([tf.reshape(F_1,(X_sub.
shape[1],-1)),StdERR],axis=1))
127         else :
128             tmp = sess.run(tf.concat([tf.reshape(F_1,(X_sub.shape
[1],-1)),StdERR],axis=1))
129             output = np.append(output,tmp,axis=0)
130             sess.close()
131             F_dist = output[:,0]
132             pval = 1 - f.cdf(F_dist,1,n-3)
133             output[:,0] = pval
134         return output
135
136
137

```

A.4 herit.py

```

1
2 def estimate(y, lik, K, M=None, verbose=True):
3     from numpy_sugar.linalg import economic_qs
4     from numpy import pi, var, diag
5     from glimix_core.glmm import GLMMExpFam

```

```

6     from glimix_core.lmm import LMM
7     from limix._data._assert import assert_likelihoood
8     from limix._data import normalize_likelihoood, conform_dataset
9     from limix.qtl._assert import assert_finite
10    from limix._display import session_block, session_line
11    lik = normalize_likelihoood(lik)
12    lik_name = lik[0]
13    with session_block("Heritability analysis", disable=not verbose
14    ):
15        with session_line("Normalising input...", disable=not
16        verbose):
17            data = conform_dataset(y, M=M, K=K)
18            y = data["y"]
19            M = data["M"]
20            K = data["K"]
21            assert_finite(y, M, K)
22            if K is not None:
23                # K = K / diag(K).mean()
24                QS = economic_qs(K)
25            else:
26                QS = None
27            if lik_name == "normal":
28                method = LMM(y.values, M.values, QS, restricted=True)
29                method.fit(verbose=verbose)
30            else:
31                method = GLMMEExpFam(y, lik, M.values, QS, n_int=500)
32                method.fit(verbose=verbose, factr=1e6, pgtol=1e-3)
33            g = method.scale * (1 - method.delta)
34            e = method.scale * method.delta
35            if lik_name == "bernoulli":
36                e += pi * pi / 3
37            v = var(method.mean())
38            return g, v, e

```

B *A. thaliana* phenotypic data

ID	Phenotype name	doi	Reference
1	FT Diameter Field	10.21958/phenotype:1	ATWELL et al., 2010
2	At2 CFU2	10.21958/phenotype:2	ATWELL et al., 2010
3	Leaf serr 16	10.21958/phenotype:3	ATWELL et al., 2010
4	Seed bank 133-91	10.21958/phenotype:4	ATWELL et al., 2010
5	Na23	10.21958/phenotype:5	ATWELL et al., 2010
6	Leaf serr 10	10.21958/phenotype:6	ATWELL et al., 2010
7	Emco5	10.21958/phenotype:7	ATWELL et al., 2010
8	Leaf roll 16	10.21958/phenotype:8	ATWELL et al., 2010
9	Leaf roll 10	10.21958/phenotype:9	ATWELL et al., 2010
10	Bs	10.21958/phenotype:10	ATWELL et al., 2010
11	2W	10.21958/phenotype:11	ATWELL et al., 2010
12	Rosette Erect 22	10.21958/phenotype:12	ATWELL et al., 2010
13	Cd114	10.21958/phenotype:13	ATWELL et al., 2010
14	Width 16	10.21958/phenotype:14	ATWELL et al., 2010
15	Storage 28 days	10.21958/phenotype:15	ATWELL et al., 2010
16	LY	10.21958/phenotype:16	ATWELL et al., 2010
17	avrRpm1	10.21958/phenotype:17	ATWELL et al., 2010
18	Width 10	10.21958/phenotype:18	ATWELL et al., 2010
19	Chlorosis 22	10.21958/phenotype:19	ATWELL et al., 2010
20	Storage 7 days	10.21958/phenotype:20	ATWELL et al., 2010
21	As2 CFU2	10.21958/phenotype:21	ATWELL et al., 2010
22	Co59	10.21958/phenotype:22	ATWELL et al., 2010

Appendix B. *A. thaliana* phenotypic data

23	FW	10.21958/phenotype:23	ATWELL et al., 2010
24	Cu65	10.21958/phenotype:24	ATWELL et al., 2010
25	Bacterial titer	10.21958/phenotype:25	ATWELL et al., 2010
26	Width 22	10.21958/phenotype:26	ATWELL et al., 2010
27	Storage 56 days	10.21958/phenotype:27	ATWELL et al., 2010
28	YEL	10.21958/phenotype:28	ATWELL et al., 2010
29	FLC	10.21958/phenotype:29	ATWELL et al., 2010
30	FT16	10.21958/phenotype:30	ATWELL et al., 2010
31	FT10	10.21958/phenotype:31	ATWELL et al., 2010
32	FT Duration GH	10.21958/phenotype:32	ATWELL et al., 2010
33	Se82	10.21958/phenotype:33	ATWELL et al., 2010
34	LDV	10.21958/phenotype:34	ATWELL et al., 2010
35	Noco2	10.21958/phenotype:35	ATWELL et al., 2010
36	8W GH LN	10.21958/phenotype:36	ATWELL et al., 2010
37	0W	10.21958/phenotype:37	ATWELL et al., 2010
38	MT GH	10.21958/phenotype:38	ATWELL et al., 2010
39	After Vern Growth	10.21958/phenotype:39	ATWELL et al., 2010
40	Aphid number	10.21958/phenotype:40	ATWELL et al., 2010
41	LN22	10.21958/phenotype:41	ATWELL et al., 2010
42	Bs CFU2	10.21958/phenotype:42	ATWELL et al., 2010
43	avrRpt2	10.21958/phenotype:43	ATWELL et al., 2010
44	Hypocotyl length	10.21958/phenotype:44	ATWELL et al., 2010
45	Germ 22	10.21958/phenotype:45	ATWELL et al., 2010
46	Leaf roll 22	10.21958/phenotype:46	ATWELL et al., 2010
47	SD	10.21958/phenotype:47	ATWELL et al., 2010
48	8W	10.21958/phenotype:48	ATWELL et al., 2010
49	FT GH	10.21958/phenotype:49	ATWELL et al., 2010
50	DSDS50	10.21958/phenotype:50	ATWELL et al., 2010

Appendix B. A. thaliana phenotypic data

51	Ca43	10.21958/phenotype:51	ATWELL et al., 2010
52	LC Duration GH	10.21958/phenotype:52	ATWELL et al., 2010
53	0W GH FT	10.21958/phenotype:53	ATWELL et al., 2010
54	B11	10.21958/phenotype:54	ATWELL et al., 2010
55	Chlorosis 10	10.21958/phenotype:55	ATWELL et al., 2010
56	RP GH	10.21958/phenotype:56	ATWELL et al., 2010
57	Chlorosis 16	10.21958/phenotype:57	ATWELL et al., 2010
58	LFS GH	10.21958/phenotype:58	ATWELL et al., 2010
59	Germ 10	10.21958/phenotype:59	ATWELL et al., 2010
60	Germ 16	10.21958/phenotype:60	ATWELL et al., 2010
61	Anthocyanin 16	10.21958/phenotype:61	ATWELL et al., 2010
62	Anthocyanin 10	10.21958/phenotype:62	ATWELL et al., 2010
63	At1 CFU2	10.21958/phenotype:63	ATWELL et al., 2010
64	Ni60	10.21958/phenotype:64	ATWELL et al., 2010
65	P31	10.21958/phenotype:65	ATWELL et al., 2010
66	Emwa1	10.21958/phenotype:66	ATWELL et al., 2010
67	As75	10.21958/phenotype:67	ATWELL et al., 2010
68	Germ in dark	10.21958/phenotype:68	ATWELL et al., 2010
69	FRI	10.21958/phenotype:69	ATWELL et al., 2010
70	As CFU2	10.21958/phenotype:70	ATWELL et al., 2010
71	Trichome avg C	10.21958/phenotype:71	ATWELL et al., 2010
72	Vern Growth	10.21958/phenotype:72	ATWELL et al., 2010
73	Mo98	10.21958/phenotype:73	ATWELL et al., 2010
74	Hiks1	10.21958/phenotype:74	ATWELL et al., 2010
75	Anthocyanin 22	10.21958/phenotype:75	ATWELL et al., 2010
76	Zn66	10.21958/phenotype:76	ATWELL et al., 2010
77	Trichome avg JA	10.21958/phenotype:77	ATWELL et al., 2010
78	LES	10.21958/phenotype:78	ATWELL et al., 2010

Appendix B. *A. thaliana* phenotypic data

79	Silique 16	10.21958/phenotype:79	ATWELL et al., 2010
80	Emoy*	10.21958/phenotype:80	ATWELL et al., 2010
81	K39	10.21958/phenotype:81	ATWELL et al., 2010
82	0W GH LN	10.21958/phenotype:82	ATWELL et al., 2010
83	At2	10.21958/phenotype:83	ATWELL et al., 2010
84	At1	10.21958/phenotype:84	ATWELL et al., 2010
85	LN10	10.21958/phenotype:85	ATWELL et al., 2010
86	FT Field	10.21958/phenotype:86	ATWELL et al., 2010
87	LN16	10.21958/phenotype:87	ATWELL et al., 2010
88	avrB	10.21958/phenotype:88	ATWELL et al., 2010
89	LD	10.21958/phenotype:89	ATWELL et al., 2010
90	Seedling Growth	10.21958/phenotype:90	ATWELL et al., 2010
91	S34	10.21958/phenotype:91	ATWELL et al., 2010
92	Leaf serr 22	10.21958/phenotype:92	ATWELL et al., 2010
93	DW	10.21958/phenotype:93	ATWELL et al., 2010
94	Seed Dormancy	10.21958/phenotype:94	ATWELL et al., 2010
95	Mn55	10.21958/phenotype:95	ATWELL et al., 2010
96	Silique 22	10.21958/phenotype:96	ATWELL et al., 2010
97	avrPphB	10.21958/phenotype:97	ATWELL et al., 2010
98	Fe56	10.21958/phenotype:98	ATWELL et al., 2010
99	8W GH FT	10.21958/phenotype:99	ATWELL et al., 2010
100	4W	10.21958/phenotype:100	ATWELL et al., 2010
101	Li7	10.21958/phenotype:101	ATWELL et al., 2010
102	FT22	10.21958/phenotype:102	ATWELL et al., 2010
103	As2	10.21958/phenotype:103	ATWELL et al., 2010
104	SDV	10.21958/phenotype:104	ATWELL et al., 2010
105	Mg25	10.21958/phenotype:105	ATWELL et al., 2010
106	Secondary Dormancy	10.21958/phenotype:106	ATWELL et al., 2010

107	As	10.21958/phenotype:107	ATWELL et al., 2010
108	Area Sweden 2009 (1st experiment)	10.21958/phenotype:108	LI et al., 2010
109	Size Planting Summer 2009	10.21958/phenotype:109	LI et al., 2010
110	Size Sweden 2009 (2nd experiment)	10.21958/phenotype:110	LI et al., 2010
111	Size Planting Summer Loc Sweden 2009	10.21958/phenotype:111	LI et al., 2010
112	Area Sweden 2009 (2nd experiment)	10.21958/phenotype:112	LI et al., 2010
113	DTF Sweden 2008 (1st experiment)	10.21958/phenotype:113	LI et al., 2010
114	Yield Sweden 2009 (2nd experiment)	10.21958/phenotype:114	LI et al., 2010
115	Size Loc Sweden 2009	10.21958/phenotype:115	LI et al., 2010
116	DTF planting Summer Loc Sweden 2009	10.21958/phenotype:116	LI et al., 2010
117	DTF loc Sweden 2008	10.21958/phenotype:117	LI et al., 2010
118	DTF loc Sweden 2009	10.21958/phenotype:118	LI et al., 2010
119	DTF Spain 2009 (1st experiment)	10.21958/phenotype:119	LI et al., 2010
120	DTF planting Loc 2008	10.21958/phenotype:120	LI et al., 2010
121	DTF Spain 2009 (2nd experiment)	10.21958/phenotype:121	LI et al., 2010
122	Yield Spain 2009 (2nd experiment)	10.21958/phenotype:122	LI et al., 2010
123	Size Sweden 2009 (1st experiment)	10.21958/phenotype:123	LI et al., 2010

124	Yield Spain 2009 (1st experiment)	10.21958/phenotype:124	LI et al., 2010
125	DTF main Effect 2009	10.21958/phenotype:125	LI et al., 2010
126	DTF main Effect 2008	10.21958/phenotype:126	LI et al., 2010
127	Size Spain 2009 (2nd experiment)	10.21958/phenotype:127	LI et al., 2010
128	Size Spain 2009 (1st experiment)	10.21958/phenotype:128	LI et al., 2010
129	DTF planting Summer 2009	10.21958/phenotype:129	LI et al., 2010
130	DTF planting Summer 2008	10.21958/phenotype:130	LI et al., 2010
131	Size Main Effect 2009	10.21958/phenotype:131	LI et al., 2010
132	DTF Spain 2008 (1st experiment)	10.21958/phenotype:132	LI et al., 2010
133	Yield Planting Summer 2009	10.21958/phenotype:133	LI et al., 2010
134	DTF Sweden 2009 (1st experiment)	10.21958/phenotype:134	LI et al., 2010
135	Yield Loc Sweden 2009	10.21958/phenotype:135	LI et al., 2010
136	DTF Spain 2008 (2nd experiment)	10.21958/phenotype:136	LI et al., 2010
137	Yield Main Effect 2009	10.21958/phenotype:137	LI et al., 2010
138	Yield Planting Summer Loc Sweden 009	10.21958/phenotype:138	LI et al., 2010
139	Yield Sweden 2009 (1st experiment)	10.21958/phenotype:139	LI et al., 2010
140	DTF Sweden 2009 (2nd experiment)	10.21958/phenotype:140	LI et al., 2010

141	DTF Sweden 2008 (2nd experiment)	10.21958/phenotype:141	LI et al., 2010
142	Mature cell length	10.21958/phenotype:142	MEIJÓ et al., 2014
143	Meristem zone length	10.21958/phenotype:143	MEIJÓ et al., 2014
144	M216T665	10.21958/phenotype:144	STRAUCH et al., 2015
145	M130T666	10.21958/phenotype:145	STRAUCH et al., 2015
146	M172T666	10.21958/phenotype:146	STRAUCH et al., 2015
261	FT10	10.21958/phenotype:261	ALONSO-BLANCO et al., 2016
262	FT16	10.21958/phenotype:262	ALONSO-BLANCO et al., 2016
269	Li7	10.21958/phenotype:269	FORSBERG et al., 2015
270	B11	10.21958/phenotype:270	FORSBERG et al., 2015
271	Na23	10.21958/phenotype:271	FORSBERG et al., 2015
272	Mg25	10.21958/phenotype:272	FORSBERG et al., 2015
273	P31	10.21958/phenotype:273	FORSBERG et al., 2015
274	S34	10.21958/phenotype:274	FORSBERG et al., 2015
275	K39	10.21958/phenotype:275	FORSBERG et al., 2015
276	Ca43	10.21958/phenotype:276	FORSBERG et al., 2015
277	Mn55	10.21958/phenotype:277	FORSBERG et al., 2015
279	Co59	10.21958/phenotype:279	FORSBERG et al., 2015
280	Ni60	10.21958/phenotype:280	FORSBERG et al., 2015
281	Cu65	10.21958/phenotype:281	FORSBERG et al., 2015
282	Zn66	10.21958/phenotype:282	FORSBERG et al., 2015
283	As75	10.21958/phenotype:283	FORSBERG et al., 2015
284	Se82	10.21958/phenotype:284	FORSBERG et al., 2015

C Genomic prediction

C.1 GP ANN

```
1
2     import os,sys,gc
3 import pandas as pd
4 import numpy as np
5 import timeit
6 from datetime import datetime
7 import keras
8 import tensorflow as tf
9 from keras import backend as K
10 from keras import layers
11 from keras.models import Sequential
12 from keras.layers import Dense, Dropout, GaussianNoise,
    AlphaDropout, Reshape
13 from keras.layers import Flatten, LocallyConnected1D,
    LocallyConnected2D
14 from keras.optimizers import Adam, Adagrad, Adadelta
15 from keras.backend.tensorflow_backend import set_session
16
17 ##set default values
18
19 learning_rate = 0.01
20 JobID = 1
21 ps = 25
22 optim = "adam"
23 X_file = "KE.geno.csv"
24 Y_file = "KE.pheno.csv"
25 CV_file = "KE_cv_pw.csv"
26 label = "DtSILK"
27 start_time = timeit.default_timer()
```

```

28 act="relu"
29 drop_rate = str('0.5,0.5,0.5')
30 arc = str('63,63')
31 DG = 'D,D,D,D,D,G'
32 LC = True
33 training_epochs = 25
34 hyp = False
35
36 ### parse command line arguments
37
38 for i in range (1,len(sys.argv),2):
39     if sys.argv[i] == "-x":
40         X_file = sys.argv[i+1]
41     elif sys.argv[i] == "-y":
42         Y_file = sys.argv[i+1]
43     elif sys.argv[i] == "-cv":
44         CV_file = sys.argv[i+1]
45     elif sys.argv[i] == "-JobID":
46         JobID = int(sys.argv[i+1])
47     elif sys.argv[i] == "-label":
48         label = sys.argv[i+1]
49     elif sys.argv[i] == "-act":
50         act = str(sys.argv[i+1])
51     elif sys.argv[i] == "-epochs":
52         training_epochs = int(sys.argv[i+1])
53     elif sys.argv[i] == "-lr":
54         learning_rate = float(sys.argv[i+1])
55     elif sys.argv[i] == "-arc":
56         arc = sys.argv[i+1]
57     elif sys.argv[i] == "-ps":
58         ps = int(sys.argv[i+1])
59     elif sys.argv[i] == "-dr":
60         drop_rate=str(sys.argv[i+1])
61     elif sys.argv[i] == "-LC":
62         LC = bool(sys.argv[i+1])
63     elif sys.argv[i] == "hyp":
64         hyp = bool(sys.argv[i+1])
65     else:

```



```
66     print('unknown option ' + str(sys.argv[i]))
67     quit()
68
69
70
71 ## change dir to data location
72
73
74 #os.chdir('/home/jaf81qa/jan_storage/tens')
75 x = pd.read_csv(X_file, index_col = 0)
76 #os.chdir("/storage/full-share/genoPred/maze")
77 y = pd.read_csv(Y_file, index_col = 0)
78 cv_folds = pd.read_csv(CV_file, index_col=0)
79
80 ## select column of phenotype file via columnname
81
82 y = y[[label]]
83 ## activity_regularizer=regularizers.l1(0.01)))
84
85 def build_network(arc, drop_rate, LC, DG):
86     def add_drops(model, drop_out, k):
87         if DG[k].upper() == 'D':
88             model.add(Dropout(drop_out[0]))
89         elif DG[k].upper() == 'G':
90             model.add(GaussianNoise(drop_out[k]))
91         elif DG[k].upper() == "A":
92             model.add(AlphaDropout(drop_out[k]))
93         else:
94             pass
95     return model
96
97 DG = DG.strip().split(",")
98 arc = arc.strip().split(",")
99 archit = []
100 for layer in arc:
101     archit.append(int(layer))
102
103 layer_number = len(archit)
104 drop_rate = drop_rate.strip().split(",")
105 drop_out = []
```

```

104     for drops in drop_rate:
105         drop_out.append(float(drops))
106     model = Sequential()
107     if LC == True:
108         model.add(Reshape(input_shape=(x_train.shape[1],),
109 target_shape=(x_train.shape[1],1)))
110         model.add(LocallyConnected1D(1,10, strides=7, input_shape=(
111 x_train.shape[1],1)))
112         model.add(Flatten())
113         start = 0
114         model = add_drops(model, drop_out, start)
115     elif LC == False:
116         model.add(Dense(archit[0], kernel_initializer='
117 truncated_normal', activation=act, input_shape=(x_train.shape
118 [1],)))
119         model = add_drops(model, drop_out, start)
120         start = 1
121         for k in range(start, len(archit)):
122             model.add(Dense(archit[k], kernel_initializer='
123 truncated_normal', activation=act))
124             model = add_drops(model, drop_out, k)
125         model.add(Dense(1, kernel_initializer='truncated_normal'))
126         return(model)
127
128
129
130 config = tf.ConfigProto()
131 #config.gpu_options.per_process_gpu_memory_fraction = 0.1
132 config.gpu_options.allow_growth = True
133 set_session(tf.Session(config=config))
134
135 if not os.path.isfile("RESULTScv50.txt"):
136     out2 = open("RESULTScv50.txt", 'w')
137     out2.write('DateTime\tCompTime\tDF\tGenos\tPhenos\tCV_fold\t
138 tArchit\tConv\tActFun\tEpochs\tdrop_rate\tAccuracy\n' )
139
140 for k in range(1,51):

```

```
136     print("Training on cv fold "+ str(k))
137     cv = cv_folds['cv_' + str(k)]
138     num_cvs = np.ptp(cv) + 1
139
140     i = 1
141     x_train = x[cv != i]
142     x_test = x[cv == i]
143     y_train = y[cv != i]
144     y_test = y[cv == i]
145
146     yhat = np.zeros(shape = y_test.shape)
147
148     model = build_network(arc,drop_rate,LC,DG)
149     model.compile(loss='mse', optimizer=Adam(lr=0.01,decay = 0.001)
150 ,metrics=['accuracy'])
151     model.fit(x_train,y_train, epochs=training_epochs , verbose=0)
152 #     score = model.evaluate(x_test, y_test, verbose=0)
153     bla = model.predict(x_test)
154     y_sub= y[np.asarray(cv == i)]
155
156     print(model.summary())
157     print('\n')
158     print(label)
159
160     comp_time = int(round(timeit.default_timer() - start_time,0))
161
162     DateTime = datetime.now().strftime('%Y-%m-%d %H:%M:%S')
163     acc = np.corrcoef(bla[:,0],np.asarray(y_sub)[:,0])[0,1]
164
165     out2 = open("RESULTScv50.txt", 'a')
166     out2.write('%s\t%i\t%s\t%s\t%s\t%i\t%s\t%s\t%s\t%i\t%s\t%0.5f\n'
167 , % (
168         DateTime, comp_time, label, X_file, Y_file, int(k), arc, LC
169 , act,int(training_epochs), drop_rate, round(acc,4)))
170
171     del model,bla, x_train, x_test, y_train, y_test
172     K.clear_session()
173     gc.collect()
```

```

171
172 config = tf.ConfigProto()
173 #config.gpu_options.per_process_gpu_memory_fraction = 0.1
174 config.gpu_options.allow_growth = True
175 set_session(tf.Session(config=config))

```

C.2 GBLUP script

```

1  geno_pred <- function(phenocsv, genocsv, cvfcsv, cvf=1, mod = "BRR"
, label, phe)
2  {
3    my_phe <- phe
4    depends<- c("BGLR", "doBy", "doParallel", "R.utils", "BBmisc", "
dplyr")
5    foo <- sapply(depends,
6                  function(X){if(!suppressPackageStartupMessages(
require(X, character.only = T)){install.packages(X)}})
7    foo <- sapply(depends, function(X){
suppressPackageStartupMessages(library(X, character.only=TRUE))})
8    rm(foo)
9
10
11    maze <- read.csv(genocsv, row.names = 1)
12    phe <- read.csv(phenocsv, row.names = 1)
13    cvffolds <- read.csv(cvfcsv, row.names=1)
14
15    X <- scale(maze)
16    y <- phe[[label]]
17    if(any(is.na(y))){
18      rms <- which(is.na(y))
19      y <- y[-rms]
20      X <- X[-rms,]
21    }
22    for(i in 1:50){
23      cvf = i
24      n=length(y)
25      seed <- sample(1:100, 1)
26
                                     #set.seed(seed)

```

```

27                                     #folds=sample(1:cvf,size=n,
replace=T)
28     folds = cvffolds[,cvf]
29     yHatCV=rep(NA,n)
30
31     for(i in 1:max(folds)){
32         cat("Predicting cv-fold ",i," of ", max(folds))
33         tst=which(folds==i)
34         yNA=y
35         yNA[tst]=NA
36         fm=BGLR(y=yNA,ETA=list(list(X=X,model=mod)),verbose =F
,nIter=7000,burnIn=1000)
37         yHatCV[tst]=fm$yHat[tst]
38         cat("    done\n")
39     }
40
41     my_cor <- cor(yHatCV,y,use = "complete.obs")
42     print(c("Corrleation of GP", mod, my_cor))
43     filename = paste0(my_phe,"_gp_results.csv")
44     print(filename)
45     if(!any(dir() == filename)){
46         res <- matrix(ncol=8, nrow = 1) %>%
47             setColNames(c("geno","pheno","cv_folds","seed","
label", "cor","method","nmark"))
48         res[1,] <- c(as.character(genocsv),as.character(
phenocsv),as.character(cvf),as.character(seed),
49                     as.character(label),as.character(my_cor),
as.character(mod),dim(X)[2])
50         print("#####")
51         print(res)
52         print("#####")
53         write.csv(res,filename)
54     }else{
55         res <- read.csv(filename,row.names = 1)
56         for(i in 1:7){
57             res[,i] <- as.character(res[,i])
58         }

```

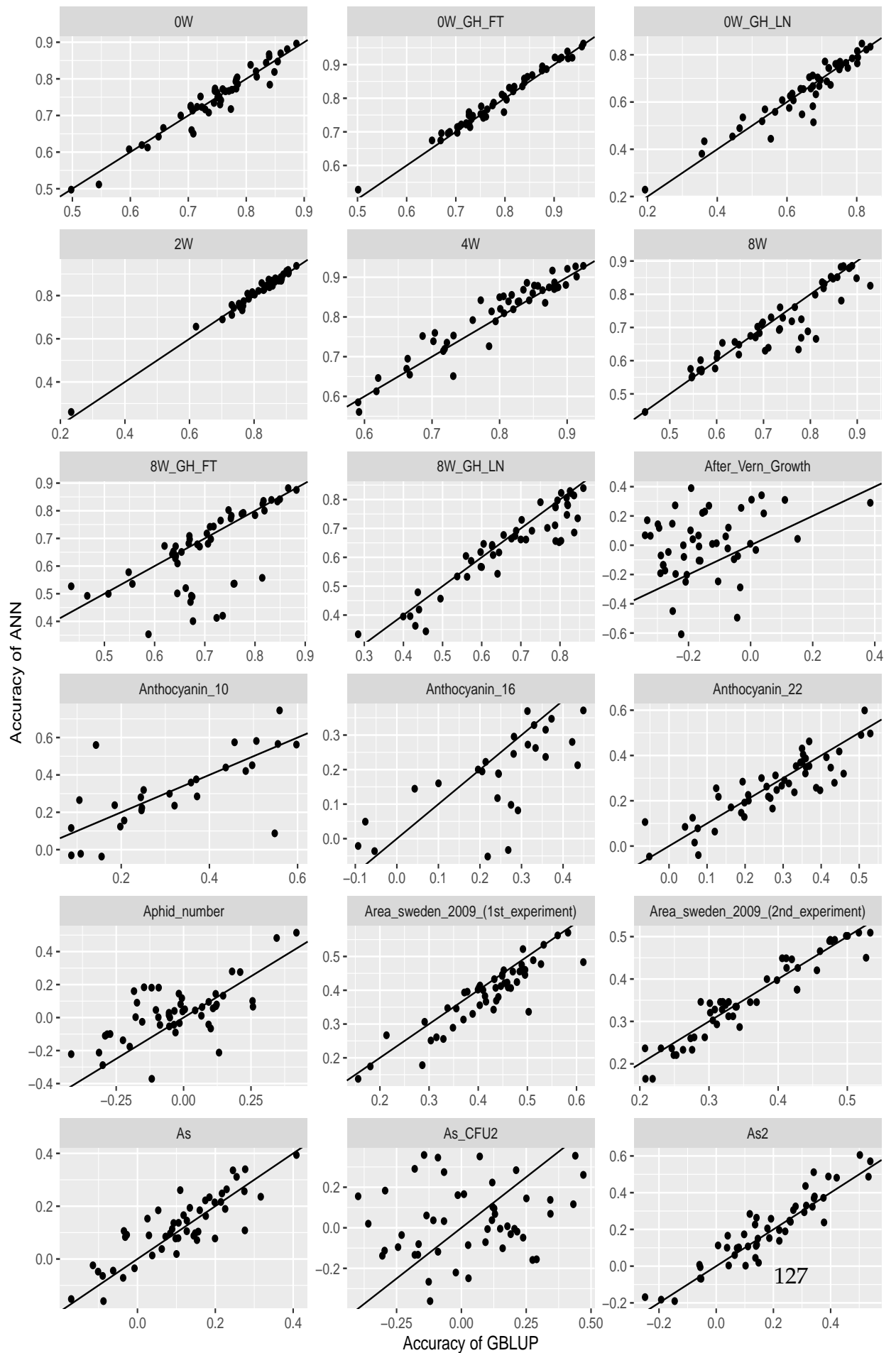
```

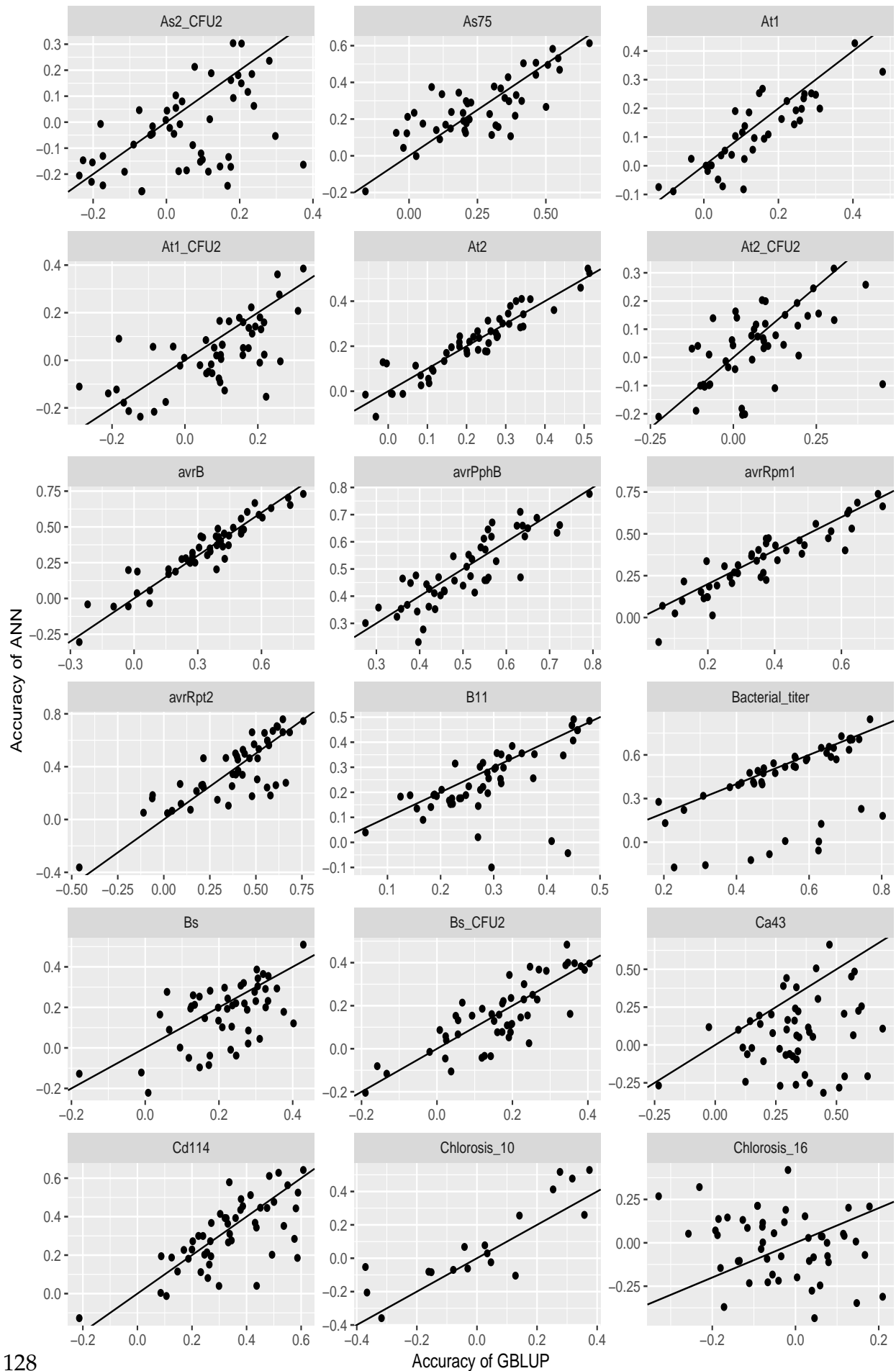
59         res[dim(res)[1]+1,] <- c(as.character(genocsv),phenocsv
, cvf, seed, as.character(label), my_cor, mod, dim(X)[2])
60         write.csv(res, filename)
61     }
62 }
63
64 }
65 ## execute this script with: Rscript ex.gblup.r -x genofile -y
phenofile -c cv file
66 source("~/PHD/Projects/gblup/bglr.r")
67
68
69 my.args <- commandArgs(trailingOnly = TRUE)
70 #my.args <- c("-x", "gent_genocsv", "-y" , "gent_pheno.csv")
71 ### set defaults
72 #cvf.name = NA
73
74 ## parsing the command line options
75 all.opts <- c("-x", "-y", "-label", "-h", "-cv", "-phe")
76 for(i in 1:length(my.args)){
77     if( i %% 2 == 1){
78         if(!my.args[i] %in% all.opts){
79             cat("unknown option", my.args[i], "Use only", all.opts
, "\n")
80             cat("use -h for help \n")
81             quit()
82         }
83     }
84     if(my.args[i] == "-x"){
85         geno.name <- as.character(my.args[i+1])
86     } else if(my.args[i] == "-y") {
87         pheno.name <- as.character(my.args[i+1])
88     } else if(my.args[i] == "-label") {
89         my_ph <- as.character(my.args[i+1])
90     } else if(my.args[i] == "-cv"){
91         cv.name = as.character(my.args[i+1])
92     } else if(my.args[i] == "-phe"){
93         my_phe <- as.character(my.args[i+1])

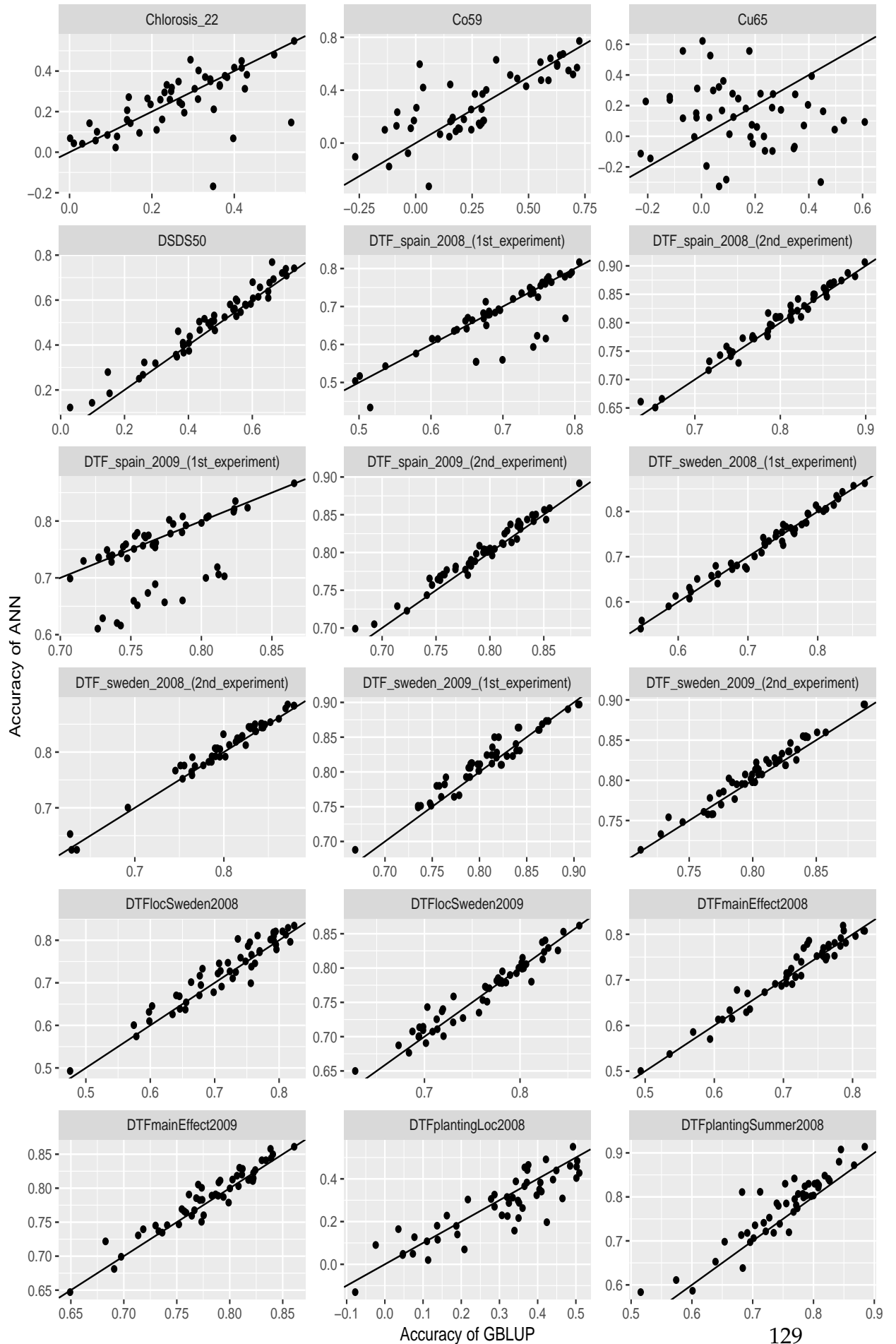
```

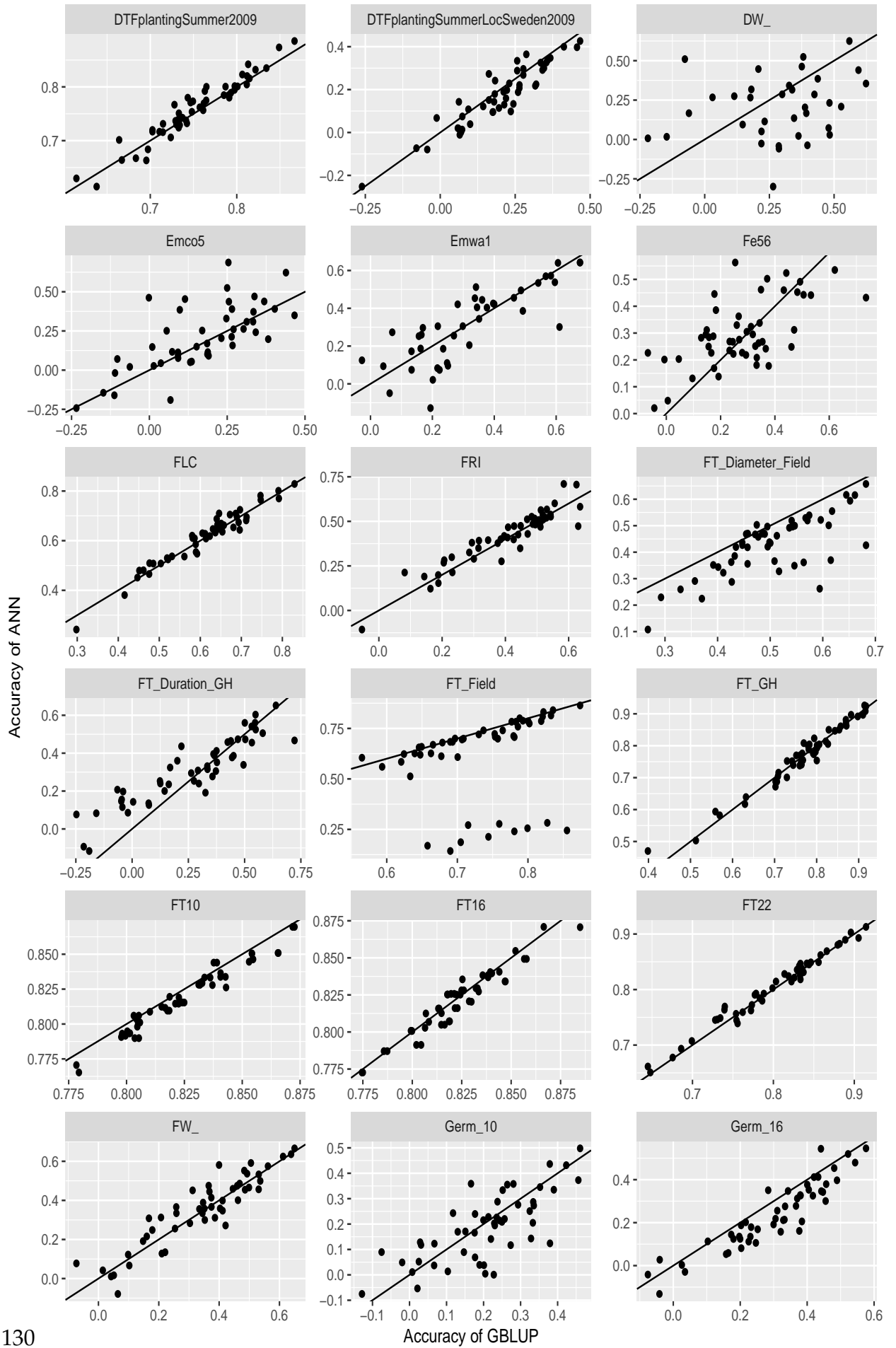
```
94     } else if(my.args[i] == "-h") {
95         print(" This script takes as a minimum two inputs\n")
96         print(" -x genotypefile")
97         print(" -y phenotypefile ")
98         print(" -cv cross-validadtion file : is optional if none is
specified random 5 fold cv will be used")
99         print(" -JobID : specify column number to use in your cross
validation file")
100        print(" -label : use header of phenotype file column you
want to use")
101        quit()
102    }
103 }
104
105
106 #pheno.name <- my.args[1]
107 #geno.name <- my.args[2]
108 #cvf.name <- my.args[3]
109
110 geno_pred(phencsv = pheno.name, genocsv=geno.name, cvfcsv = cv.name
, label=my_ph, mod = "BRR", phe =my_phe)
```

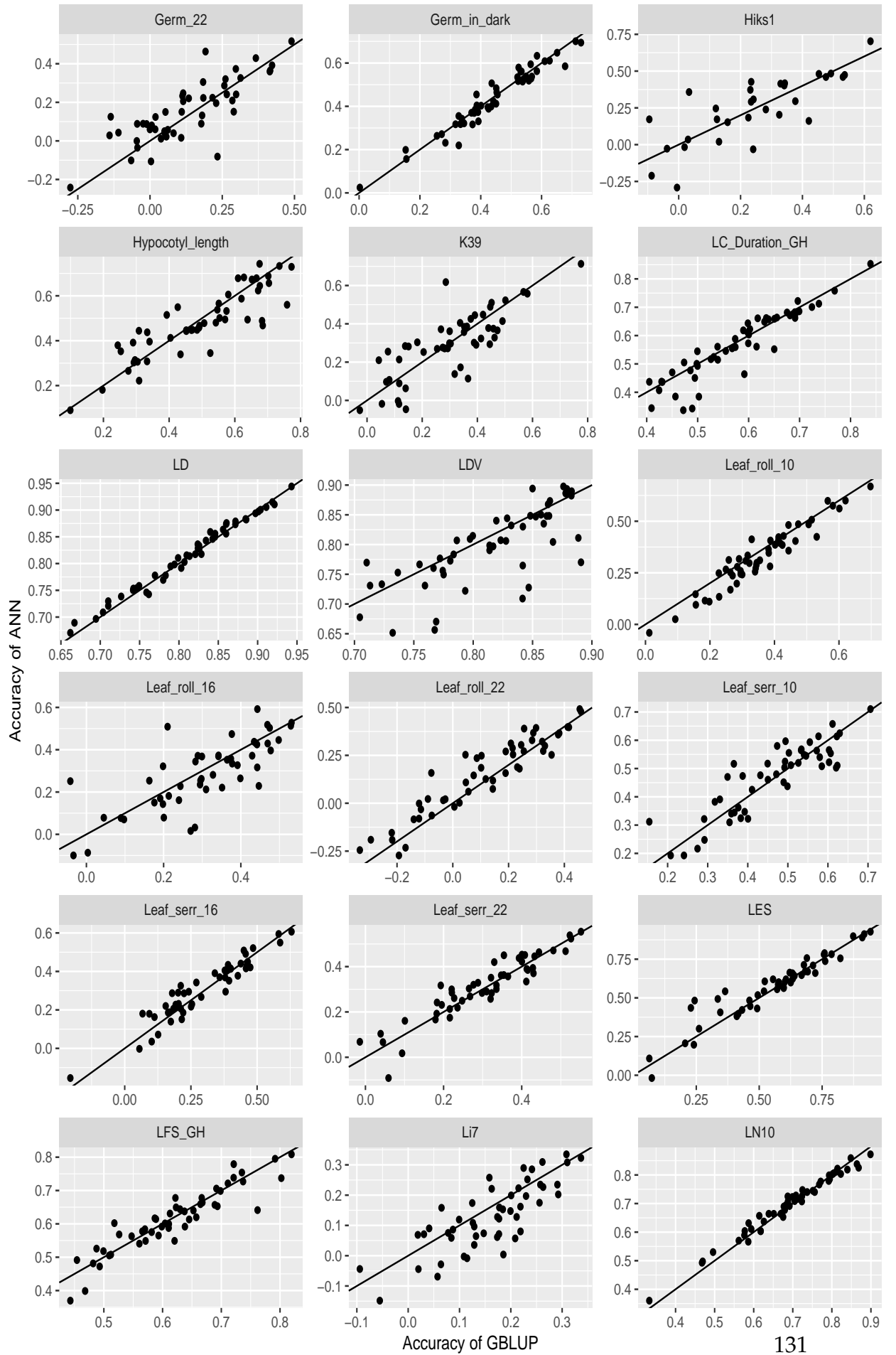

C.3 Results of GP

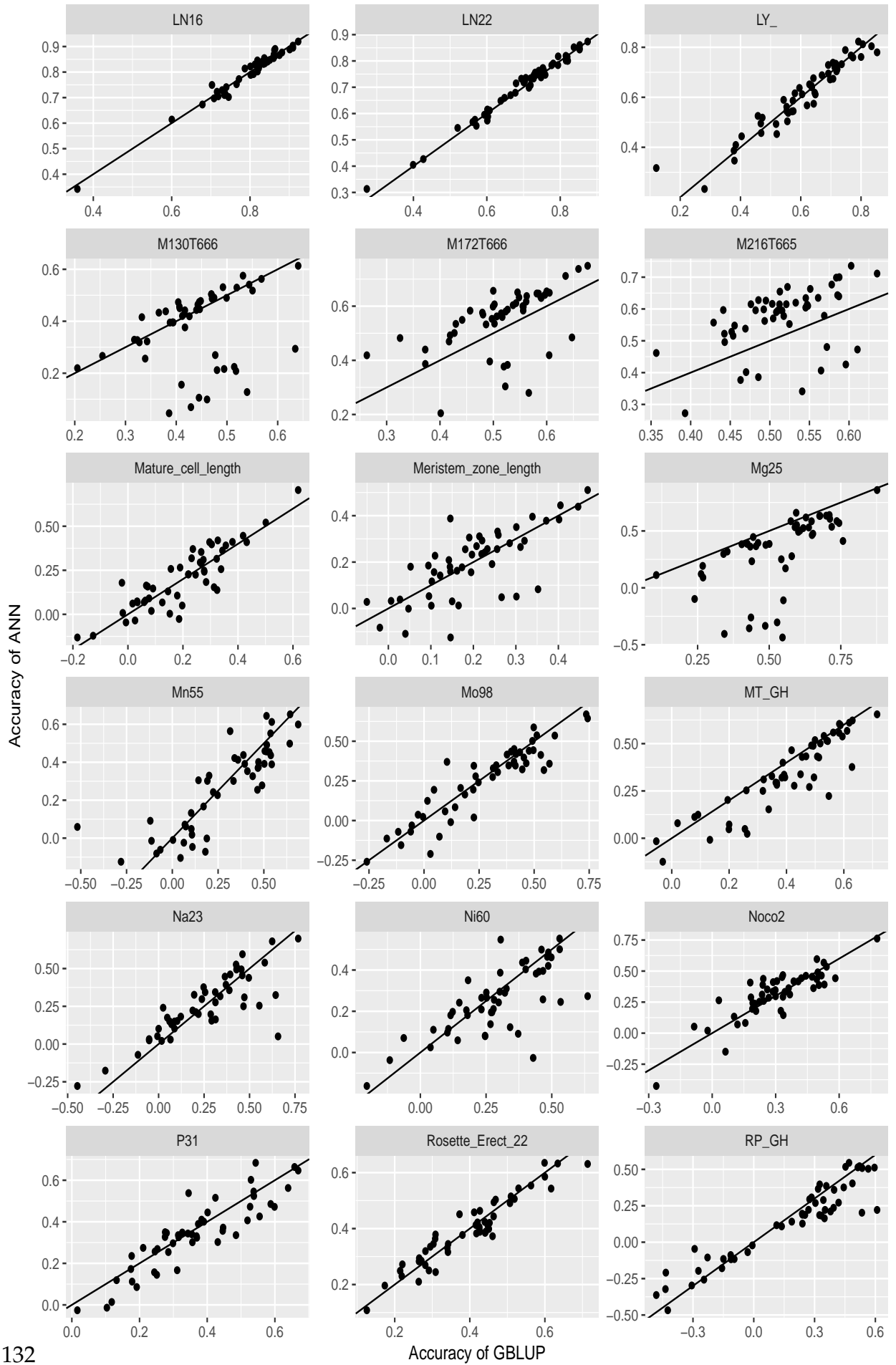


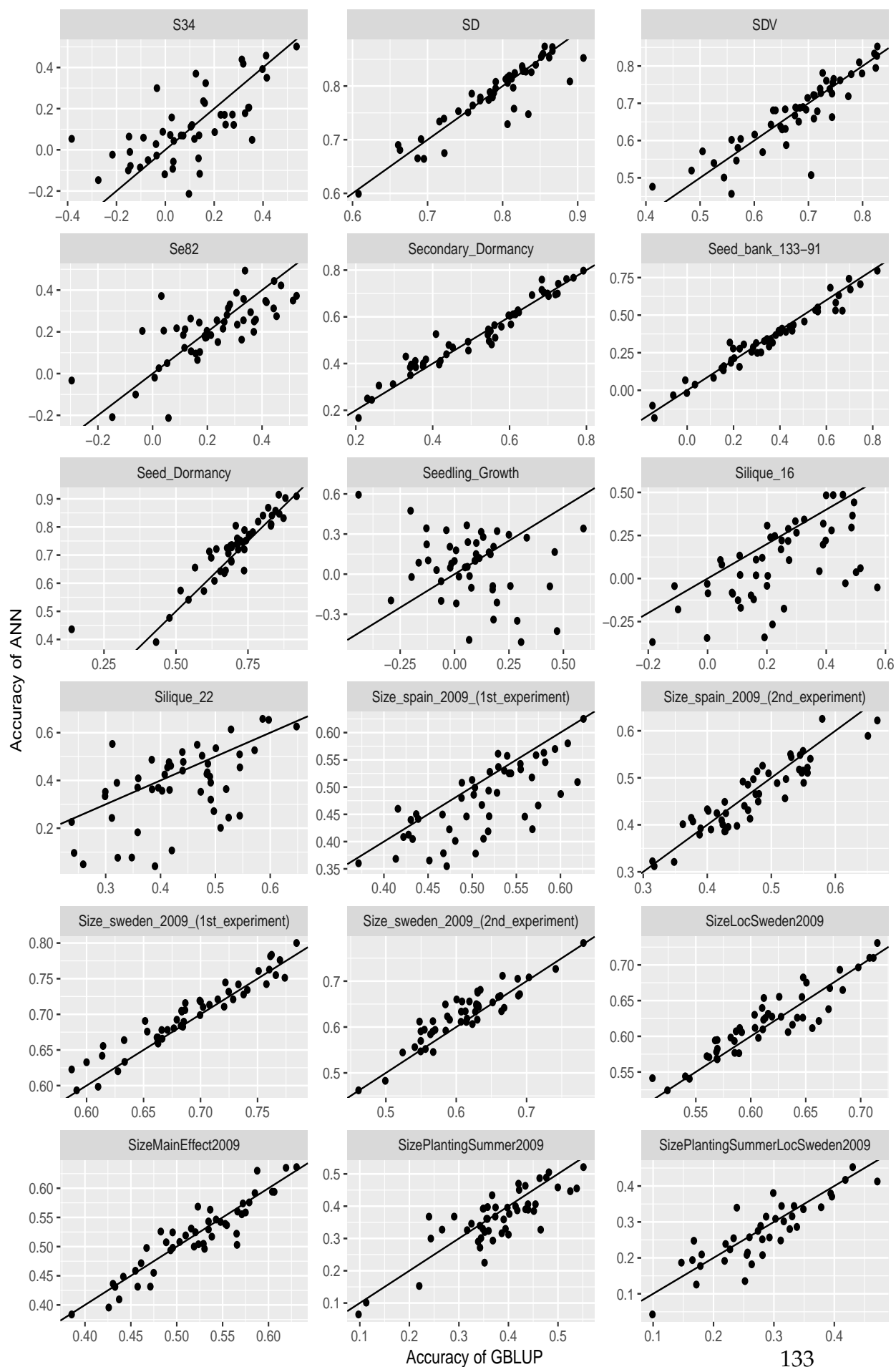


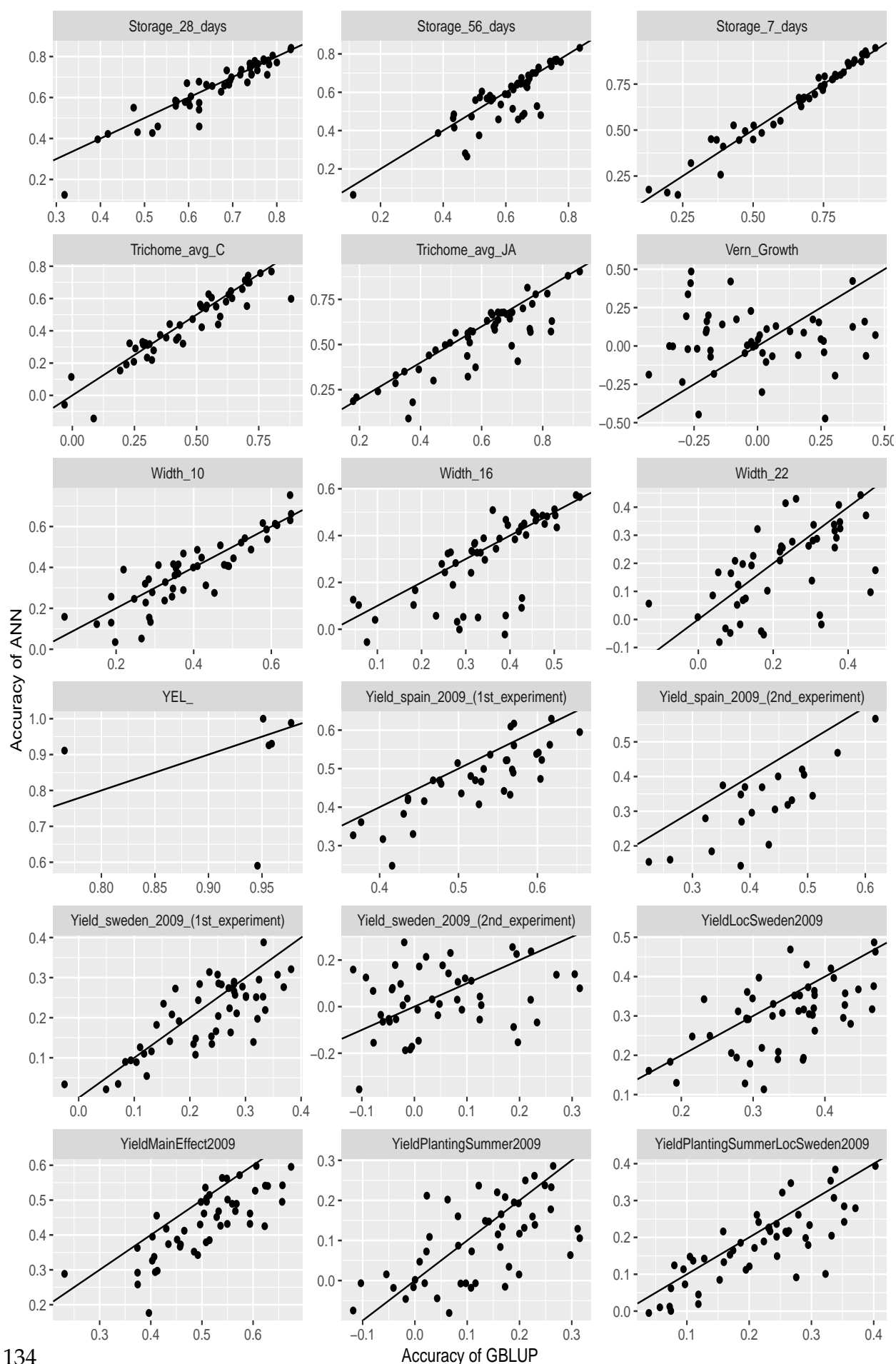


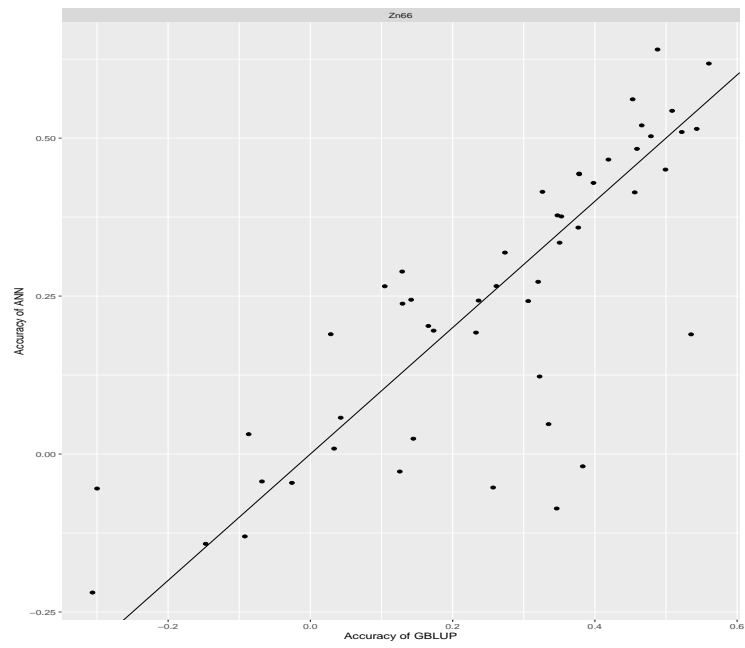












Bibliography

- ABADI, Martín et al. (2015). *TensorFlow: Large-Scale Machine Learning on Heterogeneous Systems*. Software available from tensorflow.org. URL: <https://www.tensorflow.org/>.
- ABADI, Martín et al. (2016). “TensorFlow: A System for Large-scale Machine Learning”. In: *Proceedings of the 12th USENIX Conference on Operating Systems Design and Implementation*. OSDI’16. Savannah, GA, USA: USENIX Association, pp. 265–283. ISBN: 978-1-931971-33-1. URL: <http://dl.acm.org/citation.cfm?id=3026877.3026899>.
- ALBRECHT, Theresa et al. (2011). “Genome-based prediction of testcross values in maize”. In: *Theoretical and Applied Genetics* 123.2, p. 339.
- ALLIER, Antoine et al. (2019). “Usefulness Criterion and post-selection Parental Contributions in Multi-parental Crosses: Application to Polygenic Trait Introgression”. In: *G3: Genes, Genomes, Genetics* 9.5, pp. 1469–1479.
- ALMEIDA FILHO, Janeo Eustáquio de et al. (2019). “Genomic Prediction of Additive and Non-additive Effects Using Genetic Markers and Pedigrees”. In: *G3: Genes, Genomes, Genetics* 9.8, pp. 2739–2748. DOI: [10.1534/g3.119.201004](https://doi.org/10.1534/g3.119.201004). URL: <https://doi.org/10.1534>.
- ALONSO-BLANCO, Carlos et al. (2016). “1,135 genomes reveal the global pattern of polymorphism in *Arabidopsis thaliana*”. In: *Cell* 166.2, pp. 481–491.
- AMIN, Najaf, Cornelia M VAN DUIJN, and Yurii S AULCHENKO (2007). “A genomic background based method for association analysis in related individuals”. In: *PloS one* 2.12, e1274.
- ANGERMUELLER, Christof et al. (2016). “Deep learning for computational biology”. In: *Molecular systems biology* 12.7, p. 878.
- ANKENBRAND, Markus et al. (Jan. 2018). “chloroExtractor: extraction and assembly of the chloroplast genome from whole genome shotgun data”. In: *The Journal of*

- Open Source Software* 3.21, p. 464. ISSN: 2475-9066. DOI: [10.21105/joss.00464](https://doi.org/10.21105/joss.00464). URL: <http://joss.theoj.org/papers/10.21105/joss.00464>.
- ANKENBRAND, Markus J. and Frank FÖRSTER (Apr. 2019). *Simulated Arabidopsis thaliana sequencing datasets for chloroplast assembler benchmarking*. DOI: [10.5281/zenodo.2622875](https://doi.org/10.5281/zenodo.2622875). URL: <https://doi.org/10.5281/zenodo.2622875>.
- ANKENBRAND, Markus J. et al. (June 2017). “AliTV—interactive visualization of whole genome comparisons”. In: *PeerJ Computer Science* 3, e116. ISSN: 2376-5992. DOI: [10.7717/peerj-cs.116](https://doi.org/10.7717/peerj-cs.116). URL: <https://doi.org/10.7717/peerj-cs.116>.
- ANNICCHIARICO, Paolo et al. (2015). “Accuracy of genomic selection for alfalfa biomass yield in different reference populations”. In: *BMC genomics* 16.1, p. 1020.
- ARCHIBALD, John M (2015). “Endosymbiosis and eukaryotic cell evolution”. In: *Current Biology* 25.19, R911–R921.
- ARTEAGA, María Clara et al. (2016). “Genomic variation in recently collected maize landraces from Mexico”. In: *Genomics Data* 7, pp. 38–45.
- ATWELL, S et al. (2010). “Genome-wide association study of 107 phenotypes in *Arabidopsis thaliana* inbred lines”. In: *Nature* 465(7298). DOI: [10.1038/nature08800](https://doi.org/10.1038/nature08800).
- AUINGER, Hans-Jürgen et al. (2016). “Model training across multiple breeding cycles significantly improves genomic prediction accuracy in rye (*Secale cereale* L.)” In: *Theoretical and Applied Genetics* 129.11, pp. 2043–2053.
- AZODI, Christina B et al. (2019). “Benchmarking algorithms for genomic prediction of complex traits”. In: *bioRxiv*, p. 614479.
- BAKKER, Freek T. et al. (Jan. 2016). “Herbarium genomics: plastome sequence assembly from a range of herbarium specimens using an Iterative Organelle Genome Assembly pipeline”. en. In: *Biological Journal of the Linnean Society* 117.1, pp. 33–43. ISSN: 00244066. DOI: [10.1111/bij.12642](https://doi.org/10.1111/bij.12642). URL: <https://academic.oup.com/biolinnean/article-lookup/doi/10.1111/bij.12642>.
- BELAMKAR, Vikas et al. (2018). “Genomic Selection in Preliminary Yield Trials in a Winter Wheat Breeding Program”. In: *G3: Genes, Genomes, Genetics* 8.8, pp. 2735–2747. DOI: [10.1534/g3.118.200415](https://doi.org/10.1534/g3.118.200415). URL: <https://doi.org/10.1534>.
- BENDICH, Arnold J. (1987). “Why do chloroplasts and mitochondria contain so many copies of their genome?” In: *BioEssays* 6.6, pp. 279–282. DOI: [10.1002/](https://doi.org/10.1002/)

- bies.950060608. eprint: <https://onlinelibrary.wiley.com/doi/pdf/10.1002/bies.950060608>. URL: <https://onlinelibrary.wiley.com/doi/abs/10.1002/bies.950060608>.
- BERARDINI, Tanya Z. et al. (2015). "The *Arabidopsis* information resource: Making and mining the "gold standard" annotated reference plant genome". In: *genesis* 53.8, pp. 474–485. DOI: 10.1002/dvg.22877. eprint: <https://onlinelibrary.wiley.com/doi/pdf/10.1002/dvg.22877>. URL: <https://onlinelibrary.wiley.com/doi/abs/10.1002/dvg.22877>.
- BERGSTRA, James S et al. (2011). "Algorithms for hyper-parameter optimization". In: *Advances in neural information processing systems*, pp. 2546–2554.
- BERNAL-VASQUEZ, Angela-Maria et al. (2014). "The importance of phenotypic data analysis for genomic prediction-a case study comparing different spatial models in rye". In: *BMC genomics* 15.1, p. 646.
- BERNAL-VASQUEZ, Angela-Maria et al. (2017). "Genomic prediction in early selection stages using multi-year data in a hybrid rye breeding program". In: *BMC genetics* 18.1, p. 51.
- BERNARDO, R (2010). *Breeding for quantitative traits in plants*. Tech. rep. Stemma Press.
- BERNARDO, Rex and Jianming YU (2007). "Prospects for genomewide selection for quantitative traits in maize". In: *Crop Science* 47.3, pp. 1082–1090.
- BIAZZI, Elisa et al. (2017). "Genome-wide association mapping and genomic selection for alfalfa (*Medicago sativa*) forage quality traits". In: *PLoS One* 12.1, e0169234.
- BISCARINI, Filippo et al. (2014). "Genome-enabled predictions for binomial traits in sugar beet populations". In: *BMC genetics* 15.1, p. 87.
- BOCK, Ralph (2017). "Witnessing genome evolution: experimental reconstruction of endosymbiotic and horizontal gene transfer". In: *Annual review of genetics* 51, pp. 1–22.
- BOTTOU, Léon (1991). "Stochastic gradient learning in neural networks". In: *Proceedings of Neuro-Nimes* 91.8, p. 12.
- BOTTOU, Léon and Olivier BOUSQUET (2008). "The Tradeoffs of Large Scale Learning". In: *Advances in Neural Information Processing Systems 20 (NIPS 2007)*. Ed.

- by J.C. PLATT et al. NIPS Foundation (<http://books.nips.cc>), pp. 161–168. URL: <http://leon.bottou.org/papers/bottou-bousquet-2008>.
- BOYLE, Evan A, Yang I LI, and Jonathan K PRITCHARD (2017). “An expanded view of complex traits: from polygenic to omnigenic”. In: *Cell* 169.7, pp. 1177–1186.
- BRAUNER, Pedro C et al. (2018). “Genomic prediction within and among doubled-haploid libraries from maize landraces”. In: *Genetics* 210.4, pp. 1185–1196.
- BRAUNER, Pedro C et al. (2019). “Testcross performance of doubled haploid lines from European flint maize landraces is promising for broadening the genetic base of elite germplasm”. In: *Theoretical and Applied Genetics* 132.6, pp. 1897–1908.
- BROOKER, Robert J (1999). *Genetics: analysis & principles*. Addison-Wesley Reading, MA.
- BROWNING, Brian L, Ying ZHOU, and Sharon R BROWNING (2018). “A one-penny imputed genome from next-generation reference panels”. In: *The American Journal of Human Genetics* 103.3, pp. 338–348.
- BROWNING, Sharon R and Brian L BROWNING (2007). “Rapid and accurate haplotype phasing and missing-data inference for whole-genome association studies by use of localized haplotype clustering”. In: *The American Journal of Human Genetics* 81.5, pp. 1084–1097.
- BUSTOS-KORTS, Daniela et al. (2016a). “Improvement of predictive ability by uniform coverage of the target genetic space”. In: *G3: Genes, Genomes, Genetics* 6.11, pp. 3733–3747.
- (2016b). “Improvement of Predictive Ability by Uniform Coverage of the Target Genetic Space”. In: *G3: Genes, Genomes, Genetics* 6.11, pp. 3733–3747. DOI: [10.1534/g3.116.035410](https://doi.org/10.1534/g3.116.035410). URL: <https://doi.org/10.1534>.
- CAMPOS, Gustavo De los and Paulino Perez RODRIGUEZ (2016). *BGLR: Bayesian Generalized Linear Regression*. R package version 1.0.5. URL: <https://CRAN.R-project.org/package=BGLR>.
- CHAN, Cheong Xin and Mark A. RAGAN (2013). “Next-generation phylogenomics”. In: *Biology direct* 8, pp. 3–3. ISSN: 1745-6150. DOI: [10.1186/1745-6150-8-3](https://doi.org/10.1186/1745-6150-8-3). URL: <https://www.ncbi.nlm.nih.gov/pubmed/23339707>.

- CHAT, J. et al. (July 2002). "A Case of Chloroplast Heteroplasmy in Kiwifruit (*Actinidia deliciosa*) That Is Not Transmitted During Sexual Reproduction". In: *Journal of Heredity* 93.4, pp. 293–300. ISSN: 0022-1503. DOI: [10.1093/jhered/93.4.293](https://doi.org/10.1093/jhered/93.4.293). eprint: <http://oup.prod.sis.lan/jhered/article-pdf/93/4/293/6454216/293.pdf>. URL: <https://doi.org/10.1093/jhered/93.4.293>.
- CHE, Ronglin et al. (2014). "An adaptive permutation approach for genome-wide association study: evaluation and recommendations for use". In: *BioData mining* 7.1, p. 9.
- CHOLLET, François et al. (2015). *Keras*. <https://keras.io>.
- COISSAC, Eric et al. (2016). "From barcodes to genomes: extending the concept of DNA barcoding". In: *Molecular Ecology* 25.7, pp. 1423–1428. ISSN: 1365-294X. DOI: [10.1111/mec.13549](https://doi.org/10.1111/mec.13549). URL: <https://onlinelibrary.wiley.com/doi/abs/10.1111/mec.13549> (visited on 05/16/2019).
- COLLETTE, Andrew (2013). *Python and HDF5*. O'Reilly.
- CORRIVEAU, Joseph L. and Annette W. COLEMAN (1988). "Rapid Screening Method to Detect Potential Biparental Inheritance of Plastid DNA and Results for Over 200 Angiosperm Species". In: *American Journal of Botany* 75.10, pp. 1443–1458. ISSN: 00029122, 15372197. URL: <http://www.jstor.org/stable/2444695>.
- CROSSA, José et al. (2010). "Prediction of genetic values of quantitative traits in plant breeding using pedigree and molecular markers". In: *Genetics*.
- CROSSA, José et al. (2016). "Genomic Prediction of Gene Bank Wheat Landraces". In: *G3: Genes, Genomes, Genetics* 6.7, pp. 1819–1834. DOI: [10.1534/g3.116.029637](https://doi.org/10.1534/g3.116.029637). URL: <https://doi.org/10.1534>.
- CROSSA, José et al. (2017). "Genomic selection in plant breeding: Methods, models, and perspectives". In: *Trends in plant science*.
- CUEVAS, Jaime et al. (2019a). "Deep Kernel for Genomic and Near Infrared Predictions in Multi-environment Breeding Trials". In: *G3: Genes, Genomes, Genetics* 9.9, pp. 2913–2924. DOI: [10.1534/g3.119.400493](https://doi.org/10.1534/g3.119.400493). URL: <https://doi.org/10.1534>.
- CUEVAS, Jaime et al. (2019b). "Deep Kernel for Genomic and Near Infrared Predictions in Multi-environment Breeding Trials". In: *G3: Genes, Genomes, Genetics* 9.9, pp. 2913–2924.

- DANIELL, Henry et al. (June 23, 2016). "Chloroplast genomes: diversity, evolution, and applications in genetic engineering". In: *Genome Biology* 17. ISSN: 1474-7596. DOI: [10.1186/s13059-016-1004-2](https://doi.org/10.1186/s13059-016-1004-2). URL: <https://www.ncbi.nlm.nih.gov/pmc/articles/PMC4918201/> (visited on 05/20/2019).
- DARWIN, Charles (1859). *On the Origin of Species by Means of Natural Selection, or the Preservation of Favored Races in the Struggle for Life*. London: Murray.
- DE LOS CAMPOS, Gustavo et al. (2009). "Predicting quantitative traits with regression models for dense molecular markers and pedigree". In: *Genetics* 182.1, pp. 375–385.
- DE RUBEIS, Silvia et al. (2014). "Synaptic, transcriptional and chromatin genes disrupted in autism". In: *Nature* 515.7526, p. 209.
- DEINER, Kristy et al. (2017). "Environmental DNA metabarcoding: Transforming how we survey animal and plant communities". In: *Molecular Ecology* 26.21, pp. 5872–5895. ISSN: 1365-294X. DOI: [10.1111/mec.14350](https://doi.org/10.1111/mec.14350). URL: <https://onlinelibrary.wiley.com/doi/abs/10.1111/mec.14350> (visited on 05/21/2019).
- DESTA, Zeratsion Abera and Rodomiro ORTIZ (2014). "Genomic selection: genome-wide prediction in plant improvement". In: *Trends in plant science* 19.9, pp. 592–601.
- DIERCKXSENS, Nicolas, Patrick MARDULYN, and Guillaume SMITS (Feb. 28, 2017). "NOVOPlasty: de novo assembly of organelle genomes from whole genome data". In: *Nucleic Acids Research* 45.4, e18–e18. ISSN: 0305-1048. DOI: [10.1093/nar/gkw955](https://doi.org/10.1093/nar/gkw955). URL: <https://academic.oup.com/nar/article/45/4/e18/2290925> (visited on 01/26/2018).
- Docker Hub Group for Benchmark Project. URL: <https://cloud.docker.com/u/chloroextractorteam/>.
- DOS SANTOS, Cicero and Maira GATTI (2014). "Deep convolutional neural networks for sentiment analysis of short texts". In: *Proceedings of COLING 2014, the 25th International Conference on Computational Linguistics: Technical Papers*, pp. 69–78.
- DOZAT, Timothy (2016). "Incorporating nesterov momentum into adam". In:

- EL-DIEN, Omnia Gamal et al. (2016). "Implementation of the Realized Genomic Relationship Matrix to Open-Pollinated White Spruce Family Testing for Disentangling Additive from Nonadditive Genetic Effects". In: *G3: Genes, Genomes, Genetics* 6.3, pp. 743–753. DOI: [10.1534/g3.115.025957](https://doi.org/10.1534/g3.115.025957). URL: <https://doi.org/10.1534>.
- ELIAS, Ani A et al. (2018a). "Improving genomic prediction in cassava field experiments by accounting for interplot competition". In: *G3: Genes, Genomes, Genetics* 8.3, pp. 933–944.
- (2018b). "Improving genomic prediction in cassava field experiments using spatial analysis". In: *G3: Genes, Genomes, Genetics* 8.1, pp. 53–62.
- ENCISO-RODRIGUEZ, Felix et al. (2018). "Genomic selection for late blight and common scab resistance in tetraploid potato (*Solanum tuberosum*)". In: *G3: Genes, Genomes, Genetics* 8.7, pp. 2471–2481.
- ENDELMAN, Jeffrey B. et al. (Mar. 2018). "Genetic Variance Partitioning and Genome-Wide Prediction with Allele Dosage Information in Autotetraploid Potato". In: *Genetics* 209.1, pp. 77–87. DOI: [10.1534/genetics.118.300685](https://doi.org/10.1534/genetics.118.300685). URL: <https://doi.org/10.1534/genetics.118.300685>.
- FALCONER, DS and TFC MACKAY (1996). "Introduction to quantitative genetics. 1996". In: *Harlow, Essex, UK: Longmans Green* 3.
- FAN, Jianqing, Fang HAN, and Han LIU (2014). "Challenges of big data analysis". In: *National science review* 1.2, pp. 293–314.
- FELDMAN, Moshe and Avraham A LEVY (2012). "Genome evolution due to allopolyploidization in wheat". In: *Genetics* 192.3, pp. 763–774.
- FISHER, Ronald A (1919). "XV.—The correlation between relatives on the supposition of Mendelian inheritance." In: *Earth and Environmental Science Transactions of the Royal Society of Edinburgh* 52.2, pp. 399–433.
- FORSBERG, Simon K. G. et al. (2015). "The Multi-allelic Genetic Architecture of a Variance-Heterogeneity Locus for Molybdenum Concentration in Leaves Acts as a Source of Unexplained Additive Genetic Variance". In: *PLOS Genetics* None. DOI: [10.1371/journal.pgen.1005648](https://doi.org/10.1371/journal.pgen.1005648).

- FÖRSTER, Frank and Markus J. ANKENBRAND (May 2019). *chloroExtractorTeam/benchmark: Benchmark container setup v2.0.1*. DOI: [10.5281/zenodo.2628061](https://doi.org/10.5281/zenodo.2628061). URL: <https://doi.org/10.5281/zenodo.2628061>.
- FREUDENTHAL, Jan A. et al. (2019a). "GWAS-Flow: A GPU accelerated framework for efficient permutation based genome-wide association studies". In: DOI: [10.1101/783100](https://doi.org/10.1101/783100). URL: <https://doi.org/10.1101>.
- FREUDENTHAL, Jan A et al. (2019b). "The landscape of chloroplast genome assembly tools". In: *bioRxiv*, p. 665869.
- FRIEBE, B et al. (2000). "Development of a complete set of Triticum aestivum-Aegilops speltoides chromosome addition lines". In: *Theoretical and Applied Genetics* 101.1-2, pp. 51–58.
- FUENTES, Ignacia et al. (2014). "Horizontal genome transfer as an asexual path to the formation of new species". In: *Nature* 511.7508, p. 232.
- GAPARE, Washington et al. (2018). "Historical Datasets Support Genomic Selection Models for the Prediction of Cotton Fiber Quality Phenotypes Across Multiple Environments". In: *G3: Genes, Genomes, Genetics* 8.5, pp. 1721–1732.
- GHOSH, Sreya et al. (2018). "Speed breeding in growth chambers and glasshouses for crop breeding and model plant research". In: *Nature protocols* 13.12, p. 2944.
- GIANOLA, Daniel (2013). "Priors in whole-genome regression: the Bayesian alphabet returns". In: *Genetics* 194.3, pp. 573–596.
- GIANOLA, Daniel and Johannes BCHM van KAAM (2008). "Reproducing kernel Hilbert spaces regression methods for genomic assisted prediction of quantitative traits". In: *Genetics* 178.4, pp. 2289–2303.
- GIANOLA, Daniel and Guilherme JM ROSA (2015). "One hundred years of statistical developments in animal breeding". In: *Annu. Rev. Anim. Biosci.* 3.1, pp. 19–56.
- GIANOLA, Daniel et al. (2009). "Additive genetic variability and the Bayesian alphabet". In: *Genetics* 183.1, pp. 347–363.
- GIANOLA, Daniel et al. (2016). "Genome-Wide Association Studies with a Genomic Relationship Matrix: A Case Study with Wheat and Arabidopsis". In: *G3: Genes, Genomes, Genetics* 6.10, pp. 3241–3256. DOI: [10.1534/g3.116.034256](https://doi.org/10.1534/g3.116.034256). URL: <https://doi.org/10.1534>.

- GitHub Repository for Benchmark Project. URL: <https://github.com/chloroExtractorTeam/benchmark>.
- GLOTOT, Xavier, Antoine BORDES, and Yoshua BENGIO (2011). "Deep sparse rectifier neural networks". In: *Proceedings of the fourteenth international conference on artificial intelligence and statistics*, pp. 315–323.
- GODDARD, Michael E and Ben J HAYES (2009). "Mapping genes for complex traits in domestic animals and their use in breeding programmes". In: *Nature Reviews Genetics* 10.6, p. 381.
- GODDARD, Michael E, Ben J HAYES, and Theo HE MEUWISSEN (2011). "Using the genomic relationship matrix to predict the accuracy of genomic selection". In: *Journal of animal breeding and genetics* 128.6, pp. 409–421.
- GONZÁLEZ-CAMACHO, JM et al. (2012). "Genome-enabled prediction of genetic values using radial basis function neural networks". In: *Theoretical and Applied Genetics* 125.4, pp. 759–771.
- GONZÁLEZ-CAMACHO, Juan Manuel et al. (2016). "Genome-enabled prediction using probabilistic neural network classifiers". In: *BMC genomics* 17.1, p. 208.
- GONZÁLEZ-CAMACHO, Juan Manuel et al. (2018). "Applications of machine learning methods to genomic selection in breeding wheat for rust resistance". In: *The plant genome* 11.2.
- GOODFELLOW, Ian, Yoshua BENGIO, and Aaron COURVILLE (2016). *Deep learning*. MIT press.
- GOUY, Matthieu et al. (2013). "Experimental assessment of the accuracy of genomic selection in sugarcane". In: *Theoretical and applied genetics* 126.10, pp. 2575–2586.
- GREEN, Beverley R. (2011). "Chloroplast genomes of photosynthetic eukaryotes". In: *The Plant Journal* 66.1, pp. 34–44. ISSN: 1365-313X. DOI: [10.1111/j.1365-313X.2011.04541.x](https://doi.org/10.1111/j.1365-313X.2011.04541.x). URL: <https://onlinelibrary.wiley.com/doi/abs/10.1111/j.1365-313X.2011.04541.x> (visited on 05/16/2019).
- GRENIER, Cécile et al. (2015). "Accuracy of genomic selection in a rice synthetic population developed for recurrent selection breeding". In: *PloS one* 10.8, e0136594.

- GRINBERG, Nastasiya F, Oghenejokpeme I ORHOBOR, and Ross D KING (2018). "An Evaluation of Machine-learning for Predicting Phenotype: Studies in Yeast, Rice and Wheat". In: *BioRxiv*, p. 105528.
- GUO, Zhigang et al. (2013). "Accuracy of across-environment genome-wide prediction in maize nested association mapping populations". In: *G3: Genes, Genomes, Genetics* 3.2, pp. 263–272.
- HABIER, David, Rohan L FERNANDO, and Jack CM DEKKERS (2007). "The impact of genetic relationship information on genome-assisted breeding values". In: *Genetics* 177.4, pp. 2389–2397.
- HABIER, David et al. (2011). "Extension of the Bayesian alphabet for genomic selection". In: *BMC bioinformatics* 12.1, p. 186.
- HAHNLOSER, Richard HR et al. (2000). "Digital selection and analogue amplification coexist in a cortex-inspired silicon circuit". In: *Nature* 405.6789, p. 947.
- HARRIS, BL, DL JOHNSON, RJ SPELMAN, et al. (2009). "Genomic selection in New Zealand and the implications for national genetic evaluation." In: *ICAR Technical Series* 13, pp. 325–330.
- HASSEN, Manel Ben et al. (May 2018). "Genomic Prediction Accounting for Genotype by Environment Interaction Offers an Effective Framework for Breeding Simultaneously for Adaptation to an Abiotic Stress and Performance Under Normal Cropping Conditions in Rice". In: *G3: Genes, Genomes, Genetics* 8.7, pp. 2319–2332. DOI: [10.1534/g3.118.200098](https://doi.org/10.1534/g3.118.200098). URL: <https://doi.org/10.1534/g3.118.200098>.
- HAWKINS, Charles and Long-Xi YU (2018). "Recent progress in alfalfa (*Medicago sativa* L.) genomics and genomic selection". In: *The Crop Journal* 6.6, pp. 565–575.
- HAYES, Ben and Mike GODDARD (2010). "Genome-wide association and genomic selection in animal breeding". In: *Genome* 53.11, pp. 876–883.
- HAYES, BJ, ME GODDARD, et al. (2001). "Prediction of total genetic value using genome-wide dense marker maps". In: *Genetics* 157.4, pp. 1819–1829.
- HE, Kaiming et al. (2016). "Deep residual learning for image recognition". In: *Proceedings of the IEEE conference on computer vision and pattern recognition*, pp. 770–778.

- HEFFNER, Elliot L, Jean-Luc JANNINK, and Mark E SORRELLS (2011). "Genomic selection accuracy using multifamily prediction models in a wheat breeding program". In: *The Plant Genome* 4.1, pp. 65–75.
- HEFFNER, Elliot L et al. (2010). "Plant breeding with genomic selection: gain per unit time and cost". In: *Crop science* 50.5, pp. 1681–1690.
- HENDERSON, Charles R (1975). "Best linear unbiased estimation and prediction under a selection model". In: *Biometrics*, pp. 423–447.
- HINTON, Geoffrey, Nitish SRIVASTAVA, and Kevin SWERSKY (2012). "Neural networks for machine learning lecture 6a overview of mini-batch gradient descent". In: *Cited on* 14, p. 8.
- HIRSCHHORN, Joel N. and Mark J. DALY (2005). "Genome-wide association studies for common diseases and complex traits". In: *Nature Reviews Genetics* 6.2, pp. 95–108. ISSN: 1471-0064. DOI: [10.1038/nrg1521](https://doi.org/10.1038/nrg1521). URL: <https://doi.org/10.1038/nrg1521>.
- HÖLKER, Armin C et al. (2019). "European maize landraces made accessible for plant breeding and genome-based studies". In: *Theoretical and Applied Genetics*, pp. 1–13.
- HOLLIDAY, Jason A., Tongli WANG, and Sally AITKEN (2012). "Predicting Adaptive Phenotypes From Multilocus Genotypes in Sitka Spruce (*Picea sitchensis*) Using Random Forest". In: *G3: Genes, Genomes, Genetics* 2.9, pp. 1085–1093. DOI: [10.1534/g3.112.002733](https://doi.org/10.1534/g3.112.002733). URL: <https://doi.org/10.1534>.
- HOWARD, Réka et al. (2019). "Joint Use of Genome, Pedigree, and Their Interaction with Environment for Predicting the Performance of Wheat Lines in New Environments". In: *G3: Genes, Genomes, Genetics* 9.9, pp. 2925–2934. DOI: [10.1534/g3.119.400508](https://doi.org/10.1534/g3.119.400508). URL: <https://doi.org/10.1534>.
- HU, Yaodong et al. (2015). "Prediction of plant height in *Arabidopsis thaliana* using DNA methylation data". In: *Genetics* 201.2, pp. 779–793.
- ISIK, F (2013). *Genomic Relationships and GBLUP*.
- JAN, Habib U et al. (2016). "Genomic prediction of testcross performance in canola (*Brassica napus*)". In: *PLoS One* 11.1, e0147769.
- JANOCHA, Katarzyna and Wojciech Marian CZARNECKI (2017). "On loss functions for deep neural networks in classification". In: *arXiv preprint arXiv:1702.05659*.

- JARAMILLO-CORREA, Juan-Pablo et al. (2014). "Molecular Proxies for Climate Maladaptation in a Long-Lived Tree (*Pinus pinaster* Aiton, Pinaceae)". In: *Genetics* 199.3, pp. 793–807. DOI: [10.1534/genetics.114.173252](https://doi.org/10.1534/genetics.114.173252). URL: <https://doi.org/10.1534>.
- JARQUIN, Diego, James SPECHT, and Aaron LORENZ (2016). "Prospects of Genomic Prediction in the USDA Soybean Germplasm Collection: Historical Data Creates Robust Models for Enhancing Selection of Accessions". In: *G3: Genes, Genomes, Genetics* 6.8, pp. 2329–2341. DOI: [10.1534/g3.116.031443](https://doi.org/10.1534/g3.116.031443). URL: <https://doi.org/10.1534>.
- JETTE, Morris A., Andy B. YOO, and Mark GRONDONA (2002). "SLURM: Simple Linux Utility for Resource Management". In: *Lecture Notes in Computer Science: Proceedings of Job Scheduling Strategies for Parallel Processing (JSSPP) 2003*. Springer-Verlag, pp. 44–60.
- JIANG, Yong and Jochen C REIF (2015). "Modeling epistasis in genomic selection". In: *Genetics* 201.2, pp. 759–768.
- JIN, Jian-Jun et al. (Mar. 2018). "GetOrganelle: a simple and fast pipeline for de novo assembly of a complete circular chloroplast genome using genome skimming data". In: *bioRxiv*. DOI: [10.1101/256479](https://doi.org/10.1101/256479). URL: <http://biorxiv.org/lookup/doi/10.1101/256479>.
- KADAM, Dnyaneshwar C et al. (2016). "Genomic prediction of single crosses in the early stages of a maize hybrid breeding pipeline". In: *G3: Genes, Genomes, Genetics* 6.11, pp. 3443–3453.
- KAINER, David et al. (2018). "Accuracy of Genomic Prediction for Foliar Terpene Traits in *Eucalyptus polybractea*". In: *G3: Genes, Genomes, Genetics* 8.8, pp. 2573–2583. DOI: [10.1534/g3.118.200443](https://doi.org/10.1534/g3.118.200443). URL: <https://doi.org/10.1534>.
- KALO, P et al. (2004). "Comparative mapping between *Medicago sativa* and *Pisum sativum*". In: *Molecular Genetics and Genomics* 272.3, pp. 235–246.
- KANG, Hyun Min et al. (2010). "Variance component model to account for sample structure in genome-wide association studies". In: *Nature genetics* 42.4, p. 348.
- KÄRKKÄINEN, Hanni P and Mikko J SILLANPÄÄ (2012). "Back to basics for Bayesian model building in genomic selection". In: *Genetics* 191.3, pp. 969–987.

- KIM, Sung et al. (2007). "Recombination and linkage disequilibrium in *Arabidopsis thaliana*". In: *Nature genetics* 39.9, p. 1151.
- KINGMA, Diederik P and Jimmy BA (2014). "Adam: A method for stochastic optimization". In: *arXiv preprint arXiv:1412.6980*.
- KINGSBURY, Noel (2009). *Hybrid: the history and science of plant breeding*. University of Chicago Press.
- KINGSOLVER, Joel G et al. (2001). "The strength of phenotypic selection in natural populations". In: *The American Naturalist* 157.3, pp. 245–261.
- KOCH, Marcus A and Michaela MATSCHINGER (2007). "Evolution and genetic differentiation among relatives of *Arabidopsis thaliana*". In: *Proceedings of the National Academy of Sciences* 104.15, pp. 6272–6277.
- KORTE, Arthur and Ashley FARLOW (2013). "The advantages and limitations of trait analysis with GWAS: a review". In: *Plant methods* 9.1, p. 29.
- KORTE, Arthur et al. (2012). "A mixed-model approach for genome-wide association studies of correlated traits in structured populations". In: *Nature genetics* 44.9, p. 1066.
- KRAUSE, Margaret R. et al. (2019). "Hyperspectral Reflectance-Derived Relationship Matrices for Genomic Prediction of Grain Yield in Wheat". In: *G3: Genes, Genomes, Genetics*, g3.200856.2018. DOI: [10.1534/g3.118.200856](https://doi.org/10.1534/g3.118.200856). URL: <https://doi.org/10.1534/g3.118.200856>.
- KUMAR, Rachana A., Delene J. OLDENBURG, and Arnold J. BENDICH (Sept. 2014). "Changes in DNA damage, molecular integrity, and copy number for plastid DNA and mitochondrial DNA during maize development". In: *Journal of Experimental Botany* 65.22, pp. 6425–6439. ISSN: 0022-0957. DOI: [10.1093/jxb/eru359](https://doi.org/10.1093/jxb/eru359). eprint: <http://oup.prod.sis.lan/jxb/article-pdf/65/22/6425/16935653/eru359.pdf>. URL: <https://doi.org/10.1093/jxb/eru359>.
- KUMAR, Satish et al. (2015). "Genome-Enabled Estimates of Additive and Nonadditive Genetic Variances and Prediction of Apple Phenotypes Across Environments". In: *G3: Genes, Genomes, Genetics* 5.12, pp. 2711–2718. DOI: [10.1534/g3.115.021105](https://doi.org/10.1534/g3.115.021105). URL: <https://doi.org/10.1534/g3.115.021105>.
- KURTZER, Gregory M, Vanessa SOCHAT, and Michael W BAUER (2017). "Singularity: Scientific containers for mobility of compute". In: *PloS one* 12.5, e0177459.

- KUTSCHERA, Ulrich and Karl J NIKLAS (2005). "Endosymbiosis, cell evolution, and speciation". In: *Theory in Biosciences* 124.1, pp. 1–24.
- LAN, Kun et al. (2018). "A survey of data mining and deep learning in bioinformatics". In: *Journal of medical systems* 42.8, p. 139.
- LECUN, Yann, Yoshua BENGIO, and Geoffrey HINTON (2015). "Deep learning". In: *nature* 521.7553, p. 436.
- LECUN, Yann et al. (1999). "Object recognition with gradient-based learning". In: *Shape, contour and grouping in computer vision*. Springer, pp. 319–345.
- LEGARRA, Andres, Danila A.L LOURENCO, and Zulma G. VITEZICA (2018). "Bases for Genomic Prediction". In:
- LEHERMEIER, Christina et al. (2014). "Usefulness of multiparental populations of maize (*Zea mays* L.) for genome-based prediction". In: *Genetics* 198.1, pp. 3–16.
- LEINONEN, Rasko et al. (Nov. 2010). "The Sequence Read Archive". In: *Nucleic Acids Research* 39.suppl_1, pp. D19–D21. ISSN: 0305-1048. DOI: [10.1093/nar/gkq1019](https://doi.org/10.1093/nar/gkq1019). eprint: http://oup.prod.sis.lan/nar/article-pdf/39/suppl_1/D19/7624335/gkq1019.pdf. URL: <https://doi.org/10.1093/nar/gkq1019>.
- LEUTENEGGER, Anne-Louise et al. (2003). "Estimation of the inbreeding coefficient through use of genomic data". In: *The American Journal of Human Genetics* 73.3, pp. 516–523.
- LI, Bo et al. (2018). "Genomic prediction of breeding values using a subset of SNPs identified by three machine learning methods". In: *Frontiers in genetics* 9, p. 237.
- LI, Heng (2018). "Minimap2: pairwise alignment for nucleotide sequences". In: *Bioinformatics* 34.18, pp. 3094–3100.
- LI, Jia-Yang, Jun WANG, and Robert S ZEIGLER (2014). "The 3,000 rice genomes project: new opportunities and challenges for future rice research". In: *Giga-Science* 3.1, p. 8.
- LI, Peijin et al. (2014). "Multiple FLC haplotypes defined by independent cis-regulatory variation underpin life history diversity in *Arabidopsis thaliana*". In: *Genes & Development* 28.15, pp. 1635–1640.

- LI, Xuehui and E Charles BRUMMER (2012). "Applied genetics and genomics in alfalfa breeding". In: *Agronomy* 2.1, pp. 40–61.
- LI, Xuehui et al. (2015). "Genomic prediction of biomass yield in two selection cycles of a tetraploid alfalfa breeding population". In: *The Plant Genome* 8.2.
- LI, Yan et al. (2010). "Association mapping of local climate-sensitive quantitative trait loci in *Arabidopsis thaliana*". In: *PNAS* 107. DOI: [10.1073/pnas.1007431107](https://doi.org/10.1073/pnas.1007431107).
- LIPPERT, Christoph et al. (2014). "LIMIX: genetic analysis of multiple traits". In: *bioRxiv*. DOI: [10.1101/003905](https://doi.org/10.1101/003905). eprint: <https://www.biorxiv.org/content/early/2014/05/22/003905.full.pdf>. URL: <https://www.biorxiv.org/content/early/2014/05/22/003905>.
- LITJENS, Geert et al. (2017). "A survey on deep learning in medical image analysis". In: *Medical image analysis* 42, pp. 60–88.
- LOPEZ-CRUZ, Marco et al. (2015). "Increased Prediction Accuracy in Wheat Breeding Trials Using a Marker x Environment Interaction Genomic Selection Model". In: *G3: Genes, Genomes, Genetics* 5.4, pp. 569–582. DOI: [10.1534/g3.114.016097](https://doi.org/10.1534/g3.114.016097). URL: <https://doi.org/10.1534>.
- LUO, Xiang et al. (2017). "Genomic prediction of genotypic effects with epistasis and environment interactions for yield-related traits of rapeseed (*Brassica napus* L.)" In: *Frontiers in genetics* 8, p. 15.
- LYNCH, Michael, Bruce WALSH, et al. (1998). *Genetics and analysis of quantitative traits*. Vol. 1. Sinauer Sunderland, MA.
- MA, Wenlong et al. (2017). "DeepGS: Predicting phenotypes from genotypes using Deep Learning". In: *bioRxiv*, p. 241414.
- MAMOSHINA, Polina et al. (2016). "Applications of deep learning in biomedicine". In: *Molecular pharmaceuticals* 13.5, pp. 1445–1454.
- MARTIN, William et al. (Sept. 17, 2002). "Evolutionary analysis of *Arabidopsis*, cyanobacterial, and chloroplast genomes reveals plastid phylogeny and thousands of cyanobacterial genes in the nucleus". In: *Proceedings of the National Academy of Sciences of the United States of America* 99.19, pp. 12246–12251. ISSN: 0027-8424. DOI: [10.1073/pnas.182432999](https://doi.org/10.1073/pnas.182432999). URL: <https://www.ncbi.nlm.nih.gov/pmc/articles/PMC129430/> (visited on 05/20/2019).

- MARTINI, Johannes WR et al. (2017). "Genomic prediction with epistasis models: on the marker-coding-dependent performance of the extended GBLUP and properties of the categorical epistasis model (CE)". In: *BMC bioinformatics* 18.1, p. 3.
- MARULANDA, Jose J et al. (2016). "Optimum breeding strategies using genomic selection for hybrid breeding in wheat, maize, rye, barley, rice and triticale". In: *Theoretical and applied genetics* 129.10, pp. 1901–1913.
- MARVIN, Minsky and Papert SEYMOUR (1969). *Perceptrons*.
- MAYER, Manfred et al. (2017). "Is there an optimum level of diversity in utilization of genetic resources?" In: *Theoretical and applied genetics* 130.11, pp. 2283–2295.
- MCKAIN, Michael and AFINIT (Sept. 2017). *Mrmckain/Fast-Plast: Fast-Plast V.1.2.6*. DOI: [10.5281/zenodo.973887](https://doi.org/10.5281/zenodo.973887). URL: <https://zenodo.org/record/973887>.
- MCKINNEY, Brett and Nicholas PAJEWSKI (2012). "Six degrees of epistasis: statistical network models for GWAS". In: *Frontiers in genetics* 2, p. 109.
- MCKINNEY, Wes (2010). "Data Structures for Statistical Computing in Python". In: *Proceedings of the 9th Python in Science Conference*. Ed. by Stéfan van der WALT and Jarrod MILLMAN, pp. 51–56.
- MEIJÓ, Mónica et al. (2014). "Genome-wide association study using cellular traits identifies a new regulator of root development in Arabidopsis". In: *Nature Genetics* 46. DOI: [10.1038/ng.2824](https://doi.org/10.1038/ng.2824).
- MERESCHKOWSKY, Constantin (1905). "Über natur und ursprung der chromatophoren im pflanzenreiche". In: *Biologisches Centralblatt* 25, pp. 293–604.
- MERKEL, Dirk (2014). "Docker: lightweight linux containers for consistent development and deployment". In: *Linux Journal* 2014.239, p. 2.
- MICHIE, Donald, David J SPIEGELHALTER, CC TAYLOR, et al. (1994). "Machine learning". In: *Neural and Statistical Classification* 13.
- MIN, Seonwoo, Byunghan LEE, and Sungroh YOON (2017). "Deep learning in bioinformatics". In: *Briefings in bioinformatics* 18.5, pp. 851–869.
- MISZTAL, I et al. (2013). "Methods to approximate reliabilities in single-step genomic evaluation". In: *Journal of Dairy Science* 96.1, pp. 647–654.

- MOEINIZADE, Saba et al. (2019). "Optimizing Selection and Mating in Genomic Selection with a Look-Ahead Approach: An Operations Research Framework". In: *G3: Genes, Genomes, Genetics*, g3–200842.
- MOMEN, Mehdi et al. (Aug. 2019). "Predicting Longitudinal Traits Derived from High-Throughput Phenomics in Contrasting Environments Using Genomic Legendre Polynomials and B-Splines". In: *G3: Genes, Genomes, Genetics* 9.10, pp. 3369–3380. DOI: [10.1534/g3.119.400346](https://doi.org/10.1534/g3.119.400346). URL: <https://doi.org/10.1534/g3.119.400346>.
- MONTESINOS-LÓPEZ, Osval A et al. (2015). "Threshold models for genome-enabled prediction of ordinal categorical traits in plant breeding". In: *G3: Genes, Genomes, Genetics* 5.2, pp. 291–300.
- MONTESINOS-LÓPEZ, Osval A et al. (2019a). "A benchmarking between deep learning, support vector machine and Bayesian threshold best linear unbiased prediction for predicting ordinal traits in plant breeding". In: *G3: Genes, Genomes, Genetics* 9.2, pp. 601–618.
- (2019b). "New deep learning genomic-based prediction model for multiple traits with binary, ordinal, and continuous phenotypes". In: *G3: Genes, Genomes, Genetics* 9.5, pp. 1545–1556.
- MOROTA, Gota and Daniel GIANOLA (2014). "Kernel-based whole-genome prediction of complex traits: a review". In: *Frontiers in genetics* 5, p. 363.
- MOSER, Gerhard et al. (2009). "A comparison of five methods to predict genomic breeding values of dairy bulls from genome-wide SNP markers". In: *Genetics Selection Evolution* 41.1, p. 56.
- MOUSSEAU, Timothy A and Derek A ROFF (1987). "Natural selection and the heritability of fitness components". In: *Heredity* 59.2, p. 181.
- NATIONAL CENTER FOR BIOTECHNOLOGY INFORMATION. *NCBI Taxonomy*. Accessed: 2019-10-01. URL: <https://www.ncbi.nlm.nih.gov/Taxonomy/taxonomyhome.html/>.
- NEYHART, Jeffrey, Aaron J LORENZ, and Kevin P SMITH (2019). "Multi-Trait Improvement by Predicting Genetic Correlations in Breeding Crosses". In: *bioRxiv*, p. 593210.

- NGUYEN, Derrick and Bernard WIDROW (1990). "The truck backer-upper: An example of self-learning in neural networks". In: *Advanced neural computers*. Elsevier, pp. 11–19.
- NORDBORG, Magnus et al. (2002). "The extent of linkage disequilibrium in *Arabidopsis thaliana*". In: *Nature genetics* 30.2, p. 190.
- NORMAN, Adam et al. (2018). "Optimising Genomic Selection in Wheat: Effect of Marker Density, Population Size and Population Structure on Prediction Accuracy". In: *G3: Genes, Genomes, Genetics* 8.9, pp. 2889–2899. DOI: [10.1534/g3.118.200311](https://doi.org/10.1534/g3.118.200311). URL: <https://doi.org/10.1534>.
- Oakey, Helena et al. (2016). "Genomic selection in multi-environment crop trials". In: *G3: Genes, Genomes, Genetics* 6.5, pp. 1313–1326.
- OGUTU, Joseph O, Hans-Peter PIEPHO, and Torben SCHULZ-STREECK (2011). "A comparison of random forests, boosting and support vector machines for genomic selection". In: *BMC proceedings*. Vol. 5. 3. BioMed Central, S11.
- OHYAMA, Kanji et al. (Aug. 1986). "Chloroplast gene organization deduced from complete sequence of liverwort *Marchantia polymorpha* chloroplast DNA". In: *Nature* 322.6079, p. 572. ISSN: 1476-4687. DOI: [10.1038/322572a0](https://doi.org/10.1038/322572a0). URL: <https://www.nature.com/articles/322572a0> (visited on 05/20/2019).
- OLEJNICZAK, Szymon Adam et al. (2016). "Chloroplasts: state of research and practical applications of plastome sequencing". In: *Planta* 244.3, pp. 517–527.
- OLIPHANT, Travis E (2006). *A guide to NumPy*. Vol. 1. Trelgol Publishing USA.
- OVENDEN, Ben et al. (2018). "Accounting for Genotype-by-Environment Interactions and Residual Genetic Variation in Genomic Selection for Water-Soluble Carbohydrate Concentration in Wheat". In: *G3: Genes, Genomes, Genetics* 8.6, pp. 1909–1919. DOI: [10.1534/g3.118.200038](https://doi.org/10.1534/g3.118.200038). URL: <https://doi.org/10.1534>.
- OWENS, Brenda F et al. (2014). "A foundation for provitamin A biofortification of maize: genome-wide association and genomic prediction models of carotenoid levels". In: *Genetics* 198.4, pp. 1699–1716.
- OZKAN, Hakan, Avraham A LEVY, and Moshe FELDMAN (2001). "Allopolyploidy-induced rapid genome evolution in the wheat (*Aegilops-Triticum*) group". In: *The Plant Cell* 13.8, pp. 1735–1747.

- PALMER, Jeffrey D. (1985). "COMPARATIVE ORGANIZATION OF CHLOROPLAST GENOMES". In: *Annual Review of Genetics* 19.1. PMID: 3936406, pp. 325–354. DOI: [10.1146/annurev.ge.19.120185.001545](https://doi.org/10.1146/annurev.ge.19.120185.001545). eprint: <https://doi.org/10.1146/annurev.ge.19.120185.001545>. URL: <https://doi.org/10.1146/annurev.ge.19.120185.001545>.
- PEIFFER, Jason A et al. (2014). "The genetic architecture of maize height". In: *Genetics* 196.4, pp. 1337–1356.
- POLYAK, Boris T (1964). "Some methods of speeding up the convergence of iteration methods". In: *USSR Computational Mathematics and Mathematical Physics* 4.5, pp. 1–17.
- POUDEL, Hari P. et al. (2019). "Genomic Prediction for Winter Survival of Lowland Switchgrass in the Northern USA". In: *G3: Genes, Genomes, Genetics*, g3.400094.2019. DOI: [10.1534/g3.119.400094](https://doi.org/10.1534/g3.119.400094). URL: <https://doi.org/10.1534>.
- PURCELL, Shaun et al. (2007). "PLINK: a tool set for whole-genome association and population-based linkage analyses". In: *The American journal of human genetics* 81.3, pp. 559–575.
- PURCELL, Shaun M et al. (2014). "A polygenic burden of rare disruptive mutations in schizophrenia". In: *Nature* 506.7487, p. 185.
- QIAN, Lunwen, Wei QIAN, and Rod J SNOWDON (2014). "Sub-genomic selection patterns as a signature of breeding in the allopolyploid *Brassica napus* genome". In: *BMC genomics* 15.1, p. 1170.
- QIU, Zhixu et al. (2016). "Application of machine learning-based classification to genomic selection and performance improvement". In: *International Conference on Intelligent Computing*. Springer, pp. 412–421.
- R CORE TEAM (2018). *R: A Language and Environment for Statistical Computing*. R Foundation for Statistical Computing. Vienna, Austria. URL: <https://www.R-project.org/>.
- (2019). *R: A Language and Environment for Statistical Computing*. R Foundation for Statistical Computing. Vienna, Austria. URL: <https://www.R-project.org/>.
- RAMPASEK, Ladislav and Anna GOLDENBERG (2016). "Tensorflow: Biology's gateway to deep learning?" In: *Cell systems* 2.1, pp. 12–14.

- RAMSTEIN, Guillaume P. and Michael D. CASLER (2019). "Extensions of BLUP Models for Genomic Prediction in Heterogeneous Populations: Application in a Diverse Switchgrass Sample". In: *G3: Genes, Genomes, Genetics*, g3.200969.2018. DOI: [10.1534/g3.118.200969](https://doi.org/10.1534/g3.118.200969). URL: <https://doi.org/10.1534>.
- RAMSTEIN, Guillaume P. et al. (2016). "Accuracy of Genomic Prediction in Switchgrass (*Panicum virgatum*L.) Improved by Accounting for Linkage Disequilibrium". In: *G3: Genes, Genomes, Genetics* 6.4, pp. 1049–1062. DOI: [10.1534/g3.115.024950](https://doi.org/10.1534/g3.115.024950). URL: <https://doi.org/10.1534>.
- RATCLIFFE, Blaise et al. (2017). "Single-Step BLUP with Varying Genotyping Effort in Open-Pollinated *Picea glauca*". In: *G3: Genes, Genomes, Genetics* 7.3, pp. 935–942. DOI: [10.1534/g3.116.037895](https://doi.org/10.1534/g3.116.037895). URL: <https://doi.org/10.1534>.
- RESENDE, M. F. R. et al. (2012). "Accuracy of Genomic Selection Methods in a Standard Data Set of Loblolly Pine (*Pinus taeda* L.)" In: *Genetics* 190.4, pp. 1503–1510. DOI: [10.1534/genetics.111.137026](https://doi.org/10.1534/genetics.111.137026). URL: <https://doi.org/10.1534>.
- RIEDELSEIMER, Christian et al. (2013). "Genomic predictability of interconnected biparental maize populations". In: *Genetics* 194.2, pp. 493–503.
- RINCENT, Renaud et al. (2012). "Maximizing the reliability of genomic selection by optimizing the calibration set of reference individuals: comparison of methods in two diverse groups of maize inbreds (*Zea mays* L.)" In: *Genetics* 192.2, pp. 715–728.
- RINCENT, Renaud et al. (2018). "Phenomic Selection Is a Low-Cost and High-Throughput Method Based on Indirect Predictions: Proof of Concept on Wheat and Poplar". In: *G3: Genes, Genomes, Genetics*, g3.200760.2018. DOI: [10.1534/g3.118.200760](https://doi.org/10.1534/g3.118.200760). URL: <https://doi.org/10.1534>.
- RITCHIE, Marylyn D and Kristel VAN STEEN (2018). "The search for gene-gene interactions in genome-wide association studies: challenges in abundance of methods, practical considerations, and biological interpretation". In: *Annals of translational medicine* 6.8.
- ROCAPS LAB. *CpBase*. Accessed: 2019-04-01, Version: 8/20/2017. URL: http://rocaplab.ocean.washington.edu/old_website/tools/cpbase.

- ROEBER, FK, GA GORDILLO, and HH GEIGER (2005). "In vivo haploid induction in maize. Performance of new inducers and significance of doubled haploid lines in hybrid breeding [Zea mays L.]" In: *Maydica (Italy)*.
- ROSENBLATT, Frank (1961). *Principles of neurodynamics. perceptrons and the theory of brain mechanisms*. Tech. rep. Cornell Aeronautical Lab Inc Buffalo NY.
- RUDER, Sebastian (2016). "An overview of gradient descent optimization algorithms". In: *arXiv preprint arXiv:1609.04747*.
- RUMELHART, David E, Geoffrey E HINTON, Ronald J WILLIAMS, et al. (1988). "Learning representations by back-propagating errors". In: *Cognitive modeling* 5.3, p. 1.
- SANCHO, Rubén et al. (June 2018). "Comparative plastome genomics and phylogenomics of *Brachypodium* : flowering time signatures, introgression and recombination in recently diverged ecotypes". en. In: *New Phytologist* 218.4, pp. 1631–1644. ISSN: 0028646X. DOI: [10.1111/nph.14926](https://doi.org/10.1111/nph.14926). URL: <http://doi.wiley.com/10.1111/nph.14926>.
- SANTOS DIAS, Luiz Antônio dos et al. (2004). "A priori choice of hybrid parents in plants". In: *Genet. Mol. Res* 3.3, pp. 356–368.
- SCARCELLI, N. et al. (2016). "Intra-individual polymorphism in chloroplasts from NGS data: where does it come from and how to handle it?" In: *Molecular Ecology Resources* 16.2, pp. 434–445. DOI: [10.1111/1755-0998.12462](https://doi.org/10.1111/1755-0998.12462). eprint: <https://onlinelibrary.wiley.com/doi/pdf/10.1111/1755-0998.12462>. URL: <https://onlinelibrary.wiley.com/doi/abs/10.1111/1755-0998.12462>.
- SCHMIDHUBER, Jürgen (2015). "Deep learning in neural networks: An overview". In: *Neural networks* 61, pp. 85–117.
- SCHOPP, Pascal et al. (2017a). "Accuracy of genomic prediction in synthetic populations depending on the number of parents, relatedness, and ancestral linkage disequilibrium". In: *Genetics* 205.1, pp. 441–454.
- SCHOPP, Pascal et al. (2017b). "Genomic prediction within and across biparental families: means and variances of prediction accuracy and usefulness of deterministic equations". In: *G3: Genes, Genomes, Genetics* 7.11, pp. 3571–3586.

- SCHRAG, Tobias A et al. (2018). "Beyond genomic prediction: combining different types of omics data can improve prediction of hybrid performance in maize". In: *Genetics* 208.4, pp. 1373–1385.
- SEGURA, Vincent et al. (2012). "An efficient multi-locus mixed-model approach for genome-wide association studies in structured populations". In: *Nature genetics* 44.7, p. 825.
- SEREN, Ümit et al. (2016). "AraPheno: a public database for Arabidopsis thaliana phenotypes". In: *Nucleic acids research*, gkw986.
- SHEN, Wei et al. (Oct. 2016). "SeqKit: A Cross-Platform and Ultrafast Toolkit for FASTA/Q File Manipulation". In: *PLOS ONE* 11.10, pp. 1–10. DOI: [10.1371/journal.pone.0163962](https://doi.org/10.1371/journal.pone.0163962). URL: <https://doi.org/10.1371/journal.pone.0163962>.
- SHEN, Xia et al. (2013). "A novel generalized ridge regression method for quantitative genetics". In: *Genetics* 193.4, pp. 1255–1268.
- SHINOZAKI, K. et al. (1986). "The complete nucleotide sequence of the tobacco chloroplast genome: its gene organization and expression". In: *The EMBO Journal* 5.9, pp. 2043–2049. ISSN: 1460-2075. DOI: [10.1002/j.1460-2075.1986.tb04464.x](https://doi.org/10.1002/j.1460-2075.1986.tb04464.x). URL: <https://onlinelibrary.wiley.com/doi/abs/10.1002/j.1460-2075.1986.tb04464.x> (visited on 05/20/2019).
- SIVA, Nayanah (2008). *1000 Genomes project*.
- SNOWDON, Rod J and Federico L INIGUEZ LUY (2012). "Potential to improve oilseed rape and canola breeding in the genomics era". In: *Plant breeding* 131.3, pp. 351–360.
- SOPER, HE et al. (1917). "On the distribution of the correlation coefficient in small samples. Appendix II to the papers of" Student" and RA Fisher". In: *Biometrika* 11.4, pp. 328–413.
- SOUSA, Massaine Bandeira e et al. (2017). "Genomic-enabled prediction in maize using kernel models with genotype \times environment interaction". In: *G3: Genes, Genomes, Genetics* 7.6, pp. 1995–2014.
- STEGEMANN, Sandra and Ralph BOCK (2009). "Exchange of genetic material between cells in plant tissue grafts". In: *science* 324.5927, pp. 649–651.

- STEWART-BROWN, Benjamin B. et al. (2019). "Genomic Selection for Yield and Seed Composition Traits Within an Applied Soybean Breeding Program". In: *G3: Genes, Genomes, Genetics* 9.7, pp. 2253–2265. DOI: [10.1534/g3.118.200917](https://doi.org/10.1534/g3.118.200917). URL: <https://doi.org/10.1534>.
- STOREY, John D. and Robert TIBSHIRANI (2003). "Statistical significance for genomewide studies". In: *Proceedings of the National Academy of Sciences* 100.16, pp. 9440–9445. ISSN: 0027-8424. DOI: [10.1073/pnas.1530509100](https://doi.org/10.1073/pnas.1530509100). eprint: <https://www.pnas.org/content/100/16/9440.full.pdf>. URL: <https://www.pnas.org/content/100/16/9440>.
- STRAUCH, Rene et al. (2015). "Discovery of a novel amino acid racemase through exploration of natural variation in *Arabidopsis thaliana*". In: *PNAS* 112. DOI: [10.1073/pnas.1503272112](https://doi.org/10.1073/pnas.1503272112).
- STRINGER, Sven et al. (2011). "Underestimated effect sizes in GWAS: fundamental limitations of single SNP analysis for dichotomous phenotypes". In: *PloS one* 6.11, e27964.
- SUKUMARAN, Sivakumar et al. (2016). "Genomic Prediction with Pedigree and Genotype Environment Interaction in Spring Wheat Grown in South and West Asia, North Africa, and Mexico". In: *G3: Genes, Genomes, Genetics* 7.2, pp. 481–495. DOI: [10.1534/g3.116.036251](https://doi.org/10.1534/g3.116.036251). URL: <https://doi.org/10.1534>.
- TANG, Chunlao et al. (2007). "The evolution of selfing in *Arabidopsis thaliana*". In: *Science* 317.5841, pp. 1070–1072.
- TECHNOW, Frank, Anna BÜRGER, and Albrecht E MELCHINGER (2013). "Genomic prediction of northern corn leaf blight resistance in maize with combined or separated training sets for heterotic groups". In: *G3: Genes, Genomes, Genetics* 3.2, pp. 197–203.
- TECHNOW, Frank et al. (2014). "Genome properties and prospects of genomic prediction of hybrid performance in a breeding program of maize". In: *Genetics* 197.4, pp. 1343–1355.
- TETKO, Igor V, David J LIVINGSTONE, and Alexander I LUIK (1995). "Neural network studies. 1. Comparison of overfitting and overtraining". In: *Journal of chemical information and computer sciences* 35.5, pp. 826–833.

- THAVAMANIKUMAR, Saravanan, Rudy DOLFERUS, and Bala R. THUMMA (2015). "Comparison of Genomic Selection Models to Predict Flowering Time and Spike Grain Number in Two Hexaploid Wheat Doubled Haploid Populations". In: *G3: Genes, Genomes, Genetics* 5.10, pp. 1991–1998. DOI: [10 . 1534 / g3 . 115 . 019745](https://doi.org/10.1534/g3.115.019745). URL: <https://doi.org/10.1534>.
- THORWARTH, Patrick, Eltohamy AA YOUSEF, and Karl J SCHMID (2018). "Genomic Prediction and Association Mapping of Curd-Related Traits in Gene Bank Accessions of Cauliflower". In: *G3: Genes, Genomes, Genetics* 8.2, pp. 707–718.
- TIMPSON, Nicholas J et al. (2018). "Genetic architecture: the shape of the genetic contribution to human traits and disease". In: *Nature Reviews Genetics* 19.2, p. 110.
- TOGNINALLI, Matteo et al. (2017). "The AraGWAS Catalog: a curated and standardized Arabidopsis thaliana GWAS catalog". In: *Nucleic acids research* 46.D1, pp. D1150–D1156.
- TWYFORD, Alex D. and Rob W. NESS (Sept. 1, 2017). "Strategies for complete plastid genome sequencing". In: *Molecular Ecology Resources* 17.5, pp. 858–868. ISSN: 1755-0998. DOI: [10 . 1111 / 1755 - 0998 . 12626](https://doi.org/10.1111/1755-0998.12626). URL: <http://onlinelibrary.wiley.com/doi/10.1111/1755-0998.12626/abstract> (visited on 01/26/2018).
- UNTERSEER, Sandra et al. (2014). "A powerful tool for genome analysis in maize: development and evaluation of the high density 600 k SNP genotyping array". In: *BMC genomics* 15.1, p. 823.
- VAN ROSSUM, Guido and Fred L DRAKE JR (1995). *Python tutorial*. Centrum voor Wiskunde en Informatica Amsterdam, The Netherlands.
- VANRADEN, Paul M (2008). "Efficient methods to compute genomic predictions". In: *Journal of dairy science* 91.11, pp. 4414–4423.
- VANRADEN, PM et al. (2008). "Reliability of genomic predictions for North American dairy bulls". In: *J. Dairy Sci* 91.Suppl 1, p. 305.
- VERBYLA, Klara L et al. (2009). "Accuracy of genomic selection using stochastic search variable selection in Australian Holstein Friesian dairy cattle". In: *Genetics research* 91.5, pp. 307–311.
- VIEIRA, IC et al. (2017). "Assessing non-additive effects in GBLUP model". In: *Genetics and molecular research: GMR* 16.2.

- VINGA, Susana et al. (2012). "Pattern matching through Chaos Game Representation: bridging numerical and discrete data structures for biological sequence analysis". In: *Algorithms for molecular biology : AMB* 7.1. 22551152[pmid], pp. 10–10. ISSN: 1748-7188. DOI: [10.1186/1748-7188-7-10](https://doi.org/10.1186/1748-7188-7-10). URL: <https://www.ncbi.nlm.nih.gov/pubmed/22551152>.
- WALSH, B and M LYNCH (2018a). "Short-term Changes in the Mean: 2. Truncation and Threshold Selection". In:
- WALSH, Bruce and Michael LYNCH (2018b). *Evolution and selection of quantitative traits*. Oxford University Press.
- WANG, Weiwen et al. (2018). "Assembly of chloroplast genomes with long- and short-read data: a comparison of approaches using *Eucalyptus pauciflora* as a test case". In: *BMC genomics* 19.1. 30594129[pmid], pp. 977–977. ISSN: 1471-2164. DOI: [10.1186/s12864-018-5348-8](https://doi.org/10.1186/s12864-018-5348-8). URL: <https://www.ncbi.nlm.nih.gov/pubmed/30594129>.
- WANG, Yu et al. (2014). "The accuracy of prediction of genomic selection in elite hybrid rye populations surpasses the accuracy of marker-assisted selection and is equally augmented by multiple field evaluation locations and test years". In: *BMC genomics* 15.1, p. 556.
- WARNER, Brad and Manavendra MISRA (1996). "Understanding neural networks as statistical tools". In: *The american statistician* 50.4, pp. 284–293.
- WATSON, Amy et al. (2018). "Speed breeding is a powerful tool to accelerate crop research and breeding". In: *Nature plants* 4.1, p. 23.
- WEBB, Sarah (2018). "Deep learning for biology". In: *Nature* 554.7693.
- WERNER, Christian R et al. (2018). "Effective genomic selection in a narrow-genepool crop with low-density markers: Asian rapeseed as an example". In: *The plant genome* 11.2.
- WICKE, Susann et al. (July 1, 2011). "The evolution of the plastid chromosome in land plants: gene content, gene order, gene function". In: *Plant Molecular Biology* 76.3, pp. 273–297. ISSN: 1573-5028. DOI: [10.1007/s11103-011-9762-4](https://doi.org/10.1007/s11103-011-9762-4). URL: <https://doi.org/10.1007/s11103-011-9762-4> (visited on 05/16/2019).

- WINDHAUSEN, Vanessa S et al. (2012). "Effectiveness of genomic prediction of maize hybrid performance in different breeding populations and environments". In: *G3: Genes, Genomes, Genetics* 2.11, pp. 1427–1436.
- WRIGHT, Sewall (1922). "Coefficients of inbreeding and relationship". In: *The American Naturalist* 56.645, pp. 330–338.
- WÜRSCHUM, Tobias (2012). "Mapping QTL for agronomic traits in breeding populations". In: *Theoretical and Applied Genetics* 125.2, pp. 201–210.
- WÜRSCHUM, Tobias, Stefan ABEL, and Yusheng ZHAO (2014). "Potential of genomic selection in rapeseed (*B. rapeseed* L.) breeding". In: *Plant Breeding* 133.1, pp. 45–51.
- WÜRSCHUM, Tobias et al. (2013). "Genomic selection in sugar beet breeding populations". In: *BMC genetics* 14.1, p. 85.
- XAVIER, Alencar, William M. MUIR, and Katy Martin RAINEY (2016). "Assessing Predictive Properties of Genome-Wide Selection in Soybeans". In: *G3* 6.8, pp. 2611–2616. DOI: [10.1534/g3.116.032268](https://doi.org/10.1534/g3.116.032268). URL: <https://doi.org/10.1534>.
- XIAO-MING, Zheng et al. (May 8, 2017). "Inferring the evolutionary mechanism of the chloroplast genome size by comparing whole-chloroplast genome sequences in seed plants". In: *Scientific Reports* 7.1, p. 1555. ISSN: 2045-2322. DOI: [10.1038/s41598-017-01518-5](https://doi.org/10.1038/s41598-017-01518-5). URL: <https://www.nature.com/articles/s41598-017-01518-5> (visited on 05/16/2019).
- XU, S (2010). "An expectation–maximization algorithm for the Lasso estimation of quantitative trait locus effects". In: *Heredity* 105.5, p. 483.
- XU, Shizhong (Aug. 2013). "Genetic Mapping and Genomic Selection Using Recombination Breakpoint Data". In: *Genetics* 195.3, pp. 1103–1115. DOI: [10.1534/genetics.113.155309](https://doi.org/10.1534/genetics.113.155309). URL: <https://doi.org/10.1534/genetics.113.155309>.
- YANG, Jian et al. (2010). "Common SNPs explain a large proportion of the heritability for human height". In: *Nature genetics* 42.7, p. 565.
- ZAPATA-VALENZUELA, Jaime et al. (2013). "Genomic Estimated Breeding Values Using Genomic Relationship Matrices in a Cloned Population of Loblolly Pine". In: *G3: Genes, Genomes, Genetics* 3.5, pp. 909–916. DOI: [10.1534/g3.113.005975](https://doi.org/10.1534/g3.113.005975). URL: <https://doi.org/10.1534>.

- ZEILER, Matthew D (2012). “ADADELTA: an adaptive learning rate method”. In: *arXiv preprint arXiv:1212.5701*.
- ZHANG, Yan et al. (2018). “Estimation of complex effect-size distributions using summary-level statistics from genome-wide association studies across 32 complex traits”. In: *Nature genetics* 50.9, p. 1318.
- ZHANG, Zhiwu et al. (Mar. 2010). “Mixed linear model approach adapted for genome-wide association studies”. In: *Nature Genetics* 42.4, pp. 355–360. DOI: [10.1038/ng.546](https://doi.org/10.1038/ng.546). URL: <https://doi.org/10.1038/ng.546>.
- ZHENG, Xiuwen (2013). “A Tutorial for the R Package SNPRelate”. In: *University of Washington, Washington, USA*.
- ZHONG, Shengqiang et al. (2009). “Factors affecting accuracy from genomic selection in populations derived from multiple inbred lines: a barley case study”. In: *Genetics* 182.1, pp. 355–364.
- ZHOU, Xiang and Matthew STEPHENS (June 2012). “Genome-wide efficient mixed-model analysis for association studies”. In: *Nature Genetics* 44.7, pp. 821–824. DOI: [10.1038/ng.2310](https://doi.org/10.1038/ng.2310). URL: <https://doi.org/10.1038/ng.2310>.
- ŽILINSKAS, A (2006). *Practical mathematical optimization: An introduction to basic optimization theory and classical and new gradient-based algorithms*.